THE UNIVERSITY
of EDINBURGH

Multi-analysis of Potential and Actual Above Ground Biomass in a Tropical Deciduous Forest in México.

Rogelio Omar Corona Núñez

Doctorate – The University of Edinburgh – 2017

Own Work Declaration

I declare that this thesis has been composed by me alone. I confirm that the work submitted is my own, but that appropriate credit has been given within the thesis where reference has been made to the work of others. No part of this thesis has been previously submitted or accepted for a degree or professional qualification.

Rogelio Omar Corona Núñez

May 2017

Acknowledgements

To my parents (Eugenia and Rogelio) who made me the person who I am, who gave me their unconditional support and the tools to build my life. Also, I want to thank for looking after my interests, home and cats (Micro and Nana) for these 4 long years.

To Alma Mendoza whose unconditional support after difficult times is still present. For your fruitful comments, reviews, suggestions and improvements in my research. As well, as for giving me company during my life. Not to mention, all the tough work needed to collect the field data.

I deeply thank to CONACyT for sponsoring my studies at this University under the scholarship number 187019.

Without the support of Procesos y Sistemas de Información en Geomática, SA de CV in financing my field work, data provision and interesting discussions, I would have never seen an ending.

Finally, I would like to thank to those who gave me support during my PhD

Felipe and Ayleen for the all the emotional support and your friendship during this 4 years. For helping me in not losing my head and my mind.

Emmanuel Blei for giving me R support. Without him possibly my thesis would not be in time and with the current quality.

To my examiners Heiko Balzter and Neil Stuart for your fruitful comments to improve my research, which by other means possibly it wouldn't have improved.

Rachel Cohen for your friendship and for reading my chapter.

Jeff , Theresa and Pauline Exbrayat for your friendship and fruitful academic and not academic discussions, as well as those coffee brakes.

Leopoldo Galicia Sarmiento for sharing your research and student's time, to read my chapters and give me fruitful comments, though you do not have any obligation.

Luke Smallman for your friendship and for giving me R support. I would like to have meet you earlier.

Table of contents

List of figures

List of tables

Abbreviations

A	Altitude
AGB	Above Ground Biomass
AGB_{pot}	Potential Above Ground Biomass that the landscape would have with no human disturbance
AGC	Above Ground Carbon
As	Aspect
BA	Basal Area
BRDF	Bi-directionally corrected reflectance
C	Carbon
CC	Climate Change
CDM	Clean Development Mechanism
Clit	Coarse litter
CONABIO	The National Commission for Knowledge and Use of Biodiversity (Comisión Nacional para el Conocimiento y Uso de la Biodiversidad)
CONANP	The National Commission of Natural Protected Areas (Comisión Nacional de Áreas Naturales Protegidas)
CTI	Compound Topographic Index
CV	Coefficient of Variation
CV_{maps}	Coefficient of Variation across current AGB maps
DBH	Diameter at Breast Height
DEM	Digital Elevation Model
DS	Distance to streams
Flit	Fine litter
GAM	General Additive Model
GLM	General Lineal Model
GLMM	Generalized Linear Mixed Models via Penalized Quasi-Likelihood
INECC	National Institute of Ecology and Climate Change
INEGI	The National Institute of Statistics and Geography (Instituto Nacional de Estadística y geografía)
IPCC	Intergovernmental Panel on Climate Change
IUCN	The International Union for Conservation of Nature
JB	Jarque Bera test
LAI	Leaf Area Index
LST	Land Surface Temperature
LUCC	Land Use Cover Change
MC	Monte Carlo
MODIS	Moderate Resolution Imaging Spectro radiometer
MT	Mean annual Temperature
N	Nitrogen
NFI	National Forest Inventory
NN	Neural Network
OLS	Ordinary-Least-Squares,

P	Phosphorus
PD	Probability of Deciduousness
pH	Potential Hydrogen
PmI	Potential mean solar irradiance
PSIG	Processes and Information Systems in Geomatics (R). (Procesos y Sistemas de Información en Geomática, SA de CV)
RF	Random Forest
RT	Regression Tree
SAC	Spatial Autocorrelation
SI	Solar Irradiance
SMN	The National Weathercast Service (Servicio Metereologico Nacional)
SRTM	Shuttle Radar Topography Mission
TANF	Total Areal of Natural Forest
TDF	Tropical Deciduous Forest
TOPEX	Terrain shape or exposure index
TP	Total Precipitation
W	Mann-Whitney-Wilcox test
WD	Wood density

Summary

Natural tropical deciduous forest (TDF) is considered with a medium to small height (<15 m). Particularly, in Mexico TDF shows a remnant of 36.2% of primary forest driving changes in the structure and species composition. This vegetation in Mexico is mainly transformed into grassland for cattle raising, and agriculture, primarily for self-consumption. More information about the ecology and the social pressures on this vegetation can be seen in Chapter I. The general methods, including sampling allocation and collection, characteristics of the study site, as well the procedure of the research proposal is presented in Chapter II.

The main aim of this thesis is to improve the accuracy of predictions of net carbon emissions and the spatial distribution of AGB in the Tropical Deciduous Forest of Mexico. To address this aim, it is important to take into consideration the forest structure, spatial patterns and processes in a natural forest in a multi-scale analysis; also, it is necessary to characterize the spatial socio-economic drivers that influence current AGB losses. With the understanding of such elements, it is possible to reconstruct the potential carbon stocks and estimate the allocation of net carbon emissions due to deforestation and forest degradation.

This study shows that it is possible to count net carbon emissions caused by deforestation and forest degradation at a landscape scale. To come to such estimates, it was necessary to reduce the different sources of uncertainty. Chapter III explores different elements that drive the AGB allocation in a mature forest. The AGB in the mature forest was considered as the potential AGB that the forest could get assuming that it has reached its steady state. Different field sampling strategies and allometric equations were evaluated to account for uncertainty in the AGB estimations. The results showed that small sampling design (300-400 m^2) and large-sized plots (4 ha) produce the same tree distribution for trees: ≥30 cm in DBH as well as in AGB. These results contradict what has been reported for others (Chave *et al.,* 2004 and 2005) when they refer to the general definition of tropical forest. However, those other studies referred to forests with a much higher precipitation and which can be classified as tropical rain (perennial) forest (Chave *et al.,* 2004). In the tropical deciduous forest, the kind considered in this study, AGB tends to be allocated in small-sized trees. Diverse biophysical characteristics that may drive AGB allocation were considered over different spatial scales. Water stress was the main driver for AGB density at different spatial scales. Nutrients showed little significance to explain AGB as other studies have suggested in secondary forests and/or chronosequences. With this understanding, Chapter IV shows the use of different multi-variable models. Parsimonious models were the result of the variables selection and sensitivity test. Most of the methodologies showed a better performance to explain AGB allocation than a null-model. However, when they were contrasted with independent observations over different spatial resolutions, it was possible to conclude that only GLM was capable of reproducing the spatial

patterns, and its estimations were close to observations. Nevertheless, some observations with very large AGB densities were underestimated by the model. This underestimation was related to the presence of few very large-sized trees. These two chapters depict the possibility of accounting for the potential AGB, and the uncertainty, namely whether the landscape could reach it with the absence of human disturbance.

Once the potential AGB map was built and validated, it was transformed to carbon stock, using a local carbon concentration estimate. This potential carbon stock map was contrasted to the different available maps of current carbon stocks. Consequently, it was possible to estimate net carbon emissions due to deforestation and forest degradation (Chapter V), suggesting that the general models tend to agree in the total carbon loss. However, there are some spatial discrepancies in the magnitudes of change. Main differences between maps can be reduced by diverse socio-ecological constraints that dominate the landscape. This is important because it may be possible to make future adjustments that would reduce variability, enabling more accurate AGB estimations. However, to individually account for deforestation and forest degradation, more detailed sources of local information are necessary, such as socio-economic variables. Therefore models with a bottom-up perspective would lead to a better understanding and representation of the landscape. Finally, the growing rural population will have larger demands for wood and food, so while remote or protected areas may have the potential for storing high AGB, forest close to settlements and access routes are likely to continue being disturbed, unless affordable alternatives are available for the sustainable use of the forest.

In conclusion, the estimation of spatial heterogeneity of AGB in the landscape is of great importance when measuring carbon stocks and ecological dynamics. Various elements influence the AGB allocation in the mature forest. Among all of them, water availability played the most decisive part of various spatial scales. My models support the hypothesis that water availability plays the major role in explaining AGB in Mexico on a local, sub-regional and landscape scale. Model selection produced contrasting AGB estimates and patterns. Moreover, the results of this study tell us that there is not a clear consensus among various current AGB maps. However, they also show that with a multi-model comparison it is possible to identify carbon emissions drivers and calculate total carbon emissions due to forest disturbances. Socio-economic variables played the major role in explaining AGB losses. Therefore, future studies should look into a bottom-up approach for a better understanding and representation of current AGB.

Chapter I. Introduction

I.1 Climate Change (CC)

In the last century, the world has experienced a rise in its average temperature of around 0.74 °C (Miller, 1992; Mann *et al.*, 1998; Martínez *et al.*, 2004; IPCC, 2006). Anthropogenic CC is derived from the use of fossil fuels: natural gas, mineral coal, and petroleum (Canadell *et al.*, 2007; IPCC, 2007), cement production and deforestation (Houghton, 2005b). Recently, it has been recognized that Mexico is responsible for nearly 1.5% (512 Mt CO_{2e}) of the global emissions, where the land-use and land-cover change represents 16.3% (SEMARNAT-INE, 2009).

CC will impact on hydrologic cycling, which could promote stronger and shorter periods of rain (FAO, 1996). The general trend is that evaporation rates will rise, which would reduce water availability in many regions (IPCC, 2003; Seidel *et al.*, 2008; Groppelli *et al.*, 2011) with increasing droughts (Malhi *et al.*, 2008). Relative humidity and radiation are expected to modify their patterns too (Sherwood *et al.*, 2010) as will precipitation extremes (O'Gorman, 2012). As a result, it is expected that the tropical belt widens about two degrees latitude (Seidel *et al.*, 2008). Moreover, CC will affect ecosystems processes and biodiversity; for example, Root *et al.*,(2003) suggested that CC will induce changes in plants and animals by affecting their habitats, and by promoting the intensification of anthropogenic disturbances. Ecosystems are capping differently in response to CC: some are expected to become extinct while others would expand their ecological niche, increasing their distribution range. Temperate forest is moving its tree-line to higher altitudes and latitudes; tropical ecosystems are widening their home range (Walther *et al.*, 2002; Parmesan and Yohe, 2003) as are those with a higher resilience to dry conditions, particularly dry forests (Watson *et al.*, 1997). However, a slight annual decrease in precipitation is projected to make tropical deciduous forests subject to greater risk of forest fires in the immediate future (Fischlin *et al.*, 2009). Changes in temperature and precipitation patterns could lead to a reduction in NPP of tropical ecosystems (Cao and Woodward, 1998; Del Grosso *et al.*, 2008). Finally, in drylands a change in the inter-annual climate variability is expected, mainly driven by modifications in precipitation, more extreme rainfall events and intense droughts (Maestre *et al.*, 2012). This situation may reduce forest growth for some types of forest (Bachelet *et al.*, 2003), while others with higher adaptative capacity may be capable of dealing with such changes. Moreover, tropical deciduous forests are very sensitive to changes in rainfall, which can affect vegetation productivity and plant survival (Hulme, 2005; Miles *et al.*, 2006). Cao and Woodward (1998) suggested that in tropical ecosystems some changes in vegetation productivity are mainly related to CO_2 concentrations rather than climate change itself, which will lead to a higher tropical carbon uptake. Some studies conducted in Costa Rica show that TDF is particularly sensitive to life zone shifts under climate change (Enquist, 2002). For example, little decrease in the annual precipitation would cause TDF to suffer a higher risk of forest fires.

The deforestation in the tropics has been considered an important source of carbon emissions and as a consequence a great driver of climate change (Houghton, 2005a). However, the uncertainty of such estimations is large, mainly as result of the following factors: (1) limited knowledge of carbon stocks of tropical forests (Houghton, 1999; Eva *et al.*, 2003; Fearnside and Laurance, 2003; Ometto *et al.*, 2015), processes of natural regeneration (Tucker and Townshend, 2000; DeFries *et al.*, 2002), and in understanding the impacts of deforestation, forest degradation and fires on carbon stocks (Laurance *et al.*, 1998; Laurance *et al.*, 2000; Barlow *et al.*, 2003); (2) the scale of analysis (Hansen and DeFries, 2004); and (3) the diverse methodologies to measure, simulate or predict any of the above.

Recently there have been efforts to mitigate climate change through a reduction of carbon emissions. One approach that has a worldwide application in developing countries is the carbon sequestration by afforestation and reforestation through the Clean Development Mechanism (CDM) (Santilli *et al.*, 2005). These projects depend on mapping and monitoring changes in carbon stocks over time. Though it has helped in reducing carbon emissions (Aukland *et al.*, 2002; Santilli *et al.*, 2005), it led on to relevant negative ecological impacts (Beder, 2006, 2007) mainly because of the use of monocultures of fast-growing tree species. An alternative approach is through REDD+ projects, which aim to protect natural forest. The general approach is to promote forest regeneration by reduction and avoidance of carbon emissions due to deforestation and forest degradation. REDD+ projects use as their baseline the current carbon stocks (Harris *et al.*, 2012), but they fail in the estimation of the potential of carbon stocks that can be attained in a region through the curbing of human disturbance.

I.2 Carbon cycle

The carbon cycle is the combination of different physical, chemical, and biological processes that transfer carbon between the primary storage pools (atmosphere, plants, soils, water systems and geological sediments) (Sabine *et al.*, 2004). Plants take up carbon dioxide (CO_2) from the atmosphere through photosynthesis. Photosynthesis transfers CO_2 from the atmosphere and the carbon is stored in wood and other plant tissues (Poorter *et al.*, 2009). The respiration that accompanies plant metabolism transfers some of the carbon back into the atmosphere as CO_2 (Hogberg *et al.*, 2001). When plants die they also release CO_2 into the atmosphere (Simmons *et al.*, 1996). A fraction of the dead organic material is resistant to decay, and this carbon accumulates in the soil. In this way, emissions from plants, other natural systems and human activities return carbon to the atmosphere, which renews the cycle (Kyrklund, 1990; Brown, 1997; Prentice *et al.*, 2001; Houghton, 2003; Sundquist and Visser, 2003). On land, numerous processes contribute to carbon storage. Some of these are directly influenced by human actions. For example, planting of forests, conversion to no-till agriculture among others (FAO, 2010; Ontl and Schulte, 2012). However, the amount of CO_2 emissions due to conversion of the natural forest is highly uncertain. Therefore, understanding the carbon cycle and accounting for the carbon stocks, fluxes

and changes is of primary concern, and to distinguish the effects of human actions from those of natural system (CCSP, 2003).

Temperature and precipitation, solar irradiation isolation and soil nutrients are recognized as primarily responsible for plant development (Holmgren *et al.*, 1997; Berdanier and Klein, 2011; Medeiros and Drezner, 2012; Peterson, 2012), therefore, carbon sequestration. However, depending on the scale of analysis and the ecosystem under study water availability and soil nutrients perform differently (Allen and Hoekstra, 1990; Turner, 2005; Currie, 2011). On one hand, at global scales, climatic variables are main factors to explain AGB by eclipsing species composition (Becknell *et al.*, 2012) and other local variables (Snyder and Tartowski, 2006). Different authors found that annual precipitation explains over 50% of the variation in AGB with a negative correlation (Brown and Lugo, 1982; Eaton and Lawrence, 2009; Becknell *et al.*, 2012). On the other hand, at a landscape scale variables such as solar irradiation, slope, aspect and soil texture are recognized to be the major influences on water availability for plants, mainly in dry ecosystems (Leitner, 1987). Among other factors concavity of the terrain has been thought to explain biomass allocation (Berdanier and Klein, 2011; Peterson, 2012). Moreover, the availability of a suitable microclimate is critical for the response of species distribution (Bennie *et al.*, 2008), by driving the individual development of trees (Holmgren *et al.*, 1997; Berdanier and Klein, 2011). Nevertheless, Powers *et al*., (2009) and Medeiros *et al*., (2012), in a multi-scale analysis, suggest variation in rainfall, soil properties, and nutrients are the main factors contributing to structural change in tropical deciduous forest. However, little is known about N and P patterns in mature forests (Gei and Powers, 2013) which are important factors to know in order to understand the structural differences in the tropical deciduous forest.

I.3 Forest ecosystems

Forestland plays a major role in the global carbon cycle which is closely inter-related with climate change. It is estimated that of a total of over 40 million km^2 of global forested land, 44% is in the tropics, 34% in the boreal latitudes, 13% in temperate regions, and 9% in subtropical regions (FAO, 2005; FRA, 2010). However, more than 50% of the forest is concentrated in just five countries (Russia, Brazil, Canada, United States of America and China) while Mexico is located in twelfth place (FRA, 2010).

Globally, it has been calculated to be between 289 (FRA, 2010) and 558 Gt C (Houghton, 2005a) in forest biomass, with an average reduction of 0.5 Gt C *per* year from 2005 to 2010, mainly centered in the tropics (FRA, 2010). Tropical forests represent a large reservoir of carbon, nearly 50% of carbon stored in vegetation (Houghton, 2005a). However, land-use and land-cover change (LUCC) have become of great concern in the global carbon cycle and emissions (Carpenter *et al.*, 2006). Mexico plays a particularly major role in carbon sequestration with nearly 64.8 million hectares of forested land, 20.2 million hectares of other wooded land and with over 2,043 million tons of carbon in live biomass (FRA,

2010). Even though the tropics are considered a net source of carbon emissions due to high deforestation rates (Houghton, 1995), others believe they act as a carbon sink (Lugo and Brown, 1980; Brown and Lugo, 1984). This is because some tropical forests are in recovery from previous disturbances.

Tropical forests can be grouped based on their seasonality. The three main potential drivers of phenological change on vegetation are: solar radiation, precipitation and air temperature (Ningthoujam and Mutum, 2010). As a result, their combination causes the existence of very dry forests like the tropical deciduous forest, or less water-stressed ones such as tropical semideciduous forest and tropical rain forest (FAO, 2005) - the last of these is the most studied and the first is the least studied (Janzen, 1986; Dirzo *et al.*, 2011). However, in recent times, the tropical deciduous forest is being given great importance due to its high deforestation rates (Maass *et al.*, 2005; Dirzo *et al.*, 2011; Corona, 2012). In Mexico dry ecosystems represent 53.7% (57.6 million hectares shrubland and 16.5 million hectares tropical deciduous forest) of its 138 million hectares of natural forested land (SEMARNAT, 2012).

I.4 Tropical Deciduous Forest (TDF)

Tropical deciduous forest has many homonyms according to diverse authors or research purposes, which can lead us into confusion in terminology. This study considers the following names as describing the same type of vegetation:

- Selva baja caducifolia
- Selva baja subcaducifolia
- Selva mediana caducifolia
- Selva mediana subcaducifolia
- Bosque tropical caducifolio
- Bosque tropical subcaducifolio
- Bosque tropical deciduos
- Bosque deciduo semiárido
- Bosque seco
- Selva seca
- Selva estacional seca
- Selva tropical seca
- Deciduous seasonal forest
- Deciduous forest
- Dry tropical forest
- Dry deciduous forest
- Tropical dry forest
- Short tree forests
- Tropical deciduous forest
- Seasonally dry tropical forest

This forest grows within an average temperature over 17 °C, a precipitation of 250 - 2,500 mm yearly, and a seasonality of 4-6 months (precipitation <100 mm) (Murphy and Lugo, 1986a; Trejo-Vázquez, 1999; Dirzo *et al.*, 2011). In México, this vegetation is distributed in regions where the temperature ranges from no lower than 0°C to a high that normally does not exceed 29°C (Trejo-Vázquez, 1999; Dirzo *et al.*, 2011), and with a rainfall from 600 to 1,200 mm per year, with two dry seasons. This forest is allocated on slope with shallow soils. Its altitude ranges from 0 to 1,900 m asl. According to Fischlin *et al.,* (2009) the seasonal tropical forests are characterized by a ratio of precipitation to potential evapotranspiration between 2 and 1, whereas tropical deciduous forests are characterized by a ratio <1.

TDF ecosystem is considered with a medium (10-15 m) or small height (<10 m). During the dry season the senescence is noticed, because ~75% of the elements lose their leaves (Miranda and

Hernández, 1963), However, during the rainy season the forest becomes fully green (Rzedowski, 2006). The canopy is extended and well developed. It has a shrub strata with lianas, sometimes cacti (Trejo-Vázquez, 1999; Trejo and Dirzo, 2002). Table I.2 shows ecological characteristics of this forest.

Some of the most representative species range from 6 to 10 m and they are: *Bursera excelsa*; *B. simaruba*; *B. sessiliflora*; *Amphipterygium adstringens*; *Ceiba sp.*; *Lysiloma divaricata*; *Pachycereus pecten-aboriginum*; *Plumeria rubra*; *Thevetia ovata*; *Lonchocarpus sp.*; *Lysiloma sp*; and *Pithe cellobium sp.* Some other species that range from 1.5 to 3 m are: *Acacia cochliacantha*; *Jacquinia aurantiaca*; *Randia nelsonii*; *Jatropha sp.*; *Opuntia sp.*; *Croton sp.*; *Cnidoscolus sp.*; *Bromelia pinguin*; *Bromelia pinguin*; and *Turnera diffusa.* Finally, the herbaceous strata are represented during the dry season and the genera that can be found are: *Bouteloua sp.*; *Aristida sp.*; *Setaria sp.*; and *Muhlenbergia sp*. (INEGI, 2004).

Where climatic conditions are more favorable, there are some plants that can grow larger than the average, and they can conserve their leaves during the dry season. Some examples of species than can grow up to 20 m are: *Heliocarpus sp.*; *Diphysa robinioides*; *Astronium graveolens*; *Coccoloba barbadensis*; *Enterolobium cyclocarpum*; and *Brosimum alicastrum*. Species that grow 10-15 m are: *Bursera simaruba*; *Calycophyllum candidissimum*; *Nectandra sp.*; *Apoplanesia paniculata*; *Ceiba pentandra*; *Stenocereus sp.*; *Leucaena sp.*; *Belotia insignis*; *Plumeria rubra*; *Gliricidia sepium*; and *Erythrina sp.* Tree species up to 5 m include *Cryosophilla argentea*; *Celtis sp.*; *Forchhammeria pallida*; *Luehea speciosa*; *Pedilanthus sp.*; *Pulsenia armata;* shrub strata with up to 2 m in height are *Cryosophila argentea and Bromelia sp.* (INEGI, 2004).

Table I.1 General characteristics of Mexican Tropical Dry Forest

Biodiversity	Genera	524
	Species	1,484
Density (trees/ha)	Small forest	221
	Medium and high forest	514
Basal area (m^2/ha)	Small forest	4.74
	Medium and high forest	12.03
Proportion of Biomass (%)	Aboveground	81.6
	Belowground	18.4
Organic carbon in soil (Mg ha^{-1})		47.67
Growth rate	Volume (m^3 ha^{-1} yr^{-1})	2.97
	Biomass (Mg ha^{-1} yr^{-1})	3.03
Land cover (million hectares)	Secondary forest	19.98
	Primary forest	7.37

(FRA, 2010; CONAFOR, 2012; SEMARNAT, 2012)

I.5 Deforestation

There is agreement about the role of forests in the global carbon cycle and hence global climate (Cramer *et al.*, 2004). For example, tropical forests store large quantities of carbon, but are being transformed into agricultural land and pasture land for cattle raising, and are releasing additional carbon into the atmosphere (Melillo *et al.*, 1996; Houghton, 2008; FRA, 2010). As a result, the future role of tropical forests in the global carbon cycle is a function of future deforestation rates and the degree to which remaining forests will be sustainable or even increase their carbon stock (Cramer *et al.*, 2004).

Tropical forests are the most important land-cover vegetation type in terms of area (Friday and Laskey, 1991). However, in the last decades human activities have modified and transformed such ecosystems (Vitousek *et al.*, 1997). For example, it has been reported that nearly 16 million forested hectares were transformed *per* year worldwide during 1990-2000 (FRA, 2010). Deforestation and forest degradation account for between 7% and 30% of total anthropogenic carbon emissions (Canadell *et al.*, 2007; Denman and Brasseur, 2007). Moreover, worldwide global anthropogenic deforestation flux went up to 1.6 Gt C yr^{-1} (Bolin *et al.*, 2000; Prentice *et al.*, 2001). Most of these changes have been concentrated in South America and Africa, where the annual deforestation rates exceed 4 and 3.4 million hectares, respectively. Mexico in particular has been considered to be among the top ten deforesting countries (FAO, 2005). For example, since 1950, nearly 42 million hectares have been deforested at rates of 155 to 354 thousand hectares *per* year (Table I.1) and only in recent times has there been a reduction in the rates (FRA, 2010). The highest deforestation rates are located in the south of Mexico with nearly 189.8 thousand hectares *per* year (SEMARNAP, 1998). According to Sosa-Cedillo (2008) Oaxaca shows the highest deforestation rate in the country and this is focused on the TDF. In the next table can be seen diverse deforestation rates reported to various regions of Mexico.

Table I.2 Deforestation rates reported by different studies to Mexico and Oaxaca state.

Location	Deforestation rate (%)	Deforested area (1000 ha)	Period	Reference
México	0.52	354.0	1990-2000	FRA (2010)
México	0.35	235.0	2000-2005	FRA (2010)
México	0.50	318.5	1990-2005	FAO (2005)
México	0.24	155.0	2005-2010	FRA (2010)
South of México	--	189.8	--	SEMARNAP (1998)
TDF of México	--	300.0	1990-1995	INEGI, (2000); Miranda, (1996)
TDF of México	--	163.0	1992	Rincón *et al.,* (1999)
TDF of México	1.9	--	1977-1992	Porter-Bolland *et al.,* (2007)
Oaxaca	0.35	--	1980-2001	Velázquez *et al.,* (2003)
Oaxaca	0.60	609.1	--	Céspedes-Flores and Moreno-Sánchez, (2010)
TDF of Oaxaca	0.70	67.69	1996-2002	Self estimated from from S.II and S.III (INEGI, 2001, 2005)
TDF of Oaxaca	0.85	67.26	2002-2005	Self estimated from S.III and S.IV (INEGI, 2005, 2008)
TDF of Oaxaca	0.74	128.0	1996-2007	Self estimated from S.II and S.IV

(INEGI, 2001, 2008)

While more research has been done on moist tropical forests (Skutsch *et al.*, 2009), drier tropical forests are also important: tropical deciduous forest (TDF) accounts for nearly 5% of the global carbon in vegetation and soils in terrestrial ecosystems (Houghton and Skole, 1990). Information on forest losses for TDF are sparse and uncertain. According to Chomitz *et al.,* (2007) in the tropics, nearly 78% of the TDF's original area had been modified; other researchers suggest a more optimistic 48% (Miles *et al.*, 2006; Dirzo *et al.*, 2011). WWF (2012) assessed that TDF potentially covered an area of 31.5 million hectares from the northern Mexican Pacific Ocean to Central America. The Global Land Cover 2000 calculated for Mesoamerica an extent of 18.9 million hectares (Taken from Dirzo *et al.,* 2011), while Miles *et al.,* (2006) estimated for the same year 13.4 million hectares. In particular, in Mexico TDF shows a remnant of 25-36% (Rzedowski, 1998; Portillo-Quintero and Sánchez-Azofeifa, 2010; Dirzo *et al.*, 2011; CONAFOR, 2012) of the original 33.5 million ha (INEGI, 2003a), of the primary forest driving changes in the structure and species composition. These changes have driven the growth of secondary forest (Rzedowski, 1998; Dirzo *et al.*, 2011). For example, this vegetation in Mexico is now recognized to be of great conservation importance due to high deforestation rates (Trejo and Dirzo, 2000; Maass *et al.*, 2005; Dirzo *et al.*, 2011). It is mainly transformed into grassland for cattle raising, and agriculture, mainly for self-consumption, in a less significant proportion, to irrigated agriculture (Maass, 1995; Noble and Dirzo, 1997; Janzen, 1998; Trejo and Dirzo, 2000; Corona, 2012). Others have reported transformation for wood fuel (Flint and Richards, 1994; Iverson *et al.*, 1994; Houghton, 1999; Houghton and Hackler, 1999; Achard *et al.*, 2002; Serrano-Medrano *et al.*, 2014). In some cases this can exceed biomass lost by deforestation (Gaston *et al.*, 1998). This loss explains why this vegetation type is considered as one of the most endangered (Janzen, 1986; Janzen, 1998; Dirzo *et al.*, 2011).

LUCC is considered the main driving force leading to environmental degradation, land fragmentation, loss of global biodiversity (Lambin *et al.*, 2001) and carbon losses at local scales (Corona, 2012). However, local drivers such as demographic and biophysical factors play a major role in explaining spatial patterns of LUCC across the landscape (Bürgi *et al.*, 2004; Pan *et al.*, 2004). Lambin *et al*., (2003) suggest that the driving forces for LUCC can be divided into proximate and underlying causes. Proximate causes act directly on the vegetation cover and underlying causes work at a broader scale and modify one or more proximate causes. Whereas some studies explain these dynamics through biophysical variables (Hietel *et al.*, 2005), others have focused on social, political and economic factors (Lambin *et al.*, 2001; Bürgi *et al.*, 2004). Analysis of local deforestation should ideally focus on the forest ecosystem and its uses, the landscape dynamics and the local demographic, cultural, social, economical and political characteristics that drive deforestation (McConnell *et al.*, 2004). Therefore, the systems have to be evaluated under a socio-ecological perspective (Lambin and Meyfroidt, 2010). To understand forest carbon losses due to deforestation and forest degradation, models should look into these drivers as important sources of

information to explain current AGB estimates and their potential to produce more reliable local AGB estimates.

I.6 Carbon losses

To estimate current carbon stock and the rate of loss, contrasting approaches have been taken into consideration. Some authors have estimated the loss of biomass by considering a mean deforestation rate and a mean of biomass (Achard *et al.*, 2002; DeFries *et al.*, 2002; Achard *et al.*, 2004; Houghton, 2005a) which resulted in divergent estimations. This is because AGB is distributed heterogeneously across the landscape (Slik *et al.*, 2010; Slik *et al.*, 2013; Ometto *et al.*, 2015), and deforestation rates change over temporal and spatial scales (Ewers *et al.*, 2008; Corona, 2012; Ometto *et al.*, 2015). The result is an under/over-estimation of carbon emissions, limiting its utility for environmental management or policy making. Some others have estimated AGB over different time steps (Harris *et al.*, 2012; Ryan *et al.*, 2012; Collins and Mitchard, 2015). By comparing at least 2 of those dates it is possible to estimate carbon emissions over a known time step. However, these emissions are not able to estimate the total AGB that has been lost and they can mislead understanding of where the major AGB losses occurred, mainly as a result of the saturation point of modeled AGB. Moreover, ground data, remote sensing, deforestation and forest degradation tend to have distinct spatial and temporal scales. These mismatches affect the estimation of the total area that has been deforested (Foody, 2002) based on the changes in spectral reflectance (Bolovo *et al.*, 2010), but also on the carbon emissions that can be related to such changes. These differences can lead to higher AGB estimate uncertainties than the measured AGB losses. Nevertheless, these methodologies are useful for implementing conservation strategies to reduce the impacts of deforestation on carbon stocks.

More recently, other authors have simulated carbon stocks over large temporal and spatial scales, mainly at global or continental scales (Saatchi *et al.*, 2011b; Arora *et al.*, 2013; Anav *et al.*, 2015; Walker *et al.*, 2015; Wieder *et al.*, 2015) with few examples at sub-continental scales (Saatchi *et al.*, 2007; Exbrayat and Williams, 2015). These studies help in the understanding of global dynamics on nutrient fertilization and cycling, the impact interaction across the carbon-climate system and carbon stock distributions. However, they fail in capturing the spatial heterogeneity of the carbon stocks on a regional scale, hiding ecological processes and homogenizing ecosystems dynamics that are constrained on finer scales. Moreover, these regional approaches tend to have poorly specified timing. As a consequence, it is difficult to estimate the carbon emissions (Saatchi *et al.*, 2007) and to use such information for any policy making or emissions control.

Particularly to this thesis the next definitions were used (FAO, 2000) the next definitions were used: *Carbon pool* will be understood as a reservoir or system that can accumulate or release carbon. *Carbon stock* is the absolute quantity of carbon, expressed in mass units, held within a pool at a specified time. *Carbon flux* is the transfer of carbon from one carbon pool to another in units of measurement of mass per unit area and time. *Carbon sink* is the which removes a greenhouse gas from the atmosphere. *Sequestration or uptake* is the process of increasing the carbon content of a carbon pool other than the atmosphere.

I.7 Ground-based forest inventory data

Forest inventory approach is of primary concern in biomass and carbon stock quantification. Chave *et al.,* (2004) indicate that if there is not a full representation of the forest type, the site variability will not be correctly evaluated, and the biome average could be misunderstood. Size and number of sample plots become fundamental issues to be considered during the inventory.

Chave *et al.,* (2004) quantify the error due to tree measurement. The first error comes from tree measurements. During this procedure DBH, height and wood density are defined for each tree. The common measurement errors are double counting, missing trees, or mistakes during sampling reading. The second error is due to the uncertainty in the plot sampling. Because it is argued that biomass is not normally distributed in small sampling plots - on the basis that rare large trees contribute to most of the biomass in the landscape. The general approach that has been undertaken is of having a large number of sample plots and area in order to best evaluate landscape variability in tropical ecosystems. It is expected that bigger plots could reduce the bias of under- or over-representing rare large-sized trees which are not distributed in a normal pattern, and bigger plots could reduce this bias (Keller *et al.*, 2001; Chave *et al.*, 2004; Chave *et al.*, 2005). For example, Chave *et al.,* (2004) reported a coefficient of variation of 32% in 10x10 m plots, reducing this value to 10% and 6% in plots of 50 x 50 m and 100 x 100 m, respectively, to nearly 5% in plots of 150 x 150 m, and showing no significant reduction in bigger plots. For these reasons, if a biomass average is to be estimated across the landscape or the region, it is recommended that the size and number of plots be increased to at least 0.25 to 1 ha, in concordance with Chave *et al.,* (2004). Moreover, Chave *et al.,* (2004) reported for tropical forest with a mean annual precipitation of >2,500 mm a minimum plot size >2,500 m^2. However, this tropical forest refers to tropical rainforest (Turner, 2001), and it is unknown into what extend this generic rule may apply to other tropical ecosystems. Nevertheless, this approach is complementary to others to spatialize the biomass by remote sensing and modelling (see section I.9). The idea is to aggregate under the same value all the heterogeneity, while the second approach is looking into biomass distribution across the landscape. This is because the spatial scales of biomass variability are not entirely understood, for example human disturbances, natural regeneration or climatic interactions to drive biomass allocation as well as when the aim is to measure biomass from space (Houghton, 2005a). Therefore, the scale of sampling collection would be chosen according to what it is we want to understand.

Different tropical ecosystems' biomass estimations have adopted a mixture of sampling strategies, and there is not a general methodology for making such *a priori* selection design. The sampling design is based on site characteristics, expert knowledge and/or expertise. The ideal sampling size for TDF is not clear, but this can be the result of complex topography. Thus, it is important to identify the best sampling approach for reducing the uncertainty in aboveground biomass (AGB) estimates. In Table I.3 it can be seen that the sampling strategies in other tropical ecosystems differ to those implemented in the TDF. On the one hand, savanna ecosystems with little tree densities, or tropical rain forest with large densities of

medium to large-sized trees have focused on nested sampling strategies with large-sized plots. This strategy was adopted to record the largest amount of AGB which tends to be allocated in large-sized trees. On the other hand, the strategies implemented in the TDF are particular. Some have adopted the measurement of all trees within a small area, while a few others have done the sampling collection over large-sized plots but limiting the AGB estimations to a minimum DBH. In none of the reports was it possible to calculate the sampling density base on their study site. For example, in the TDF most of the sampling approaches have been by small plots ≤100 m^2 (Hubbell, 1979; Jha and Singh, 1990; Castellanos *et al.*, 1991; Martínez-Yrízar *et al.*, 1992; Cairns *et al.*, 2003; Jaramillo *et al.*, 2003; Gallardo-Cruz *et al.*, 2005; García *et al.*, 2005), 100-400 m^2 (Sagar and Singh, 2006; Bijalwan *et al.*, 2010; Burquez and Martínez-Yrizar, 2010) and 500 m^2 (Eaton, 2005; Sagar and Singh, 2006; Bijalwan *et al.*, 2010; Burquez and Martínez-Yrizar, 2010; Návar, 2010) with several repetitions. Very few examples exist of plots with sizes near 10,000 m^2 or bigger (Jaramillo *et al.*, 2003; Gasparri *et al.*, 2010) (Table 1.3). Moreover, and particularly to Mexico, the Mexican National Forest Inventory (NFI) is a national inventory database that provides information of forest resources (degradation processes, biomass stocks, biodiversity, etc). The field plot of this inventory varies accordingly to the vegetation type and they are allocated systematically all over the country. The TDF's NFI is based on rectangular plots of 10x40 m, where all trees ≥7.5 cm in DBH were recorded (DBH and height). For recording trees under 7.5 cm in DBH, the NFI subsampled each of the plots in subplots of 12.56m^2. In each of the subplots number of trees and height was recorded (CONAFOR, 2007). In any case, it is not clear if the sampling strategy implemented in the TDF that was adopted as a standardized sampling approach, was the ideal sampling size because of the inner homogeneity in tree size density, or because of the difficulty of sampling this kind of forest in the field.

Table I.1 Sampling collection in tropical sites for biomass estimation.

	Parcel size (m^2), DBH measurement (cm) and number of samples				
Site	**0-500**	**500-5,000**	**5,000-10,000**	**>10,000**	**Reference**
Mozambique	314 m^2; 5-10 cm DBH; N=90		5,700 m^2; >30 cm DBH; N=30		Woolen *et al.,* (2012)
Mozambique		2,500 m^2 and 5,000 m^2; >5 cm DBH; N=30 and 5	10,000 m^2; >5 cm DBH; N=15		Ryan *et al.,* (2011)
Panama		1,600 m^2 and 3,200 m^2; >1 cm and 10 cm DBH; N=35 and 9	10,000 m^2; >10 cm DBH; N=45		Chave *et al.,* (2004)
India, TDF	100 m^2; >1 cm DBH; N=420				Jha and Singh (1990)
India, TDF	100 m^2; >9.6 cm DBH; N=100				Sagar and Singh (2006)
India, TDF	400 m^2; DBH and N not reported				Bijalwan *et al.,* (2010)

Argentina, TDF		8,000 m^2; >10 cm DBH; N=15	Gasparri *et al.*, (2010)
Costa Rica, TDF	400 m^2; >2 cm DBH; N=336		Hubbell (1979)
Mexico, TDF	100 m^2; >3.2 cm DBH; N=4		Castellanos *et al.*, (1991)
Mexico, TDF	25 m^2; >3 cm DBH; N=40		Martínez-Yrizar *et al.*, (1992)
Mexico, TDF	100 m^2; >3 cm DBH; N=16	12,000 m^2; DBH not reported; N=1	Jaramillo *et al.*, (2003)
Mexico, TDF	100 m^2; >10 cm DBH and <10 cm N=50 and 15		Cairns *et al.*, (2003)
Mexico, TDF	100 m^2; >1 cm DBH; N=30		Gallardo, *et al.*, (2005)
Mexico, TDF	100 m^2; >1 cm DBH; N=34		García *et al.*, (2005)
Mexico, TDF	400 m^2; >7.5 cm DBH; N=40		Navar *et al.*, (2010)
Mexico, TDF	500 m^2; >1cm DBH: N=36		Eaton and Lawrence, (2009)
Mexico, TDF	25 m^2; >1cm DBH: N=34		Rodriguez *et al.*, (2010)
Mexico, shrubland	25 m^2; >1 cm DBH; N=20		Burquez and Martínez-Yrizar, (2010)
Mexico, TDF	400 m^2; ≥7.5 cm DBH		National Forest Inventory (CONAFOR, 2007)

I.8 Allometric equations

After a ground-based forest inventory, a critical step for biomass estimation is the use of allometric equations (Chave *et al.*, 2004). Some equations can be developed from destructive harvesting during the field survey where DBH and height of each tree are measured to relate them to its total biomass. From this relation, allometric equations can be developed and further applied to other trees for biomass estimation. According to Brown (2002) 95% of the variation in above-ground tropical forest carbon stocks can be explained by the DBH alone, even in diverse regions. In recent years, different authors have noticed the necessity to develop general allometric equations for tropical ecosystems (Brown *et al.*, 1989; Brown, 1997; Chave *et al.*, 2004). However, because of the high diversity of species, to develop a species-specific equation is very impractical. Moreover, on most occasions there are not site or region specific equations. As a result, it is necessary to use equations developed from other sites, which can lead to an under- or over- biomass estimation. For example, it has been reported that high estimates are based on direct and destructive sampling, while lower estimates are based on volumetric equations which are

transformed to biomass (Brown and Lugo, 1984; Palm *et al.*, 1986; Hall and Uhlig, 1991). During the last years diverse allometric equation reports have been done about tropical forest under contrasting precipitation conditions for biomass estimation (Table I.4).

The general approach for tropical forests biomass estimation across the landscape is to estimate the aboveground biomass of each tree in a stand by applying to its measured diameter the most proper available biomass allometric relation, and then to sum the tree estimates (Brown, 1997; Chave *et al.*, 2004). From this can be derived an average biomass *per* site, which later could be transformed by other means into a spatial representation.

Table I.2 Allometric equations in diverse tropical sites for biomass estimation

Equation	Ecosystem	R2	Source
$Kg= 0.0841* (D^{2.41})$	TDF, Sinaloa, Mex	0.79	Návar (2009)
$kg=10^{((-0.5352)+\log_{10}(BA))}$	TDF, Jalisco, Mex, <900 mm	0.94	Martínez-Yrizar *et al.,* (1992)
$kg=p*exp(-0.667 + (1.784*ln(D)) + ((0.207*ln(D))^2)-((0.0281 * ln(D))^3))$	Dry forest, tropics	--	Chave *et al.,* (2005)
$kg=0.112*((pD^2H)^{0.916})$	Dry forest, tropics	--	Chave *et al.,* (2005)
$kg=p*exp(-0.667 + (1.784*ln(D)) + ((0.207*ln(D))^2)-((0.0281*ln(D))^3))$	Dry forest, tropics	--	Chave *et al.,* (2005)
$Kg=0.0673 \times (pD^2H)^{0.976}$	Pantropics	--	Chave *et al.,* (2014)
$kg=34.4703 - (8.0671*D) + (0.6589*D^2)$	Dry forest, tropics	0.67	Brown *et al.,* (1989)
$kg= exp ((-2.4090 + (0.9522*ln (D^2 *H*p))$	Dry forest, tropics	0.99	Brown *et al.,* (1989)
kg=exp(-1.996 + 2.32*ln(D))	Dry forest, tropics, 900-1,500 mm	0.89	Brown, (1997)
kg= exp (-2.134 + 2.530*ln(D))	Moist forest, tropics, 1,500-4,000 mm	0.97	Brown, (1997)
$Kg= (21.297 - (6.953*D) + (0.74*D^2)$	Wet forest, tropics, >4,000 mm	0.92	Brown, (1997)

p= wood density
D= DBH
H=height
BA=Basal area

I.9 Biomass spatialization

Natural forest is spatially heterogeneous due to particular environmental and topographic conditions, and human disturbance (Houghton *et al.*, 2001; Houghton, 2005a; Ryan *et al.*, 2012; Woollen *et al.*, 2012). For that reason, it is hard to measure all the sites and components to make a proper estimation of carbon or biomass density *per* unit area, (see section I.6). As a result, other approaches have been taken into consideration for spatializing the field sampling across the landscape. Moreover, the higher spatial resolution facilitates coordination of ground data collection with diverse information sources, thus assuring homogeneity of vegetation conditions within pixels. For example, some researchers have used remote sensing data to map surface area characteristics, including spectral mixture analysis (Lu *et al.*, 2005); regression tree modelling (Michaelsen *et al.*, 1994; Baccini *et al.*, 2012a; Cartus *et al.*, 2014); decision tree classification (Dougherty *et al.*, 2004); subpixel classification (Civco *et al.*, 2002); neural network classification (Civco and Hurd, 1997); maximum entropy algorithms (Saatchi

et al., 2011a; Rodriguez-Veiga, 2016; Rodriguez-Veiga *et al.*, In Press) and regressions (Bauer *et al.*, 2005). Besides that, remote sensing coupled with modelling has been used as a proxy to estimate biomass. Remote sensing techniques show pros and cons, being the most common problem the signal saturation, mainly as a result of dense canopy closure in perennial forest (Gibbs *et al.*, 2007) and less common in deciduous forest (Gasparri *et al.*, 2010). While these approaches are useful to reconstruct current biomass estimates, there is still a lack of understanding of how these techniques may be used to reconstruct the potential biomass under non-human disturbance ecosystems.

In recent years different authors (Baccini, 2008; Goetz *et al.*, 2009; Mitchard *et al.*, 2011; Baccini *et al.*, 2012b; Mitchard *et al.*, 2013; Avitabile *et al.*, 2016) have worked on developing tools for understanding, validating and/or measuring current AGB estimates over pan-tropical regions. Some other authors (Cartus *et al.*, 2014) have worked at a national scale to access field plot density information (eg. National Forest Inventory), or because it is recognized that areas such as Mexico with high diversity in ecosystems and complex topography present a real challenge for AGB estimation (Rodriguez-Veiga, 2016). Despite the validation of previous AGB maps produced for Mexico, currently there is still high uncertainty across these predictions. It is unknown to what extent those validations apply at global or national scales, and how they can be used for better decision making at regional scales (Saatchi *et al.*, 2007). According to Mitchard *et al.,* (2013) Baccini´s and Saatchi´s maps produce similar total AGB estimates at a national scale, but sub-regional scales suggests that AGB allocation is significantly different. However, understanding why or to what extent diverse AGB maps differ at the landscape scale is missing. Recent studies have undertaken different approaches to improve the accuracy of AGB maps. Avitabile *et al.,* (2016) used different sources to improve Baccini's and Saatchi's maps. Cartus *et al.,* (2014) and Rodriguez-Veiga (2016) and Rodriguez-Veiga *et al.,* (2016) focused on just one country with many more field observations than any other map. However, there is still a lack of consensus in the results of such maps. Besides Rodriguez-Veiga (2016) and Rodriguez-Veiga *et al.,* (2016) there is also no independent validation of these maps at the scale of their applicability. Therefore, the total carbon forest emissions due to anthropogenic actions by deforestation and forest degradation processes is unknown.

Moreover, distinctive approaches have been considered to reconstruct natural biomass. Dynamic Global Vegetation Modelling (Cramer *et al.*, 2001) and Ecosystem Demographic Modelling (Moorcroft *et al.*, 2001). These models simulate the successions until steady state, based on vegetation structure and the magnitude and spatial pattern of the carbon sink. Another approach, as it is proposed in this thesis is to understand the main drivers of biomass allocation in mature forest. Mature forest biomass is assumed as the potential biomass that a landscape could reach with no human disturbance due to a multi-scale interaction of factors that have directly or indirectly driven its allocation.

I.10 Justification and aims

Climate change will have impacts on the permanence of forest and therefore on forest carbon stocks (Meir and Pennington, 2011). The change will result from alterations to the frequency, intensity, duration, and timing of fire (Flannigan *et al.*, 2000), droughts (Cox *et al.*, 2008; Lewis *et al.*, 2011), hurricanes and windstorms (Dale *et al.*, 2001). Because temperature is a key environmental factor that regulates biological processes (Dougherty *et al.*, 2004; Davidson and Janssens, 2006; Piao *et al.*, 2010), climate change will also lead to alterations in forest structure, with the expansion of species with higher adaptative capacity. It is expected that climate change may influence inter-annual variations of temperature and precipitation in dry forests (Diffenbaugh *et al.*, 2008). For instance, TDF can increase its distribution range and may displace tropical wet forest according to the future dry and warmer environmental conditions. Moreover, arid ecosystems can shift towards a desert condition by decreasing rainfall (Solé, 2007). As a result, it is important to understand current carbon stocks, as well as potential carbon stocks that are expected under a non-human disturbance scenario. While much attention has been focused on tropical moist forests, little attention has been paid to TDF. According to Skutsch *et al.*, (2009) TDF carbon emissions are also important, because more carbon losses may occur even though their carbon content is considerably lower *per* hectare than other tropical forests. This forest has a little commercial value, which promotes traditional techniques of production in local populations, similar to observations done for Mexico (Burgos and Maass, 2004; Castillo *et al.*, 2005; Dirzo *et al.*, 2011; Corona, 2012). However, how much carbon has been lost due to anthropogenic activities have not been quantified because of a lack of understanding of potential carbon stocks. Consequently, it is important to analyze the TDF as a socio-ecological system and to understand the different impacts (topographic, climatic and socio-economic) that can promote change in the TDF carbon stocks distribution.

In accordance with this point, the general aim of this thesis is to estimate the net carbon losses and its spatial variability in a Tropical Deciduous Forest in Mexico. To address this aim, not only is it important to take into consideration the mature forest structure, spatial patterns and processes in a multi-scale analysis; also, it is necessary to characterize the spatial bio-physical drivers that influence mature AGB and the socio-economical drivers to understand the current AGB patterns and losses. With the understanding of such elements, it is possible (1) to reconstruct the potential carbon stocks and (2) to estimate the allocation of net carbon losses due to deforestation and (3) to understand the impact of forest degradation. Thus the critical questions of this thesis are:

- What are the main factors that control the AGB distribution in a natural landscape?
- Which are the main responsible factors for understanding AGB allocation in the landscape and its associated bias?
- How much AGB has been lost in a tropical deciduous forest and what are the main drivers of such losses?

Chapter II. Data and Methods

II.1 General thesis outlines diagram

The general methods are comprised in 3 general steps (Figure II.1; the different steps are identified by different colouring lines). In chapter III field data collection, biophysical variables and selection of mature forest observations were done. In the same chapter III field observations of mature forest were contrasted against different predictor variables to understand the relationship to AGB. This general process can be seen within the dashed green line. Within the blue solid line are highlighted the different elements used for Chapter IV. This chapter tested different statistical models to reproduce the potential AGB that could be expected under a no disturbance scenario. Finally, within the red solid line the process of chapter V is highlighted. In this chapter, driver forces of carbon emissions were identified.

In a particular manner, the different steps were disaggregated in sources of information, results and interactions between any of the previous. The first step was the sampling collection (green box). This sampling strategy was the base of all the next stages of this research. From it a probability map of deciduousness was built as a predictor variable including topographic and climatic variables (violet box) to understand the drivers of mature AGB allocation (Chapter III). Through a multi- variable and model analysis the potential AGB was reconstructed (orange box) (Chapter IV). By contrasting different current AGB estimates (grey box) and the potential AGB developed in chapter IV it was possible to estimate the net carbon losses (yellow box) (Chapter V). In the same Chapter V patterns and processes of carbon losses were evaluated with regression trees (blue box). From it, it is possible to identify promissory places for carbon sequestration through forest restoration.

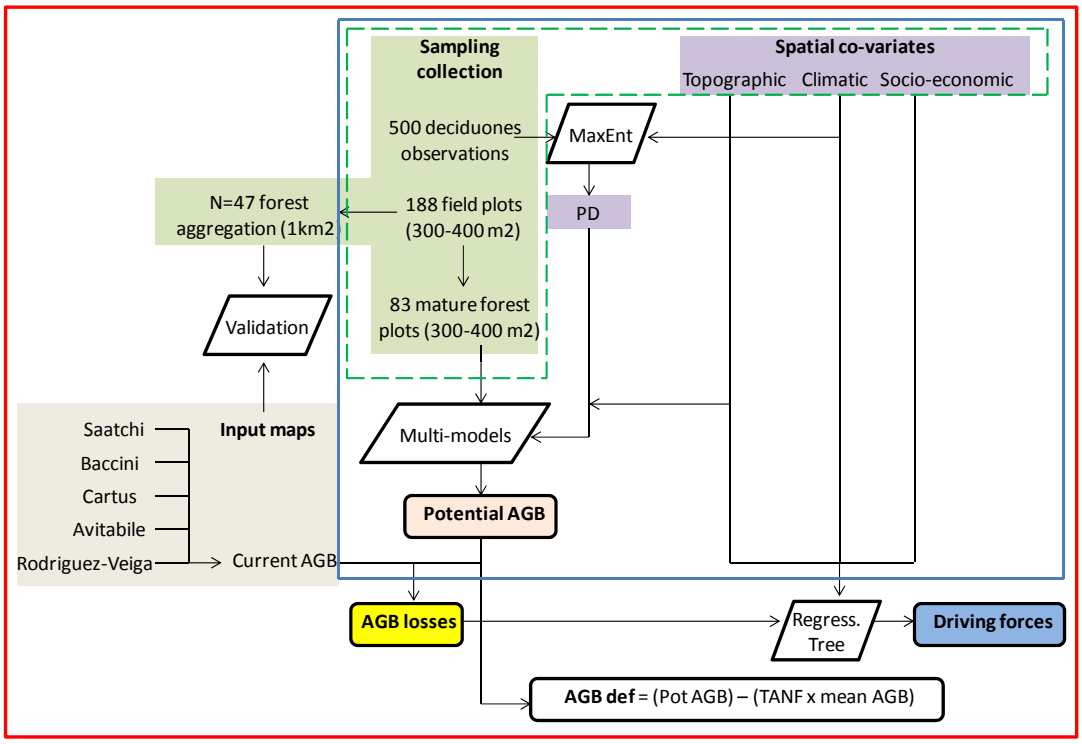

Figure II.1 The diagram flow chart shows the different steps followed during this thesis.

II.2 Study site

The study site comprises five municipalities with an area of ~21,570 km^2. This region is known as the Southern Coast of Oaxaca (CIEDD, 2012). The extreme coordinates are 15.63' N and 15.96° N and -96.03° W and -95.97° W (Figure II.2).

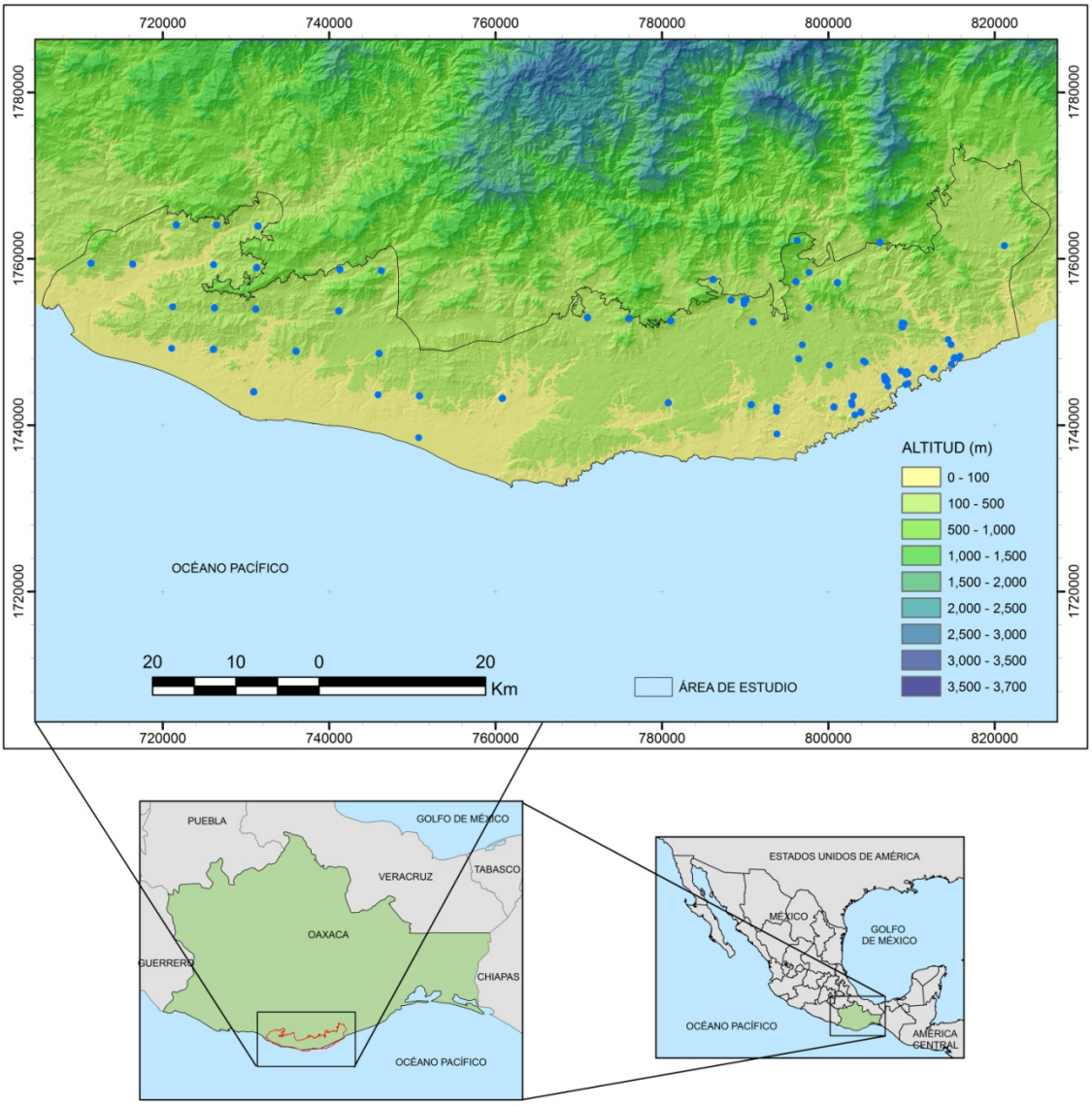

Figure II.2 The figure shows the sampling location of 83 plots of mature forest over an altitude grid map. The *bottom left-hand panel* highlights in red the study site in the State of Oaxaca and the *bottom right-hand panel* shows the location of the State of Oaxaca.

It's regional topofeatures (geoforms) are characterized by knolls with plains, and some small mountain ranges. Geomorphologically this region can be grouped in folding low hills near the coast followed by block hills with low dissection and pre-mountainous with low dissection (Corona, 2009; INEGI, 2009). According to the INEGI (2009), this region is dominated (~90%) by intrusive igneous and metamorphic rocks like Gneis. The most widely distributed soil type is the regosol with a lithic phase and sandy texture, followed by cambisol and lithosol (Corona, 2009; INEGI, 2009) with less representation of alluvial soils and littorals.

Corona (2009) reported different pedogeomorphologic profiles. The profiles included processes of soil formation, geomorphology, geology, slope, aspect, geomorphology, potential vegetation and degradation,

and analyses forest and soil dynamics over an altitudinal gradient (Annex 1 & 2). On the hilltops were found the most stable landscapes. However, from microtopography derives micro-watersheds, which promotes sites with high soil fertility and water availability. Convex terrain curvatures are more exposed to erosion processes promoting higher water deficiencies. Karstic montain slopes show contrasting differences in water reservoir and soil formation. On this units, slash burn agriculture is mainly located. On the one hand, the karstic units are characterized for sites with underground water reservoirs. On the other hand, the mountain slopes promotes water runoff. Consequently, microtopography drives important differences in soil and water accumulation. Alluvial deposits are rich in nutrients and water availability, similar processes observed at lower altitudes with the alluvial deposit plain. These has promoted colonization of agricultural activities, mainly for irrigation.

Total precipitation **Mean annual temperature**

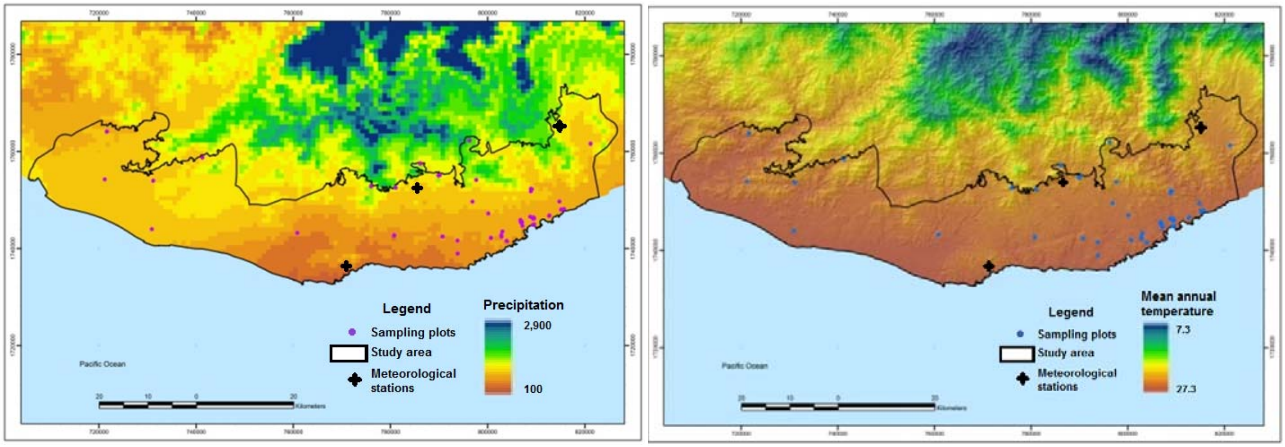

Figure II.3 Total precipitation (mm) and mean annual temperature (°C) comes from a WorldClim data set (Hijmans *et al.*, 2005). In all figures the study site boundary was drawn and sampling plots allocations were highlighted with dots. Colors selection for boundaries and dots were based on background colors. In all cases, an extended area of the boundaries can be noticed. The meterorological stations are in order from left to right Puerto Angel, Huatulco and Xadani.

The climate is considered Aw(w) (Köppen, modified by García (2004)) ranging from the dry (w_o), in most of the region, to the humid (w_2) in higher altitudes (>1,000 m asl) (Figure II.3) 'warm sub-humid with summer rains with inter-winter droughts and two annual dry seasons'. The main dry season lasts about seven months with a mean annual precipitation of <1,600 mm falling >75% during June to September. The warmest months are between May and August, and the less warm are between December and February. The average annual temperature is 19-33°C with a mean annual evaporation about 1,700 mm with maximum values >170 mm during March to May (Hijmans *et al.*, 2005; SMN, 2014) (Figure II.3).

- Puerto Angel: The $Aw_o(w)$ class ranges between 0-500 m asl. The average temperature of 27.6°C with a maximum average of 32.7°C, with the coldest average of 26.7°C. The precipitation is 797 mm. Between February and April the monthly rain average is 0.95 mm, while from June to September it is 185 mm (INEGI, 2004, Figure II.3 and II.4a).
- Huatulco: The $Aw_1(w)$ is concentrated in between 0-1,000 m asl. The average temperature of 26.8°C with a maximum average of 34.3°C, with the coldest average of 19.2°C. The precipitation is 1,351

mm. In December and January the monthly rain average is 1.7 mm, while from June to September there is the highest (290 mm) (INEGI, 2004, Figure II.3 and II.4b).

- Xadani: The $Aw_w(w)$ is observed in >1,000 m asl. The average temperature of 25.8°C with a maximum average of 33.8°C, with the coldest average of 17.7°C. The precipitation is 1,356 mm. From December to March the monthly rain average is 4.2 mm, while from June to September it is the highest (568 mm). In contrast to the other two types of climate, this does not present two dry seasons (INEGI, 2004) (Figure II.3 and II.4c).

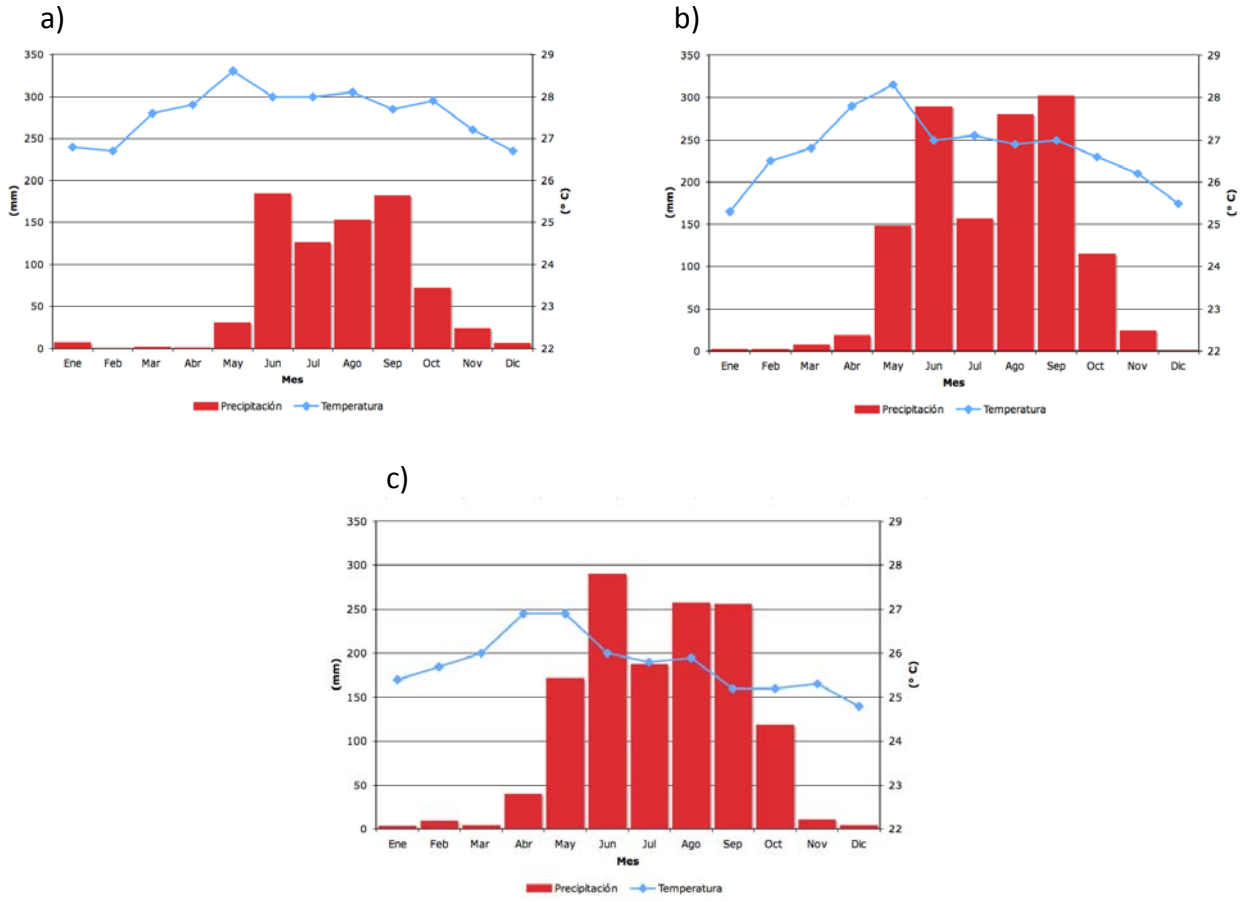

Figure II.4 Monthly average temperature and precipitation.
a. Meteorological station 20-092 'Puerto Angel' 15°52'N, 96°27'W, 485 m asl.
b. Meteorological station 20-333 'Huatulco' 15°49'N, 96°19'W, 225 m asl.
c. Meteorological station 20-256 'Xadani' 15°58'N, 96°04'W, 361 m asl.
Source, SMN (2014)

In this region the characteristic vegetation is the Tropical Deciduous Forest (TDF) (Corona, 2012). More than 80% of the land cover has natural vegetation with different conservation degrees (Corona, 2009; Lira and Ceballos, 2010; Corona, 2012; Mendoza, 2015; Corona *et al.*, 2016). The TDF shows different phonological characteristics (Figure II.5). Along the TDF, in the region are other vegetation types. Semiperennial tropical forest occurs in medium-height areas, and at the floodplains of intermittent and perennial streams, with riparian vegetation along the margins. Mangroves and aquatic vegetation occur at the mouth of the river basins (Copalita, Huatulco, Coyula, Sal, Aguacate and Tonameca) and lagoons (La

Salina, Chacahua and Palmar). Temperate forest can be observed in the northern part of the study site at higher altitudes (>2,000 m asl) (Corona, 2009), but isolated examples of *Quercus spp* can be seen at >600 m asl. Locally the flora has been classified into more than 91 families, 391 genera, and 736 species. The dominant families in terms of the number of species are *Leguminosae* (146), *Euphorbiaceae* (48), *Asteraceae* (42), and *Convolvulaceae* (37) (Salas-Morales *et al.*, 2007).






Figure II.5 Tropical deciduous forest with different phenological aspects. All the photos were taken during the dry season of 2012 within a one-week interval and are organized by leaf senescence.

This forest has little commercial value, which promotes traditional techniques of production in local populations (Corona, 2012). The agriculture is dominated by subsistence production maize and beans. The average field size of farmed land ranges from 0.5 to 2 hectare. Agriculture production starts by cutting down branches and trees, prior to the rainy season, then setting fire (Corona, 2012). Wood extraction for fuel wood production is by selective logging, and branches and lianas are also removed. PSIG (2015) reported that this region is mainly dominate by a natural cover (169,617 ha) with a forest loss of 2.3% between 2006-2011. In 1998 an area of 6,375 ha was declared as a Natural Protected Area (NPA) for biodiversity of TDF conservation.

The land-use and land-cover changes have been driven by slash and burn agriculture and pastureland for raising cattle (Figure II.6). The agriculture involves production of maize and beans for self-consumption (Corona *et al.*, 2016). The average parcel size ranges from 0.5 to 2 hectares. The agriculture production starts with the cutting down of branches and trees, previous to the rain season, then setting fire to them. This technique is known as slash-burn agriculture and for centuries has been practiced among these communities. The annual yield is in between 600 to 1,000 kg per hectare of maize. However, the production cannot be maintained for more than three years. As a result, those parcels need to be left fallow and new forested areas opened. This cycle is maintained for ten to fifteen years, and sometimes twenty years, before production comes back to the first parcel (Corona, 2012). The pastureland is induced by frequent burning, and is used mainly to raise cattle, though some use goats. The stratum is not higher than 5-10 cm and the main genera used are: *Bouteloua*; *Cathestecum*; *Hilaria*; *Trachypogon*; and *Aristida.* However, the family *Fabaceae* is also used (INEGI, 2004). Commercial forestry is absent in the TDF, but extraction of selected timber species happens on a small scale mainly for local consumption for construction.

Pastureland during rainy season

Pastureland with cattle during rainy season

Slash

Burn

Slash and burn agriculture

Maize production

Figure II.6 Anthropogenic land-use and land-covers distributed in a matrix of TDF

II.3 Data collection and biomass estimation

To capture the spatial heterogeneity of AGB allocation forest over the landscape, it is necessary to have a good representation of the landscape heterogeneity. However, mature forest is mainly restricted to isolated places with limited accessibility, and/or in protected areas. These make it very difficult to acquire field information over large areas. In consequence, our field campaigns were designed to record

the landscape variability by sampling not only the most common biophysical regions, but also the rare elements of the landscape.

Our field campaigns (N=60) were complimented with the National Forest Inventory (NFI) (CONAFOR, 2007; CONAFOR, 2012). which systematically allocated the sampling plots (N=128). The field campaigns were carried out during summer 2012 and spring 2013, and for the NFI in the year 2007. Field data collection is of 188 field plots in total. 60% of the data was collected by the NFI and the rest was collected by this study.

The NFI plots measure 10 x 40 m, where all trees ≥7.5 cm in DBH were recorded (DBH and height). For recording trees under 7.5 cm in DBH, the NFI subsampled each of the plots in subplots of 12.56m^2 in a sub-plot of 3.54x3.54 m. All trees within a DBH of 1.0-7.5 cm and over 0.25 m in height were sampled, recorded in height classes and classified into species (CONAFOR, 2007). Particularly to this thesis, from all the sampled trees, a linear regression was constructed to estimate DBH for trees <7.5 cm in DBH based on their height, and the number of plants in the sub-plot was extrapolated to the forest plot (Figure II.7).

Our sampling design consisted of plots of 10x30 m, where all the plants ≥1 cm in DBH and ≥1.3 m in height were measured (Figure II.7). Complementing these samples, 2 plots of 4 hectares each were collected. These plots were allocated in two different altitudes (50 and 250 m asl) within a distance of ~7 km. In each of those large plots, all trees ≥30 cm in DBH were sampled and geotagged (N=365) and DBH and height were recorded.

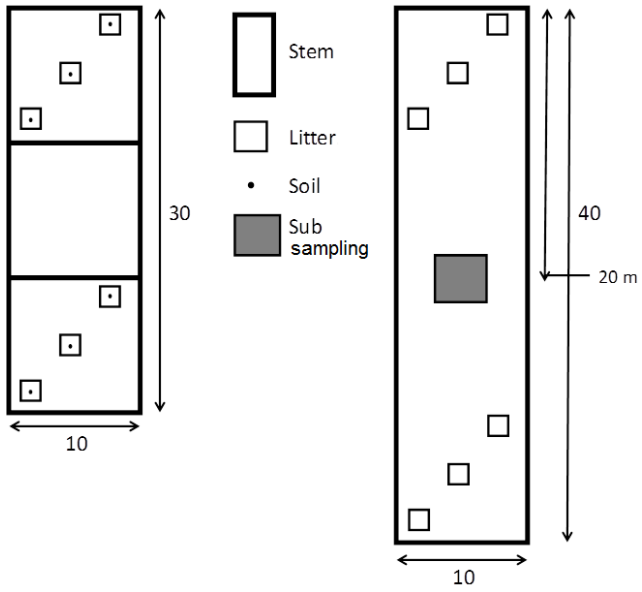

Figure II.7 Diagram of the general sampling strategy for stems, litter and soils at two spatial scales. The left-hand panel refers to our sampling strategy, while the right-hand panel refers to the National Forest Inventory approach with our modifications for litter collection. In our sampling collection, all trees with a DBH≥1 cm were measured, while in the NFI plots all trees ≥7.5 cm in DBH were recorded. Complementary to the NFI a sub-plot of 3.54x3.54 cm (grey square) was established in the middle of the plot where all trees between 1-7.5 cm in DBH and over 0.25 m height were sampled. For any case, coarse scale refers to the mean estimates in Mg ha^{-1} for AGB and MgC ha^{-1} for litter and soil samples, when applicable. *Fine-scale* refers to

litter (small and white squares) and soils collection (small black dots) by triplicate in extreme side plots.

The allometric variables consisted of DBH, height and wood density. For every tree, the DBH was measured using diametric tapes while height was estimated with a laser rangefinder Bushnell Sport 850 with an error of ±0.9 m (Bushnell, 2016). While it is recommended to use species-specific wood density (WD) for improvement for AGB estimation models (Chave *et al.*, 2005), this process is not always possible. In the Mexican TDF this approach was not practical because of the remarkably high biodiversity. This forest in Mexico has a very high *alpha* and *beta* diversity, as well as an elevated number of endemism and rare species (Trejo and Dirzo, 2002; Castillo-Campos *et al.*, 2008; Dirzo *et al.*, 2011) with more than 700 spp in this region. We used a stand-level WD average as suggested by Baker *et al*., (2004). WD was constructed based on a collection of 28 plots during the dry season 2013 (N=121 trees). The wood cores measured 0.515 cm in diameter with variable length. For dry weight estimation, all samples were dried in the oven to a constant weight at 70°C and weighed on a digital scale with an error of ±1mg. For carbon content, we collected six mixed samples from different stems and plots. The samples were analyzed in a Shimadzu TOC analyzer by combustion method.

AGB estimations and uncertainty were calculated by using 7 different allometric equations (Table II.1), 2 equations built for Mexico (Martínez-Yrízar *et al*., 1992; Návar, 2009), 2 for the Pantropic (Chave *et al*., 2005) and 3 for the world (Brown, 1997; Brown *et al*., 1989). This study has not included the recent equation reported by Chave *et al.,* (2014) because it shows similar performance to those published in 2005 (Chave *et al.*, 2014). The equation that produced the highest and the lowest estimates was excluded from further analysis. Five of the seven equations were selected to calculate a mean value for AGB and the seven equations as a measure of uncertainty in our estimates. The allometric equation built by Brown *et al.,* (1989) is not recommended to use in trees <5 cm in DBH, so trees that fell into that category were adjusted by using the mean value from the other six allometric equations.

To identify the minimum plot sampling for a normal distribution for trees with a DBH ≥30 cm a pseudo-sampling was carried out within the two 4 ha plots. The pseudo-sampling consisted in building multiple virtual plots of different plot sizes. For each sampling design the mean, median, and normality test was calculated.

Table II.1 Selection of different allometric equations tested

Reference	Ecosystem	Location	Precip.	Equation for AGB in kg *per* tree
Brown *et al.,* 1989	T. moist	World	1500-4000	e^(-2.409+0.9522*ln(DBH^2*H*D))
Brown *et al.,* 1989	T. Dry	World	<1500	34.4703 - (8.0671*DBH) + (0.6589*DBH^2)
Brown, 1997	T. Dry	World	>900	e^(-1.996+2.32*ln(DBH))
Chave *et al.,* 2005a	T. Dry	Pantropic	<1500	0.112*(D * DBH^2*H)^0.916
Chave *et al.,* 2005b	T. Dry	Pantropic	<1500	D*e^(-0.667+(1.784*ln(DBH)) + (0.207*ln(DBH)^2)-(0.0281*ln(DBH)^3))
Martínez-Yrízar *et al.,* 1992	T. Dry	Mexico	<900	10^(-0.535 + LOG(BA))
Návar, 2009	TDF	Mexico	<700	0.0841*(DBH^2.41)

e= Euler's constant; DBH= Diameter at breast height in cm; H= Height in m; D= Wood density in g cm^{-3}; and BA= Basal area in cm^{-2} *per* stem

Litter (fine and coarse) was collected during the dry season of 2013 when it reached its maximum (Martínez-Yrízar, 1995). Fine litter (F_{lit}) ≤2 cm in diameter, leaves, and twigs, was collected in 9 sub-samplings of 30x30 cm within each of the 40 AGB plots. Each subsample was weighed in the field on a digital scale with an error of ±1g. For dry weight estimation, the subsample was dried in the oven to a constant weight at 70°C. All dried subsamples were mixed and sent for chemical analysis (N=120, Carbon and Nitrogen). The data collected on a fine scale (10x10 m) were treated independently for local spatial autocorrelation analysis and grouped in 40 mean samples for landscape analysis. Coarse litter (C_{lit}), and woody debris ≥2 cm in diameter, were collected in one subsample of 2x30 m *per* plot with a total of 19 plots sampled. Each subsample was weighed in the field on a digital scale with an error of ±1g. For dry weight estimation, about 30% of the biomass *per* plot was dried in the oven to a constant weight at 70°C.

The top soil (0-5 cm) properties were composed of mixtures of 6 sub-samplings (N=38), turning into 19 mean values for 10x30m plots. Deeper soil (0-20 cm) cores were collected in a subsampling in the same sites as was done for topsoil (N=10). For all cases, to obtain undisturbed soil samples we used a soil core sampler with a hammer attachment. The top soil core had a volume of 98.175 cm^3 and deep soil of 392.70 cm^3. Each subsample was weighed on a digital scale with an error of ±1g. For dry weight estimation, all samples were dried in the oven to a constant weight at 70°C. The chemical and physical analysis measured carbon (C), nitrogen (N) and phosphorus (P) content, pH, bulk density and Boyoucos texture (clay, silt and sand content). P extraction technique was selected based on pH (Bray and Kurtz, 1945; Olsen *et al.*, 1954).

II.4 Selection of mature forest plots

Out of a total number of 188 samples distributed across the entire area, 83 plots were selected because they were at least 50 years old (Figure II.2) and considered as mature forest. A total of 42 plots were inventoried for this study, and 41 were further used from the NFI, in addition to the two 4 ha plots. The sampling plots had a maximum distance between any two plots of 80 km and a mean distance between all the plots of 26.6 km. About 80% of the plots have at least another neighbouring plot in a distance ~320 m and ~50% of the plots have at least another plot in less than 100 m.

To ensure that only mature forest was included different approaches were considered. (1) About 70% of the plots were visited to ensure the absence of: human tracks, invasive species, logging or any kind of wood extraction or burned areas, and showing no evidence of cattle inside or around the plot; (2) The plots had to be located over 2 km from agricultural fields; (3) to ensure that the forest did not have human disturbance in the past a remote sensing time series was built. Different aerial photos were used (1985 and 1995), and Google Earth-DigitalGlobe imagery (2004-2010, when available for 2013-2014), and complemented with LandSat (2013 and 2014), a similar approach followed by Powers *et al.,* (2009). By visually analyzing aerial photographs (Shoshany, 2000; Shoshany, 2002) since 1985 they had to show

mature forest surrounded by a matrix of natural forest. In Figure II.8 can be seen an example of remote sensing time series to identify a mature forest plot.

II.5 Characterization of the landscape

All topographic variables were built in the QGIS (QGIS-2.6.0, 2014) platform. From digital contour lines every 20 m acquired from INEGI (2003b), a Digital Elevation Model (DEM) with a resolution of 20x20 m *per* pixel was built, and from it, altitude, slope, terrain curvature, topographic indexes and hydrological network were derived (Figure II.9). We further calculated the distance to the hydrological network (streams) and distance to the coast.

Terrain shape or exposure (TOPEX) was derived from estimating the difference between mean altitude neighbourhood pixels and the elevation at the central pixel. Negative values represent exposed positions (convex curvatures) while positive estimates represent shelter (concave curvatures) (Zimmerman, 1999). The compound topographic index (CTI) summarizes soil moisture by considering flow direction and accumulation (Beven, 1977; Burrough *et al.*, 1998). It is dimensionless and higher scores are associated with moist sites (Spadavecchia *et al.*, 2008) (Figure II.9).

Potential mean solar irradiance (PmI) in W m^2 *per* day during the dry season was estimated. This factor suggests the maximum heat that can potentially strike, and it works as a limiting factor on soil moisture and plant productivity (Wright and van Schaik, 1994). It was built by calculating the potential incoming shortwave radiation over the dry season and at the hour of maximum heat strike, by changing the solar geometry (between 11:00 and 16:00 hrs, local time). The geometry was adjusted for every 60 min by changing the azimuth and altitude depending on the month and hour (Kumar *et al.*, 1997; NOAA, 2015). Shadows were projected on the surface at each time step. The potential solar irradiance was transformed into W m^2 by using the constant, reported *per* hour and season for the region (SMN, 2014) (Figure II.9).

Different authors have suggested that AGB correlate strongly to climatic variables (Murphy and Lugo, 1986b; Martínez-Yrízar *et al.*, 1992; Jaramillo *et al.*, 2003; Read and Lawrence, 2003). Temperature and precipitation exert direct influence on plants' water stress. In this study the climatic variables were selected from WorldClim (Hijmans *et al.*, 2005) with a spatial resolution of ~1 km^2 and were not transformed during analysis (Figure II.3). The data layers are the result of the interpolation of average monthly climate data from weather stations, elevation, latitude and longitude In cases where stations show multiple years, averages were calculated. The information represent the 1950-2000 time period. The selected variables were: mean annual temperature (Bio1), mean diurnal range (Bio2), isothermality (Bio3), maximum temperature of warmest month (Bio5), mean temperature of wettest quarter (Bio8), mean temperature of warmest quarter (Bio10), total precipitation (Bio12), precipitation of driest quarter (Bio17) and precipitation of warmest quarter (Bio18). Because it is recognized that the dry season is a main characteristic of this ecosystem other climatic variables were derived from the monthly

datasets: maximum, minimum and mean temperature during dry and rainy season (MTRS).; seasonal climate amplitude based on the maximum-to-minimum temperature ratio; and precipitation-mean temperature ratio.

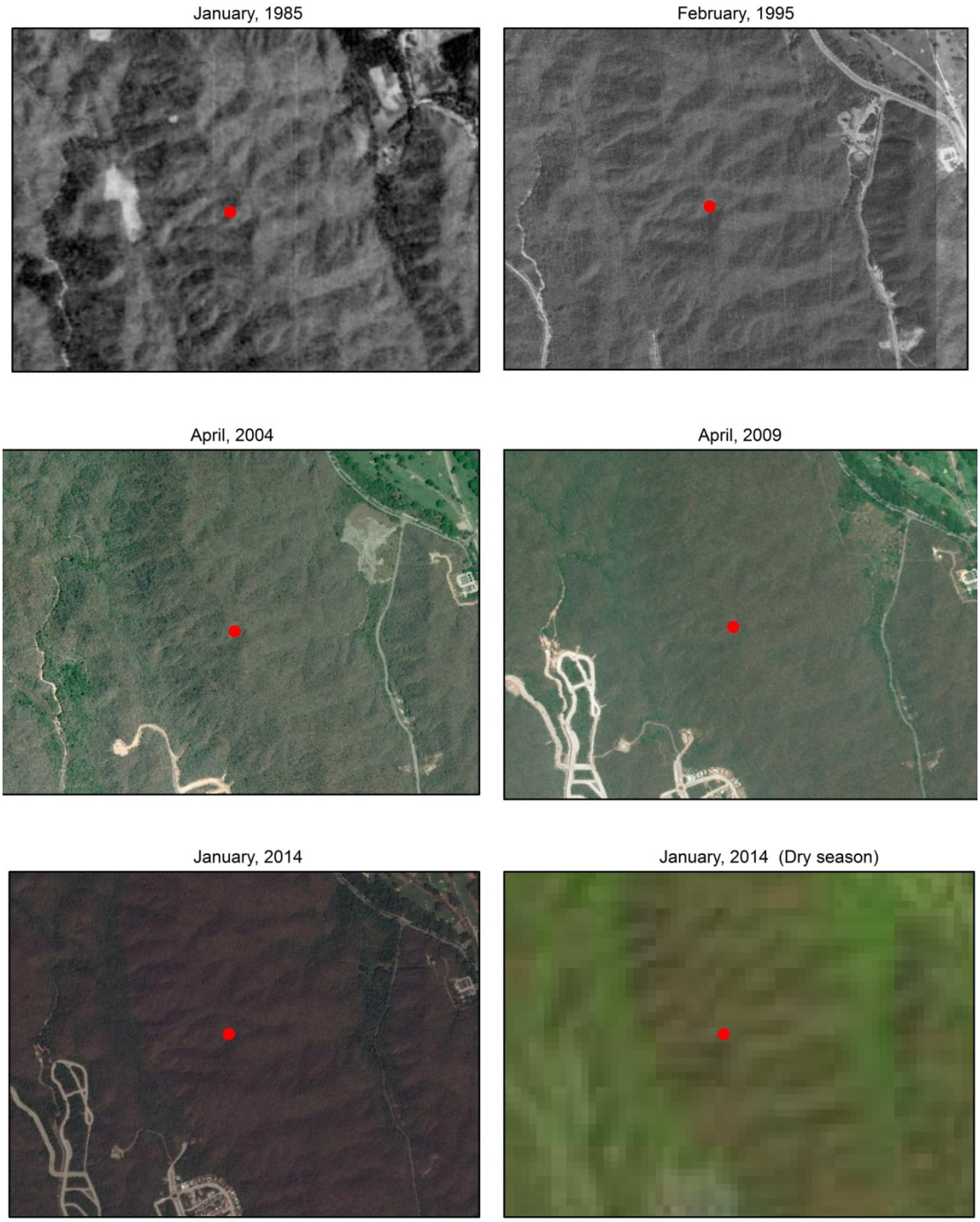

Figure II.8 Example for identifying by remote sensing time series the mature TDF sampling plots. Images collected in the years 1985 and 1995 correspond to aerial photographs orthorectified. The scenery collection for the years 2004, 2009 and January 2014 comes from the Google Earth-DigitalGlobe while the image from January 2014 comes from LandSat 8.

Time series for Leaf Area Index (LAI) was used as an indicator of deciduousness based on leaf span expression. It was obtained from MODIS Terra (NOAA, 2014) from an eight-day mean composite from 2002 to 2014. Low quality data was excluded from the analysis. A mean yearly eight-day composite was calculated with a resolution of 1 km^2. Because the reconstruction of potential LAI may drive high uncertainty, it was considered that the probability deciduousness (PD) would work as a proxy for LAI. Under the MaxEnt platform a probability deciduousness PD map was developed. During the dry season, when at least 70% of the landscape was leafless, from aerial images, 500 points were allocated in places where there was a fully green canopy. All observations fell on natural forest with no anthropogenic cover. The predictive variables used were: aspect; altitude; distance to streams; solar irradiation; CTI; total precipitation; and mean annual temperature.

Different socio-economical and biophysical data was derived from photo interpretation at a scale of 1:25,000. Aerial photos for the year 2011 were used to digitalize roads (dirt and paved), coast and perennial rivers contours. All the land-use and land-cover maps (LUCC) including human settlements were obtained from PSIG (2015) in shape file format. The distance from any of the previous attributes to each pixel was calculated with a cell size of 30m and then aggregated into a 1 km^2. In all cases, diverse transformations of the data were applied when possible to improve the model's fit.

Altitude

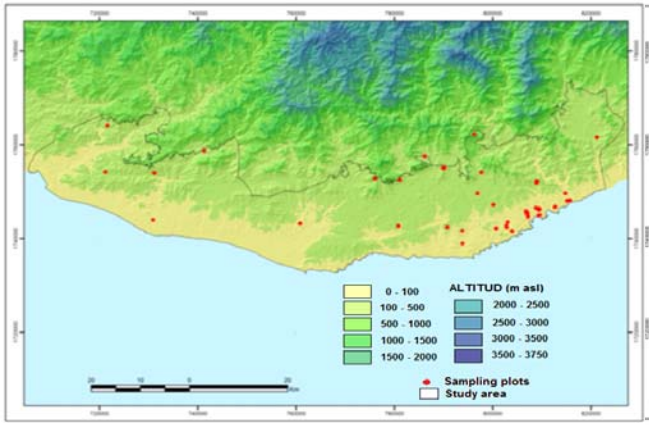

Slope

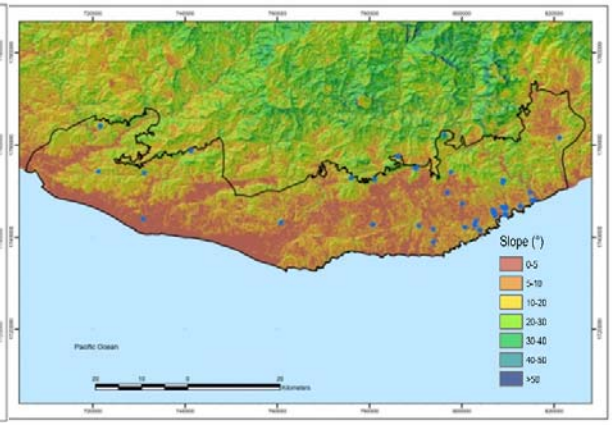

Aspect

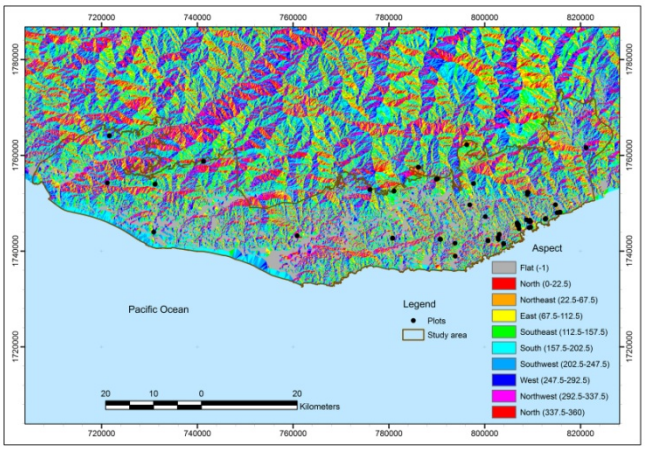

Terrain curvature

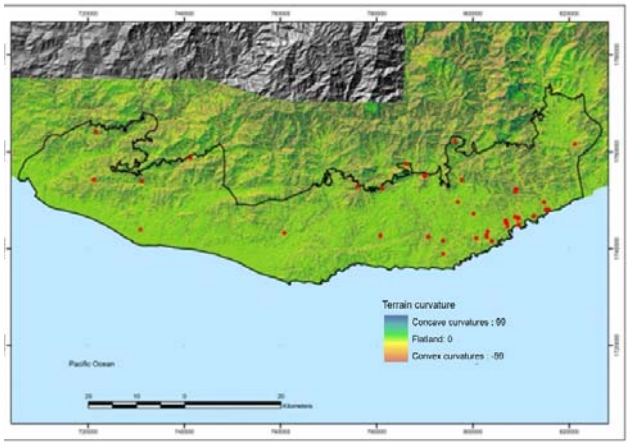

Compound topographic index **Mean solar irradiance**

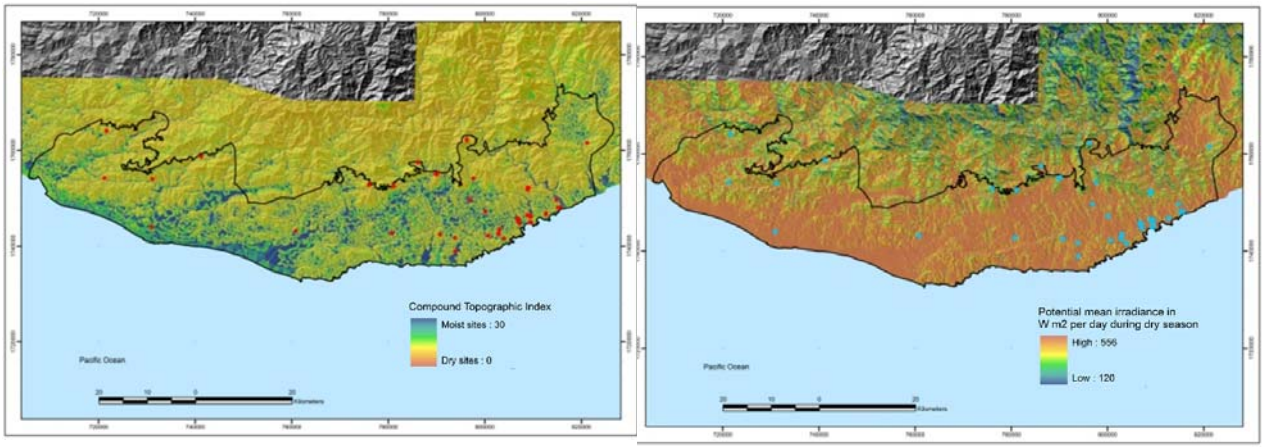

Figure II.9 Biophysical variables for the study site. Topographic variables were derived from a DEM with a resolution of 20x20m. In all figures the study site boundary was drawn and sampling plots allocations were highlighted with dots. Colors selection for boundaries and dots were based on background colors. In all cases, an extended area of the boundaries can be noticed.

II.6 Spatial heterogeneity and multi-model agreement in potential AGB predictions

AGB predictions were tested to understand their capability to capture the spatial heterogeneity in the landscape. These test approaches were: (1) linear regressions between observations and predictions for diverse spatial scales: (2) spatial discrepancies among models (RMSE, bias, CV and CI); and (3) spatial autocorrelation of AGB predictions.

Different model's predictions were contrasted against multiple spatial scales (400 m^2, 2,500 m^2, 1 ha and the landscape as a single unit). A simple linear regression was applied to observations and estimations over multiple spatial scales. The observations were evaluated regarding proximity to the mean predictions and in between the CI. In all cases, bias and RMSE were calculated as indices of a model's performance to reproduce the observations. The CV and CI for each model were evaluated at the landscape scale to understand the strengths and weakness of the models to represent the landscape. Also, the CV was contrasted with various biophysical variables with a linear regression. Doing this meant that it would be possible to establish how well the models performed and where the modeled AGB estimates might fail.

To calculate the spatial discrepancies along AGB estimates all the models were tested against each other. If the models returned the same estimates, the spatial heterogeneity across the models would be the same and a simple linear regression would be the best approach to contrast it. For testing the correlation across the paired comparisons the r^2 adjusted index and *p-value* were calculated. To reduce the bias

during the visual exploration of the linear regressions, the smothered scatter plot was adopted. The AGB differences (bias) were contrasted with the biophysical variables to break down the spatial trends of bias. It was considered there was an absence of bias when the linear regression between the predictor variable and AGB changes produced no correlation. Mayor divergences were considered for cases where AGB were skewed.

Finally, to carry on with the spatial autocorrelation analysis in all cases, we adopted the semivariogram models fitted as inversely proportional to approximate variance (weighted Cressie). This approach was selected because we were dealing with a small to moderate sample size (Cressie, 1985, 1993). Spatial dependence in the data was estimated from the nugget-to-sill ratio (Rossi *et al.*, 2009). Lack of spatial dependence would occur if measurement errors are large at zero separation distances (large nuggets), or if considerable variability occurs at smaller spatial extent than data resolution. For more details refer to the section II.8.a.

II.7 Other sources of aboveground biomass

This study took into consideration all the sources of information regarding current AGB. The input maps used for this study were the three pan-tropical datasets and two wall-to-wall datasets for Mexico published by Avitabile *et al.,* (2016), Baccini *et al.,* (2012b), Cartus *et al.,* (2014), Rodriguez-Veiga (2016) and Saatchi *et al.,* (2011b), here after referred to as the "Avitabile", "Baccini", "Cartus", "Rodriguez-Veiga" and “Saatchi” maps individually, or as “input” maps collectively. The input maps refer to different epochs for the 2000s however the reference data mostly spanned the period 2000 – 2013.

Avitabile combined two existing datasets of vegetation AGB (Saatchi *et al.*, 2007; Baccini *et al.*, 2012b) into a pan-tropical AGB map at 1 km^2 resolution using an independent reference dataset of field observations and locally calibrated high-resolution AGB maps. The method was applied independently in regions with homogeneous error patterns of the input maps (Saatchi and Baccini maps), which were estimated from the reference data and additional covariates. They considered the representativeness of the plot over the 1 km^2 pixels, and the finer resolution data (for Mexico the Cartus map, and for site location some plots of the NFI) was screened to discard plots not representative of the map cells in terms of AGB density.

The Cartus study used a randomForest for modelling the relationship between the field observations from the Mexican NFI at 1 ha aggregation (MgC ha^{-1}), the multi-sensor imagery (L-Band radar data from ALOS PALSAR and Landsat) and a digital elevation data were obtained as part of NASA’s Shuttle Radar Topography Mission (SRTM). From the NFI trees>7.5 cm were considered for AGB estimation and allometric equations applied at species, genus-specific or generalized level were used to identify the optimal allometric equation for each plot location. By aggregating different field plots a mean value of AGB per hectare was estimated with a mean central coordinate. The output of the Cartus

study was a map across Mexico for the early 2000s with a spatial resolution of 30 x 30 m. For the purposes of this study and to make AGB comparisons across the maps, estimates of MgC ha^{-1} were transformed into AGB (Mg ha^{-1}) by applying the regional carbon content measured for wood (47.3%, results of Chapter III)

Baccini used a randomForest model to identify the relationship between the field AGB data and a combination of remote sensing data. The minimum measured DBH was 5 cm for all live trees. They used satellite-based light detection and ranging (LiDAR) together with 500 m multispectral surface reflectance imagery and other geospatial data layers. LiDAR waveform measurements were acquired by the Geoscience Laser Altimeter System (GLAS) onboard NASA's Ice, Cloud, and land Elevation Satellite (ICESat). Surface reflectance data were provided by the Moderate Resolution Imaging Spectro radiometer (MODIS) onboard NASA's Terra and Aqua satellites, MODIS Land Surface Temperature (LST) as long as bi-directionally corrected reflectance (BRDF), EVI2, NII2 and SRTM. The resulting Baccini output map has a resolution of 500 x 500 m for the epoch 2007-2008.

Rodriguez-Veiga used a data fusion model based on the maximum entropy (MaxEnt) in combination with ALOS PALSAR dual polarization (2007, 2008, 2009), MODIS VI (2008), SRTM and a forest probability layer that was built under the same platform. The model extrapolated the information by including approximately 16,000 field national inventory plots for Mexico. The Rodriguez-Veiga map shows above ground woody biomass in Mexican forests and represents the epoch 2008 (2004-2012).

Saatchi used MaxEnt in addition to spatial imagery from multiple sensors; MODIS (LAI and NDVI), SRTM, and quick scatterometer (QSCAT) on earth-observing satellites to extrapolate AGB measurements from inventory plots and GLAS data. The Saatchi output is a model for the spatial distribution of AGB ha^{-1} in forests across three continental regions for the epoch 2000-2001 with a spatial resolution of 1 km^2.

The input maps were harmonized by first projecting the Saatchi map to a UTM 14 N with a geographic reference system WGS-84 and then aggregating the other maps to match its spatial resolution and grid. Spatial aggregation was performed by computing the mean value of the pixels whose centre was located within each 1 km^2 cell of the Saatchi map. To allow direct comparison of the results among the input maps, the analysis was performed only for the area common to all maps.

II.8 Statistical analysis

II.8.1 Identify factors that drive AGB accumulation in mature forest (Chapter III)

All descriptive statistical analyses were performed in the R software version x64 2.15.1 (R-Core-Team, 2014). The Mann-Whitney-Wilcox test (W) was used to test to establish that two samples came from the same population. A Jarque Bera test (JB) was used to test the normality of the observations. It was used linear regression (ordinary-least-squares, OLS) and boxplots to examine the relationships between each measure of environmental heterogeneity.

Spatial dependence of a location on neighbouring sites was measured by spatial autocorrelation (SAC) (nugget, partial sill and range). The SAC was estimated by using the library geoR (Ribeiro and Diggle, 2001). The semivariograms were fitted to a spherical model, for optimal performance variable lags, and binds were selected for each variable. The semivariogram models were fitted as inversely proportional to approximate variance (weighted Cressie). This approach was chosen because there is a small to moderate sample size (Cressie, 1985, 1993). Spatial dependence in the data was estimated from the nugget-to-sill ratio. A strong spatial dependence in the data set is defined by a ratio below 0.25, and a ratio between 0.25 and 0.72 a moderate spatial dependence (Rossi *et al.*, 2009). Lack of spatial dependence will occur if measurement errors are large at zero separation distances (large nuggets), or if considerable variability occurs at smaller spatial extents than data resolution.

II.8.2 Characterize interactions among the predictor variables and a sensitivity test in the mature forest (Chapter IV)

Firstly, it was tested that all the predictor variables sampled across the observations fell in the landscape range. With this, extrapolations over the range of the observations could be avoided. Correlated variables were excluded from the analysis. All the variables were tested in pairs using the Spearman correlation test and correlations $\geq|0.75|$ were excluded.

Secondly, all the variables that fully filled these requirements were introduced in the models to test their significance to AGB_{pot}. For each model, the ten most influential variables were retained. For GLM, the backward step-wise data reduction was adopted. For the regression tree, variables that came from the first 3 splits were considered. With random forest, it was used the node purity index and variable importance index (%IncMSE) (Breiman, 2001; Strobl *et al.*, 2007; Altmann *et al.*, 2010). In MaxEnt, the variables reduction was done via Jackknife which allowed the estimation of the significance of each predictor variable (Saatchi *et al.*, 2011b). The predictor variables selected from the models were re-grouped and re-tested. This group of variables was re-introduced in each model, except MaxEnt, and by removing and reintroducing them one by one, it was possible to identify the variables that impacted the most in the model. Finally, if any of the last variables correlated with any of those originally eliminated

we re-tested the model for any improvement. To reduce the sensitivity of AGB towards a single variable, all the final selected variables were tested for sensitivity under a Monte Carlo (MC) analysis. MC was tested using the library mc2d (Poillot *et al.*, 2013). To reconstruct the distribution of each predictor variable a distribution function was built using the library fitdistrplus (Delignette-Muller and Dutang, 2015). When a single predictor variable promote an over- or under-estimation in AGB $\geq$ 500 Mg ha^{-1} over the mean, the variable was excluded.

II.8.3 Calibrate the models and predict the potential AGB (Chapter IV)

The AGB reference data were randomly split for training the models and for independent validation (Cochran, 1977). The same training and validation data were used for each model to allow a comparison across the methods. To assess the accuracy and the uncertainty of the predictions of the models the independent validation data (Friedl, 1997; Hill *et al.*, 2013) was employed. From the 83 field measurements of mature forest, 86% (N=73) were used for training and 14% (N=10) for validation.

An additional independent validation was conducted by 32 quarter of a hectare and eight 1 ha plots. Thereby it was possible to analyze the modelling performances not only for local predictions, but also for multi-scale comparisons. To test the accuracy across the models, r^2 was utilized, adjusted for the calibration, and RMSE and bias statistics for the validation. To test the improvements in modelled AGB estimations, the results were contrasted with a null model. The null model was built by considering the mean estimate from field observations as a prediction. Finally, Wilcoxon signed-rank test was used to decide whether the corresponding models' population distributions were identical to observations. It was considered that models came from repeated observations of the same subject, and population distribution were identical to field AGB estimates (Crawley, 2013).

A total of 7 contrasting methods were tested and compared for their ability to estimate AGB from field samples and biophysical properties. All the analyses were carried out with the software R version x64 2.15.1 (R-Core-Team, 2014) and the libraries caret (Kuhn, 2015), gam (Hastie, 2015), mass (Ripley *et al.*, 2015), nnet (Ripley and Venables, 2015), randomforest (Breiman, 2001) and tree (Ripley, 2015), and the software MaxEnt (Elith, 2011).

The regressions modelling was conducted by the following techniques: (1) Multi-Lineal Regression (GLM) and (2) General Additive Model (GAM), both with a Poisson error distribution. GLM was selected because it is assumed to have linear effects on some transformations of the dependent variable (McCullagh, 1989), while GAM has the capability of finding the appropriate smoothness for each applicable model term using prediction error criteria or likelihood-based methods (Hastie, 2015). Moreover, regressions processes were adopted. (3) Regression Tree (RT) and (4) Generalized Linear Mixed Models via Penalized Quasi-Likelihood (GLMM). RT is capable of capturing nonlinear relationships between the response and predictor variables by not making assumptions regarding the distributional properties of the input data (Friedl, 1997). While GLMM represents the clusters for a

normally distributed random intercept (Schall, 1991). In this case, a model was fitted for AGB with predictor variables and by using a fixed effect, the best performance was achieved using altitude.

Two learning machines were selected: (5) Random forest (RF) and (6) Automated neural networks (NN). RF creates a large number of trees containing a bootstrap sample of the data with the same number of cases as the original data, and by using a randomly selected subset of the predictor variables. The final prediction is the average of the values predicted by all the previous trees (Breiman, 2001). Compared with the standard RT model, RF is less sensitive to noise in the training data and tends to result in more accurate model predictions (Baccini, 2008). NN on the other hand is good at learning patterns to find relationships from training data and to apply these sets or rules into new data. These models produce weights and estimate the bias for minimizing the error between the trained data and actual output for all predictor variables (Bishop, 1995; Dreiseitl, 2002). The final NN model was built with two hidden layers and the optimum weighting was selected over 1,000 iterations. Increasing the complexity of the model improved the prediction of the calibration estimates, but it failed against independent data by increasing the RMSE and the bias. As a result, the best model had a lower complexity but it was capable of reproducing validation estimates.

For all the models, except MaxEnt, a bootstrapping aggregation (bagging) was applied (Breiman, 1996). This method averaged multiple predictions from a collection of bootstrap samples; in this case, 75% of the training data was used (N=55 out of 73). The main goal of doing this was to capture the uncertainty of the predictions along multiple proportions of the observed information. For all the models it was set at 1,000 runs; this number was chosen based on the minimum number of runs in each model that produced akin predictions allowing reliability of our analysis. The 1,000 predictions were aggregated into 1 mean with the 95% CI of the mean, standard deviation and the 95% CI of the predictions. Finally, to test confidence about the predictions the Coefficient of Variation (CV) was calculated as the ratio of the standard deviation to the mean (Crawley, 2013), where lower values of CV suggest less dispersion over the 1,000 predictions.

According to Saatchi *et al.,*(2011b) a data fusion model based on the maximum entropy model (MaxEnt) outperforms parametric methods and some other nonparametric models in predicting AGB, such as RF. Because of that, we tested (7) MaxEnt and adopted the methodology reported by Saatchi *et al.,*(2011b). The training data was split into biomass classes. In total MaxEnt was run eight times for each biomass group. Each of the eight aggregates was developed from sub-aggregating the data in different ranges (4 to 9 aggregations). The ranges used across the eight groups were diverse, and repeat any interval category was at all times avoided to eliminate double counting of the probabilities. The minimum number of observations *per* ranges was 3. The mean value from the range was estimated based on the observations that fell within that range. To improve the capability of the predictions two approaches of data aggregation were considered to convert the predictions into a single AGB map. The first option was selecting the maximum probability class observed for each pixel across all the models. A high value of probability for a particular pixel indicates that the pixel is predicted to be suitable for having related

characteristics to the training pixels (Elith, 2011; Saatchi *et al.*, 2011b). The second method was the same applied by Saatchi's *et al.*,(2011b), in which a weighted mean was estimated across the probability classes for each pixel. For this study, Saatchi's approach was preferred because the probabilities across the classes were not consistent. By repeating the latter process with the eight groupings, various statistics and uncertainties of the model performance were calculated.

A detailed description of how these models perform is beyond the scope of this chapter but more information can be found in these sources (McCullagh, 1989; Bishop, 1995; Breiman, 1996; Friedl, 1997; Dreiseitl, 2002; Baccini, 2008; Elith, 2011; Saatchi *et al.*, 2011b; Clark, 2013; Hastie, 2015).

II.8.4 Identify patterns and processes of AGB losses (Chapter V)

In order to identify similarities in mean AGB estimates (input maps vs field observations) at different scales of analysis two different approaches were used: Firstly a t-test on paired samples was used to contrast AGB estimates at site location where at least 3 observations fell in a 1 km^2 grid and compared against different input maps (N=47 observations). This test assumes errors are normally distributed and come from paired observations, particularly from the same location (Crawley, 2013). Secondly a Wilcoxon rank-sum test was used to contrast AGB estimates at landscape scale (field observations N=188; and map grid cells N=1,764). This test assumes independence in the samples and that errors are not normally distributed (Crawley, 2013). Finally, a median comparison was carried out using the notch option build for boxplots. All tests were carried out at the 95% confidence level.

Higher resolution maps and field observations were averaged within 1 km^2 grid cells. All the re-scaled maps were aggregated into one single mean. To test the uncertainty of different input maps, and as a measure of the AGB uncertainty at the pixel scale, the Coefficient of Variation (CV) was calculated as the ratio of the standard deviation to the mean (Crawley, 2013), where lower values of CV suggest less dispersion among the AGB estimates from different input maps at a pixel resolution. In contrast higher values of CV represent higher variability among the input maps. To identify if high values in CV of the maps (CV_{maps}) are related to highly heterogeneous sites, a Spearman correlation coefficient was applied between CV_{maps} and the CV measured in 1 km^2 grid cells with at least three AGB field observations. To test the spatial bias of the uncertainty across the input maps, CV_{maps} was compared against different explanatory variables using a Spearman correlation coefficient and regression tree as a multivariate test to characterize spatial bias and to identify driving forces of carbon losses.

All the statistical analyses were carried out using R statistical software version x64 2.15.1 (R-Core-Team, 2014) and the library tree (Ripley, 2015). For spatial analyses, and generation of all the topographic and socio-economic variables GIS software QGIS was used (QGIS-2.6.0, 2014).

Chapter III. To reduce the uncertainty in above ground biomass in mature forest it is necessary to understand the forest structure, topography and soils: a multi-scale analysis of a Tropical Deciduous Forest

III.1 Abstract

Land-use and land-cover changes and selective logging have led to losses in carbon storage of diverse tropical ecosystems. Globally, tropical deciduous forest (TDF) has been one of the most impacted of these, but the outcomes have been poorly quantified. Little is known of ecological processes of AGB distribution over various spatial scales in natural and non-human disturbed ecosystems, as most studies have been focused on different disturbed vegetation stages. The understanding of TDF aboveground biomass has been biased towards the secondary forest with few samples of mature forest. The aim of this chapter is to quantify, allocate and understand the natural factors responsible for driving the accumulation of the mature biomass in a Mexican TDF. Remote sensing time series (1985-2014) across field sites were used to identify suitable sampling locations for mature forests. Plot inventories indicated that >90% of the trees have their diameter at breast height (DBH) <10 cm. Large trees (≥30 cm) were found at similar frequencies in small (300-400 m^2) and large (4 ha) plots. AGB is normally distributed with a mean of 118±44 Mg ha^{-1}. Depending on the selected allometric equation, at least 60% of the AGB is allocated in trees with a DBH<28.7cm. At the local scale, large trees (≥30 cm in DBH) did not show spatial autocorrelation, and in the landscape, the AGB showed a spatial correlation in distances <250 m. Because there were low densities of very large trees (DBH≥75 cm), the mean AGB estimates across different allometric equations only resulted in differences of <11%. Climate, land and soil properties variables such as leaf area index, altitude, rainfall and precipitation-temperature ratio were positively correlated to AGB. Solar irradiance, distance to streams and mean annual temperature showed an inverse relation to AGB. Soil texture and pH were the most important soil properties in explaining AGB, with stronger effects than nutrients. Across different scales of analysis, higher biomass estimates were related to sites with less water stress**.** This information can support spatial estimates of biomass storage capacity for Mexican TDF, crucial information for land and carbon management.

III.2 Introduction

Forest land plays a major role in the global carbon cycle, with nearly 50% of the carbon stored in tropical forests (Houghton, 2005a; Pan *et al.*, 2011), and significant land-use and land-cover change (LUCC) leading to forest loss. While more research has been done on moist tropical forests (Skutsch *et al.*, 2009), drier tropical forests are also important: TDF account for nearly 5% of the carbon stored in terrestrial ecosystems (Houghton and Skole, 1990).

To achieve the goal of better understanding of the carbon cycle and to account for the carbon stocks, fluxes and changes, as well as to distinguish the effects of human actions from those of natural system, variability turns out to be of primary concern (CCSP, 2003). Biomass and carbon stock estimations depends on forest inventories. Therefore, forest inventories should be able to make a full representation of the forest type. Chave *et al*., (2004) suggest that primary sources of uncertainty are due to tree measurement and plot size. In the TDF most of the sampling approaches have been by small plots with several repetitions. However, the ideal sampling size for TDF is not clear, but this can be the result of complex topography. Thus, it is important to identify the best sampling approach for reducing the uncertainty in AGB estimates. Another source of uncertainty in biomass estimates comes from the proper selection of the allometric equation (Chave *et al.*, 2004). While this can count for much of the uncertainty in AGB estimates, it is tough to tackle. Equations are built under precise site-specific conditions, inevitably significant bias remains when these equations are used in a specific location (Brown *et al.*, 1989; Brown, 1997; Chave *et al.*, 2004).

Biophysical factors such as water availability and nutrients are recognized as primarily responsible for plant development (Holmgren *et al.*, 1997; Berdanier and Klein, 2011; Medeiros and Drezner, 2012; Peterson, 2012). However, depending on the scale of analysis and the ecosystem under study, they differently perform (Allen and Hoekstra, 1990; Turner, 2005; Currie, 2011). In a local context, species composition (Becknell *et al.*, 2012), slope, aspect and soil texture (Leitner, 1987), concavity (Berdanier and Klein, 2011; Peterson, 2012) are recognized to be the major influences on water availability for plants and/or biomass allocation. Microclimate is critical for the response of species distribution (Bennie *et al.*, 2008), by driving the individual development of trees (Holmgren *et al.*, 1997; Berdanier and Klein, 2011). Nevertheless, Powers *et al*., (2009) and Medeiros *et al*., (2012), in a multi-scale analysis, suggest variation in rainfall, soil properties, and nutrients are the main factors contributing to structural change in TDF. However, little is known about N and P patterns in mature forests (Gei and Powers, 2013) and how they may affect the structural differences in the TDF.

This lack of integrity across scales complicates the understanding of the drivers of AGB, making it even more complex in a heterogenic natural landscape. Because of this, it is necessary to implement a multi-scale approach. Thus, the critical question to be addressed by this study is, what are the main factors that control the AGB distribution in a natural landscape? To be capable of answering this key question and in light of current knowledge the following questions were developed:

Q1. Is there an AGB spatial autocorrelation beyond the local scale in a TDF?

Q2. Are the large stems the major contributors in AGB estimates in a TDF ecosystem?

Q3. Is the water availability the major limiting factor for AGB in the TDF?

III.3 Results

III.3.1 Community structure, tree size distribution and basal area

In this study records were made for woody plants, 94 genera and 248 species. More than 70 species were not possible to classify and represent ~20% of all the plants. The top five genera represent about 20% of the total species recorded and these are: *Tabebuia* (4.8%); *Calophyllum* (4.5%); *Hura* (3.7%); *Acacia* (3.4%); and *Cochlospermum* (3.3%). The most common species are: *Tabebuia chrysantha* (4.7%); *Calophyllum brasiliense* Cambess (4.5%); *Hura polyandra* (3.7%); *Guazuma ulmifolia* Lam. (3.3%); and *Cnidoscolus tubulosus* (2.9%).

The tree size distribution follows an inverse J-shape typical of natural forests with good regeneration and continuous replacement (Hall and Bawa, 1993; Lykke, 1998; El-Sheick, 2013). On average there are ~6,450 trees ha^{-1} (DBH ≥ 1 cm) (Figure III.1). About 90% of trees are DBH <10 cm. Trees with a DBH ≥30 cm represent less than 1% of the total (56 stems *per* hectare). From a pseudo-sampling it can be inferred that the minimum sampling plot size for reaching a normal distribution in AGB for trees with DBH ≥30 cm is 2,500 m^2. The two sampling approaches (300-400 m^2 and 4 ha plots) for number of trees DBH ≥30 cm *per* ha, do not differ statistically (W=131.5, p=0.13) and the data came from identical populations. By excluding six outliers, the mean basal area (BA) (± standard deviation) was 27.6±8.9 m^2 ha^{-1} with a median of 27.2 m^2 ha^{-1}, with a normal distribution (JB, p=0.34, Figure III.2a). BA and AGB correlated strongly (Figure III.3a), and AGB correlated to number of trees but only for DHB ≥30 cm ha (Figure III.3c).

Mean wood density is 0.51±0.16 g cm^{-3} (JB, p=0.78). The range was comprised between 0.09 and 0.93 g cm^{-3}. When contrasting the tree DBH against its wood density, there was no evidence to suggest that they were related (r^2=0.001, p=0.74). Our stand wood density was similar to that reported for other dry ecosystems and smaller than those of tropical moist ecosystems (Brown *et al.*, 1989; Brown, 1997; Fearnside, 1997; Jaramillo *et al.*, 2003; Read and Lawrence, 2003; Baker *et al.*, 2004; Ribeiro *et al.*, 2011). Mean wood carbon content (%) showed a normal distribution of 47.25±0.79%, with a range from 46.18 to 48.11%. This estimate falls in between the range reported for tropical forest, tropical angiosperms (Thomas and Martin, 2012) and another TDF in Mexico (Eaton, 2005; Eaton and Lawrence, 2009). Some authors have suggested that local wood carbon content can reduce the uncertainties in 5-7% (Martin and Thomas, 2011; Saner et al., 2012; Thomas and Malczewski, 2007) and up to 10% (Elias and Potvin, 2003). In this study we account for 5.5% in carbon estimates. Finally, carbon content in litter was

relatively smaller than other estimates (36.3%) (Anaya *et al.*, 2007; Firdaus *et al.*, 2010; Petit-Aldana *et al.*, 2011), which can significantly drive important changes in the AGC estimates for this pool.

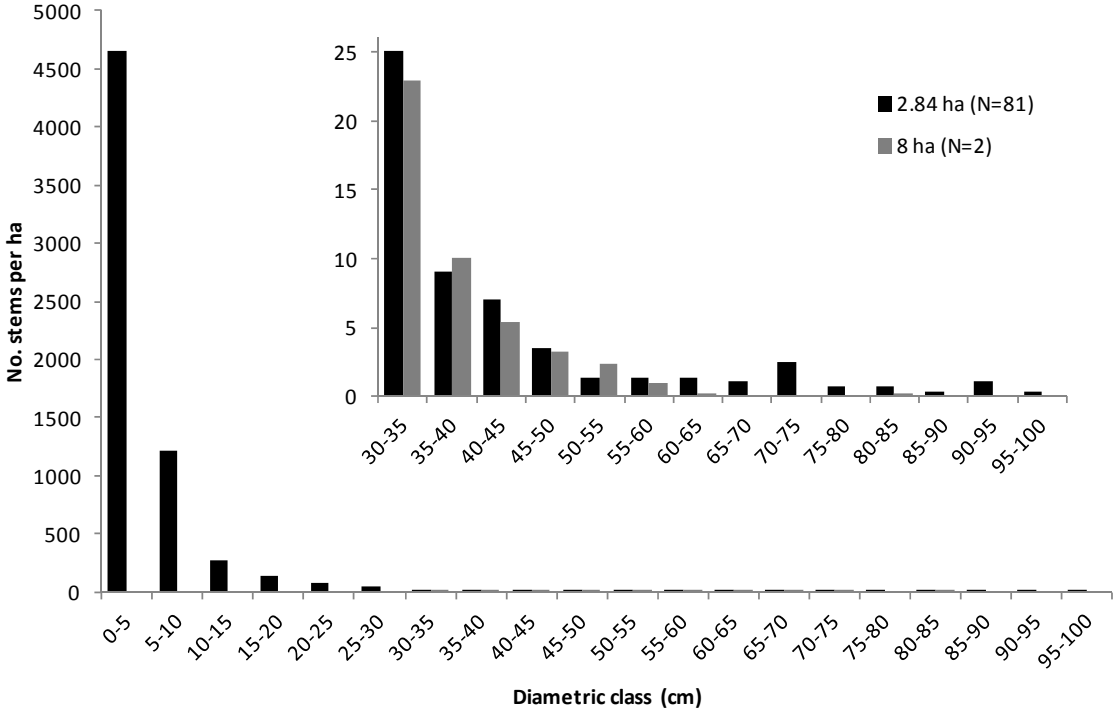

Figure III.1 Tree size distribution *per* diametric class for 2 sampling designs (small and large sampling plots). The X axis refers to the diametric class and the Y axis refers to the number of trees *per* hectare measured for both sampling strategies. Black bars apply to small sampling plots (300-400 m^2, N=81) with a total area sampled of 2.84 ha. Grey bars apply to large sampling plots (200x200 m, N=2) with a total area of 8 ha.

III.3.2 Soil properties

Soils textures were characterized by a sandy loam, with a few examples of sandy clay loam. The textural classification did not show changes in different depths. The mean composition of the topsoil is 62.6±12.9% sand, 19.7±7.0% silt, and 17.7±6.8% clay. On the 0-20 cm composite sand content increased by 3.6±1.7%, while silt and clay showed a reduction of 2.4±1.8 and 1.2±0.8%, respectively.

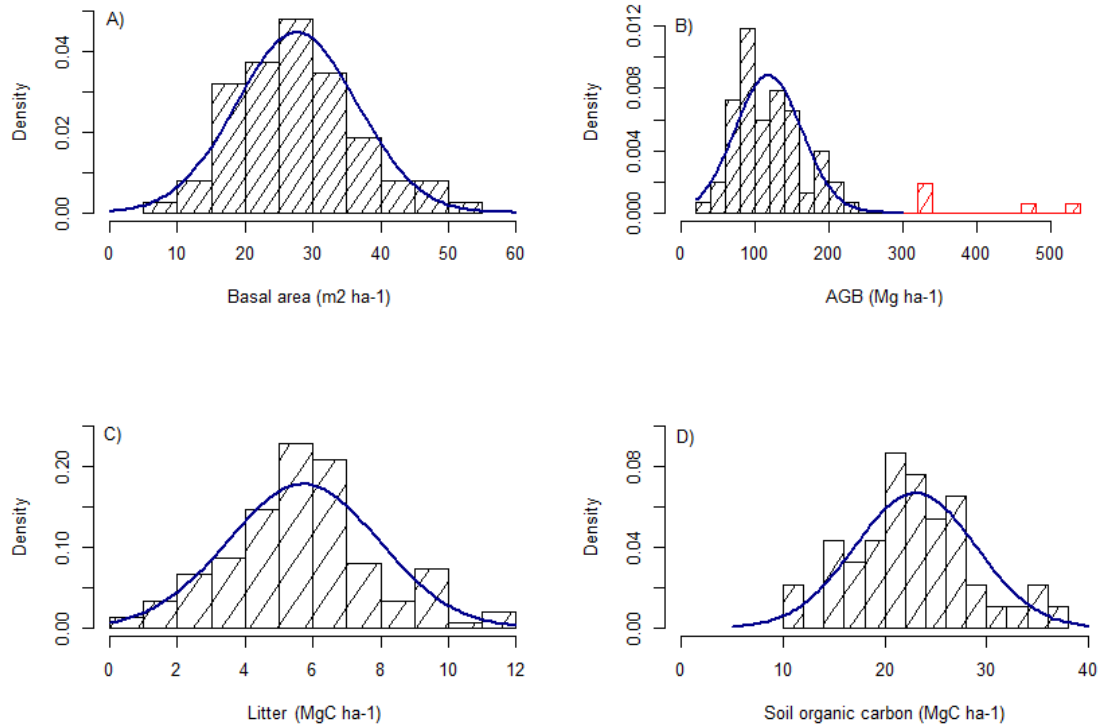

Figure III.2 Frequency graphs for the basal area (A) and AGB (B) come from coarse spatial scale, red bars refers to the outliers in AGB. Litter (C) and soil carbon stocks (D) frequency graphs come from a fine spatial scale. The solid line refers to the expected normal distribution.

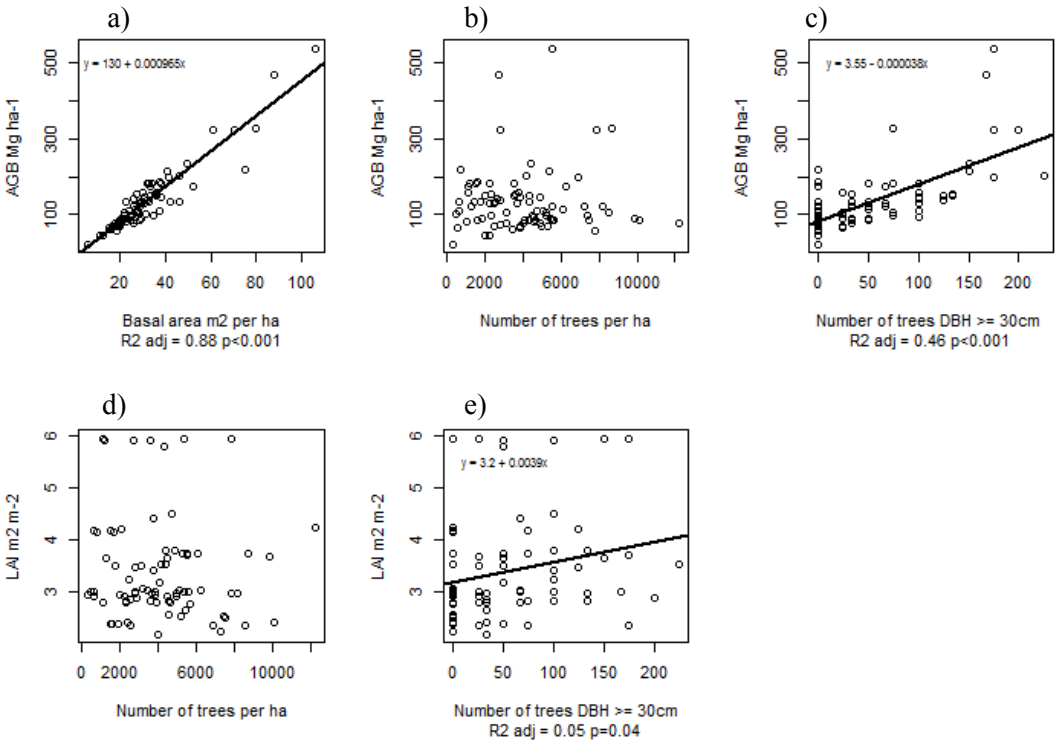

Figure III.3 Community structure lineal regression plots. (a) Correlation between basal area, (b) number of trees *per* ha and (c) number of trees with a DBH≥30 cm, (d) number of trees *per* ha and (e) number of trees with a DBH≥30 cm and LAI. The outliers were not excluded from these analysis. When the regressions was significant , the equation was included.

All measured soil properties showed a normal distribution. The soil was acidic to neutral with a pH of 6.44±0.90, being steady at both depths. The topsoil C content had a mean of 4.68±1.37%, ranging from 2-9%. The N in the soil ranged from 0.1-0.66% with a mean value of 0.35±0.13%. The total extractable P has a geometric mean of 4.95 mg kg^{-1} (+1.00, -0.84; log transformation, JB, p=0.79). However, in the composite 0-20 cm depth showed a reduction in these figures. Deeper soil proved to have on average 35.1±10.4% less C content, 10.0±9.2% less N content and 9.8% (+7.1% and -5.5%; log transformation) less P content in comparison to the top soil. Regarding the stocks, on the top 5 cm of the soil, the mean N stock was 1.68±0.62 MgN ha^{-1} (JB test p=0.62) and 15.12±6.39 MgN ha^{-1} for the top 50 cm. This is similar to stock reported for a semi-deciduous forest (16.7 MgN ha^{-1}) and higher than the deciduous forest (6.7 MgN ha^{-1}), both reported for the Chamela region (Jaramillo *et al.*, 2011). The P stock for the top soil represented 25.3 kgP ha^{-1} (+16.3, -8.9; log transformation, JB test p= 0.61) and up to 228.2 kg P ha^{-1} (+147.0 and -80.3; log transformation, JB test p= 0.81) for the first 50 cm. Finally, the mean C:N stoichiometric ratio estimated was 11.3:1 (+3.2 and -2.5; log transformation, JB, p=0.30). Regarding the mean N:P stoichiometric ratio is 18.8:1 (+22.9 and -10.3; log transformation, JB, p=0.83). Most of the observations fell in the range 10-12.5:1 and 12.5-25:1 for the C:N and N:P, respectively.

III.3.3 AGB estimates and its uncertainty

From the seven allometric equations tested, two were excluded and they are those developed by Martínez-Yrízar *et al.*, (1992) and Chave *et al.,* (2005b) (Table III.1). The former equation used the logarithm of BA and showed the lowest figures in AGB estimates, mainly in trees with DBH >20 cm. The latter showed the highest AGB estimates due to the use of exponential DBH, inducing a steep rise with the increase of DBH (Table III.1). The equations built for dry forests by Brown *et al.,* (1989) and Brown (1997) showed similar values. The mean biomass in the landscape derived from different allometric equations across the plots was 132.8±83.4 Mg ha^{-1} (Table III.1 & Figure III.4a). However, when three outliers were excluded it was observed to be a normal distribution (JB, p= 0.08, Figure III.2b) with a mean estimate of 118.1±44.0 Mg ha^{-1} and a median of 107.9 Mg ha^{-1}.

On average, at least 60% of the AGB ($DBH_{60\%AGB}$) was allocated in trees with a DBH<28.7 cm (Figure III.4a) with little variation among the diverse equations (Table III.1 & Figure III.4b). The range in DBH was between 25.3 cm (Martínez-Yrízar *et al.*, 1992) and up to 31.5 cm (Návar, 2009). The same approach used to identify what diameter the 80% of the AGB ($DBH_{80\%AGB}$) lay within showed higher variability. The mean $DBH_{80\%AGB}$ was 50.7 cm with a median of 48.4 cm. The DBH could be as low as 40.4 cm (Martínez-Yrízar *et al.*, 1992) and as high as 63.0 cm when using Návar's (2009) equation (Table III.1 & Figure III.4b). When the mean biomass estimate was ≥100 Mg ha^{-1} 70% of the AGB was allocated in trees with a DBH <40 cm and increasing to ~95% in plots when AGB <100 Mg ha^{-1}. Contrastingly, plots where AGB <50 Mg ha^{-1} did not contain trees ≥30 cm in DBH.

Table III.1 Mean AGB for each allometric equation and minimum DBH to reach 60 and 80% of the AGB.

Equation	AGB (Mg ha^{-1})	$DBH_{60\%AGB}$ (cm)	$DBH_{80\%AGB}$ (cm)
Brown *et al.*, 1989 (T.moist)	105.8	29.1	49.5
Brown *et al.*, 1989 (T. dry)	124.1	27.5	48.4
Brown, 1997	124.8	30.3	60.5
Chave *et al.*, 2005a	98.4	28.1	45.3
Chave *et al.*, 2005b	145.4	29.0	47.5
Martínez-Yrízar *et al.*, 1992	77.6	25.3	40.4
Návar, 2009	103.6	31.5	63.0
Mean	132.8±83.4	28.7	50.7
Median	110.1	29.0	48.4

When contrasting different allometric equations, uncertainty in biomass estimates *per* tree increased with DBH, mainly occurring in classes ≥75 cm. However, because of their low densities they accounted for 7.7-12.4 Mg ha^{-1}, which represents ~10% of the total AGB (Figure III.4b). On the other hand, the primary source of uncertainty was related to more populated trees (DBH<35 cm) which, with little variation in AGB *per* tree, their large densities represented about 66.3% of the AGB estimates, with a range of 65.1-81.9 Mg ha^{-1} (Figure III.4a & b).

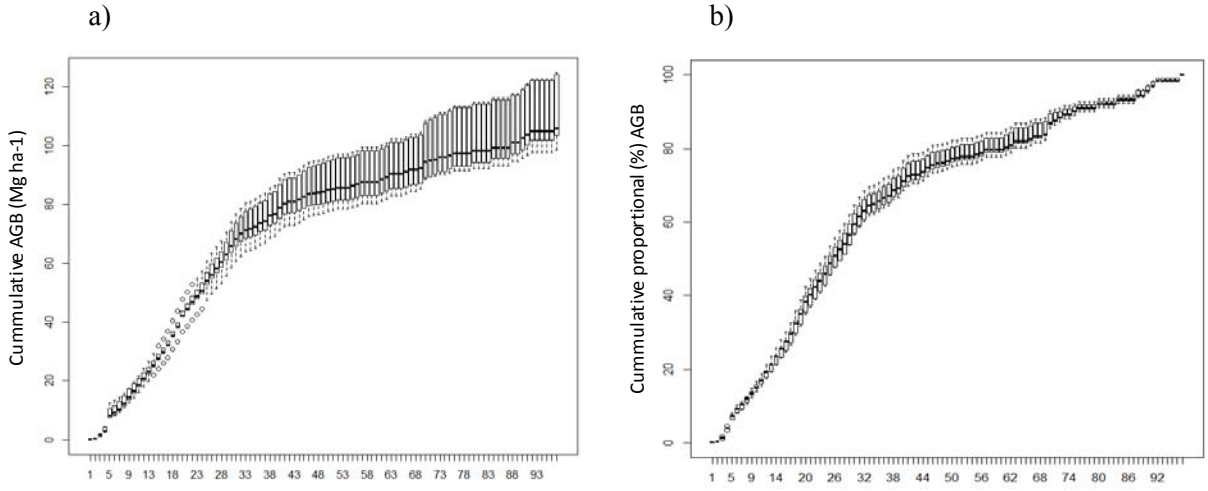

Figure III.4 Cumulative AGB *per* diametric class in cm for five allometric equations. (a) Cumulative AGB is expressed in Mg ha^{-1} and in (b) in percentages. In all cases bars refer to the upper and lower quartile, a solid black line refers to the median, white dots refer to outliers while the greatest and the lowest values, excluding outliers, are expressed with whiskers.

III.3.4 Carbon stock estimates

This ecosystem reached a mean above (live and dead) ground carbon (AGC) stock of 64.1 MgC ha^{-1} (+24.0, -23.5). About 87% referred to live AGB, 9% to fine litter and 4% to coarse litter. Considering the uncertainty in the estimates of biomass and carbon content the live AGC stock was 55.8±20.8 MgC ha^{-1}. Regarding other C stocks, litter showed a normal distribution (JB test p=0.08) with a mean value of

5.78±2.14 MgC ha^{-1} (Figure III.2c), similar to other regions (Brown and Lugo, 1982; Delaney *et al.*, 1997; Delaney *et al.*, 1998). Coarse litter showed a geometric mean C stock of 2.48 MgC ha^{-1} (+1.05, -0.56; log transformation, JB p-value = 0.84). On the top 5 cm of the soil, the mean C stock was 23.00±5.95 MgC ha^{-1} with a normal distribution (JB test p=0.70) (Figure III.2d). Considering a depth of 50 cm, the carbon stock in soils was found to be 149.27±3.46 MgC ha^{-1}. The total AGC and below carbon (BGC) stock was ~213±28 MgC ha^{-1}. The proportion of SOC in the top 50cm and AGC stocks was 2.3:1, which falls in the upper limit of other dry ecosystems (Delaney *et al.*, 1997; Walker and Desanker, 2004; Ryan *et al.*, 2011).

III.3.5 Spatial autocorrelation analysis

The spatial dependence among different variables and scales of analysis showed that the landscape is highly heterogeneous. For example, at the local scale, the different biological and soil properties, and carbon content (N=38) showed a high semivariance between neighbouring plots or did not exhibit spatial autocorrelation. We detected a non-monotonic variogram 'hole effect' for the measured variables, where the semivariance was larger at distances <40 m than those in the range of 40-80 m. However, it seems that variograms were dampened because of an irregular sampling design inducing a super-imposition of multiple continuity structures (Journel and Froidevaux, 1982; Pyrcz and Deutsch, 2003). At the local scale, AGB and BA in large trees (≥30 cm in DBH, N=365) did not show spatial autocorrelation.

Table III.2 Semivariogram parameter estimates for measured variables at a coarse spatial scale derived from a fitted spherical model.

	Units	Range (m)	Sill	Nugget	Nugget/Still ratio	r^2
Basal area	m^2 ha^{-1}	86.6	120.0	42.2	0.35^{M}	0.42
Live AGB	Mg ha^{-1}	228.5	3,028.6	1,265.4	0.42^{M}	0.29
Fine litter	Mg C ha^{-1}	1,506.0	4.7	0.4	0.08^{S}	0.76

**Spatial dependence: (S) strong (M) moderate (L) low.

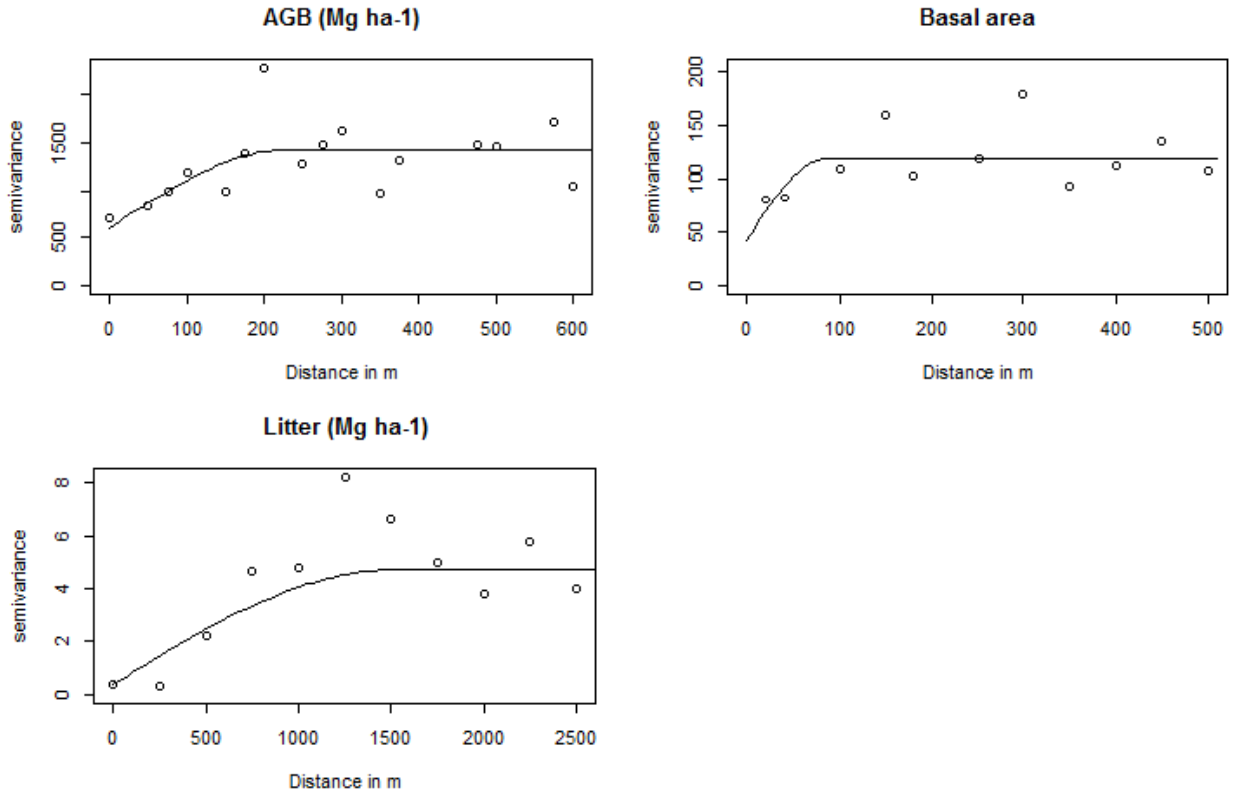

Figure III.5 Semivariograms of AGB, basal area and fine litter.

At a landscape scale, the range of spatial autocorrelation showed 2 contrasting figures (Table III.2 and Figure III.5). On the one hand we have BA and AGB (N=81) which showed a range of <250m, both with a moderate spatial dependence. Fine litter carbon (N=40) stock had a range of ~1.5 km with a strong spatial dependence. On the other hand, soil properties did not show spatial autocorrelation (N=19).

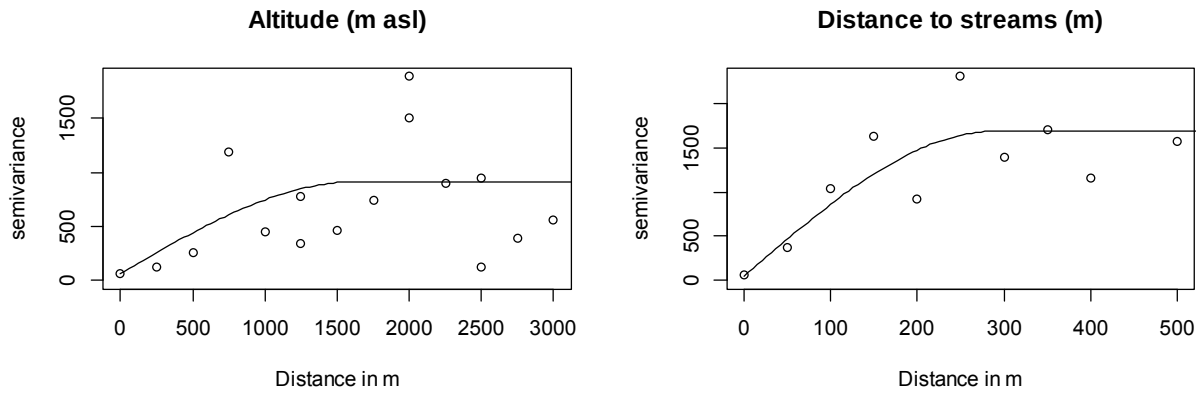

Figure III.6 Semivariograms of altitude and distance to streams.

III.3.6 Biophysical properties regresses to live AGB

There is a strong correlation of AGB to variables that may account for water stress, and less correlation with soil nutrients. For example, LAI is an important proxy for many biological processes like water and nutrient availability, and to some extent AGB. In the TDF mean annual LAI was the strongest factor (r^2 adj =0.19, p<0.000) (Figure III.7a) to explain AGB. The LAI time series suggested that the main differences across AGB groups occurred during the dry season (Figure III.8a). During this season low-high AGB groups (<200 Mg ha^{-1}) showed the lowest LAI figures (1.4-1.9 m^2 m^{-2}), whereas very high AGB (≥200 Mg ha^{-1}) reached values of 3.7 m^2 m^{-2}. During the rainy season different groups showed similar means: 4.6 m^2 m^{-2} for low and medium AGB group (<100 Mg ha^{-1}), and 4.9 m^2 m^{-2} for high and very high groups (≥100 Mg ha^{-1}), with a maximum LAI of ~6.5 m^2 m^{-2} (Figure III.8a). Interestingly, number of trees or any combination of different classes of number of trees *per* diametric class did not correlate to LAI (Figure III.3d). The best correlation was identified for number of trees DBH ≥30 cm (r^2=0.05, p=0.040) (Figure III.3e).

AGB regressed positively to altitude (r^2 adj =0.12, p<0.001; Figure III.7b). At higher altitudes (>500 m a.s.l) mean AGB was ~180 Mg ha^{-1}, while at lower altitudes (<200 m a.s.l) the mean estimates were ~115 Mg ha^{-1}. This can be related to the relative humidity that is in the air, where at higher altitudes the humidity is higher. PmI regressed inversely to AGB (Figure III.7c), places with low PmI during the dry season (420-440 W m^{-2}) reached the highest figures with a mean estimate >260 Mg ha^{-1}, and when PmI ≥500 W m^{-2} AGB was ~120 Mg ha^{-1}. Aspects facing West and North showed the highest AGB with mean figures ~140 Mg ha^{-1}, while East and South faces showed lower mean estimates (Figure III.7d). About 30% of plots with the lowest AGB were allocated in the South-East orientation (Figure III.8b), and ~30% of the plots with the highest AGB were orientated South-West and West aspects, where only 40% were found in the North and East orientations. Terrain curvature showed importance in places where dry climate dominates (mean annual temperature >26°C and total precipitation <850 mm). Concave curvatures showed AGB figures ~110 Mg ha^{-1}, while in more exposed positions the estimates were ~85 Mg ha^{-1} (Figure III.7e). Distance to streams showed a spurious inverse regression only for the first 140 m (r^2 adj=0.07, p=0.055; Figure III.7f). CTI was used as an index to express soil wetness and nutrient deposition. For example, values <5.0 showed a mean AGB of ~110 Mg ha^{-1}, and values between 7.5 and 10 showed the highest AGB estimates (>150 Mg ha^{-1}). Variables such as slope and distance to the coast did not show any explicative power to AGB estimates.

Regarding climatic variables, mean annual temperature showed an inverse regression to AGB (r^2 adj=0.13, p<0.001; Figure III.7g). Places with a mean temperature <25°C showed the highest estimates (~210 Mg ha^{-1}), in sites with temperature >26°C the AGB was ~110 Mg ha^{-1}. Seasonal climate amplitude during the dry season showed a positive regression (r^2 adj=0.09, p<0.001; Figure III.7h). When the amplitude was <1.9, mean AGB showed the lowest figures (~115 Mg ha^{-1}) and when it was ≥1.9, mean AGB increased (~150 Mg ha^{-1}).

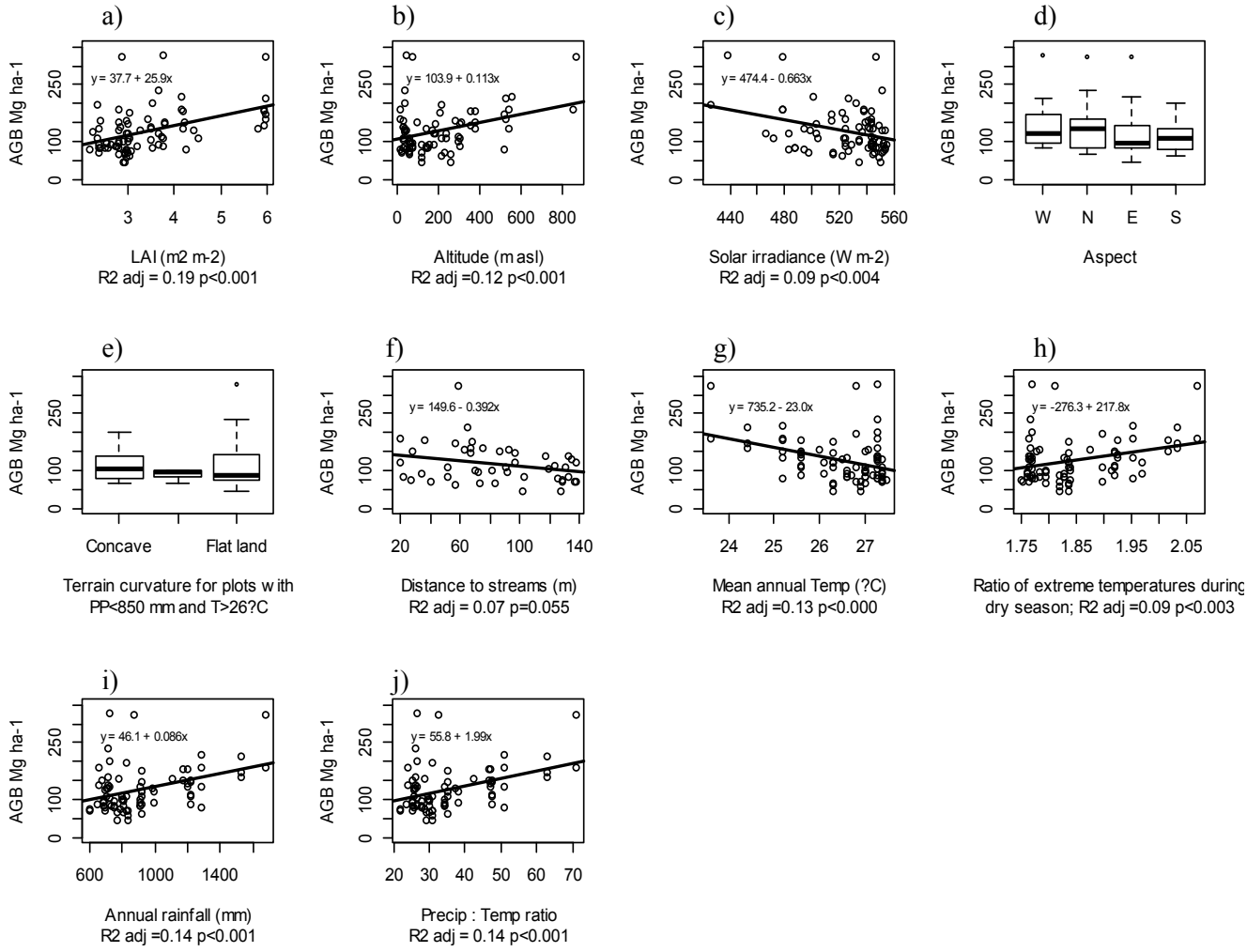

Figure III.7 Significant biophysical variables tested against AGB. (a) Mean annual LAI comes from a MODIS-Terra with a spatial resolution of 1x1 km. (b) Altitude, (c) Solar irradiance, (d) Aspect, (e) Terrain curvature and (f) Distances to streams are derived from a digital elevation model with a spatial resolution of 20x20m. (g) Mean annual temperature, (h) Ratio of extreme temperatures during dry season, (i) Annual rainfall and (j) Precipitation:Temperature ratio, come from WorldClim (Hijmans *et al.*, 2005) with a spatial resolution of 1x1 km. Linear regressions come from ordinary least squares. The regressions report adjusted r^2 and their significance p-value (*p*).

Total precipitation was an important positive factor (r^2 adj=0.14, p<0.001; Figure III.7i). Places with a limited rainfall (<1,000 mm yr^{-1}) showed the lowest mean estimates (~115 Mg ha^{-1}), increasing to ~160 Mg ha^{-1} when the precipitation exceeded 1,000 mm *per* year. Precipitation:mean annual temperature ratio showed a positive correlation with AGB (Figure III.7j): when the ratio was ≥50 mm $°C^{-1}$ mean AGB reached its highest figures (~185 Mg ha^{-1}), reducing the estimates (~120 Mg ha^{-1}) when the ratio was <50 mm $°C^{-1}$.

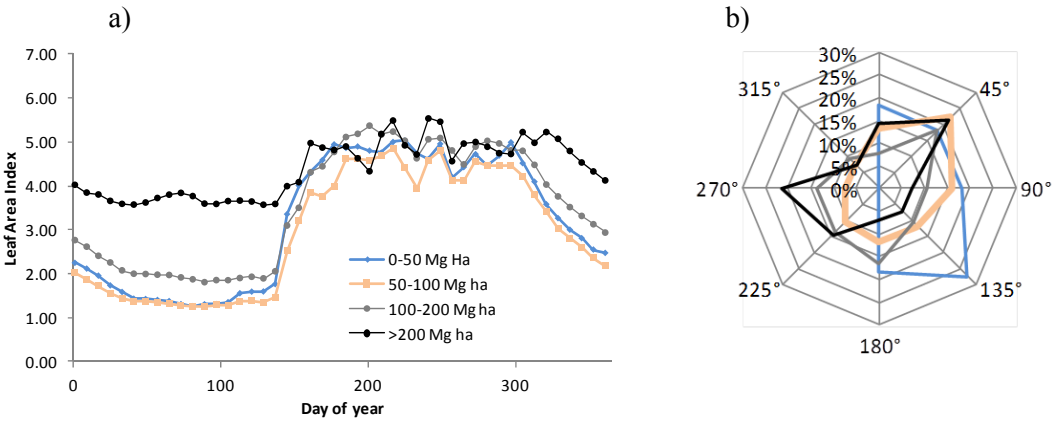

Figure III.8 AGB groups for time series of (a) mean leaf area index (202-2014) and (b) radar chart for samples distribution over different aspect orientations. LAI time series is expressed in m^2 m^{-2} *per* day and aspect is referred to in degrees (°) where 0° is North, 90° is East, 180° is South and 270° is West orientation.

Soil texture was an important factor in explaining AGB. Clay and silt content were inversely related to AGB (r^2 adj =0.38, p=0.003; and r^2 adj=0.18, p=0.041; Figure III.9a and III.9c), while sand content was positively related (r^2 adj=0.30, p=0.009; Figure III.9b). The pH classes showed that strong acidic soils (pH<5.5) had the lowest AGB estimates (~55 Mg ha^{-1}), followed by moderate to slightly acidic soils and neutral soils (~120 Mg ha^{-1}; pH= 5.5-7.3). However, slightly alkaline soils showed the biggest variation in AGB estimates but concentrating its median in ~90 Mg ha^{-1} (Figure III.9d).

The SOC on the top 5 cm did not show any apparent tendency to explain AGB (Figure III.9e). The N stock on the top soil suggested that when the N stock is <1.0 MgN ha^{-1} AGB would be ~130 Mg ha^{-1}, reducing to ~85 Mg ha^{-1} when N stocks are 1.50-1.75 MgN ha^{-1} (Figure III.9f). The highest mean AGB estimate (~115 Mg ha^{-1}) was identified when the mean P stocks <25 kgP ha^{-1} , and reducing to ~95 Mg ha^{-1} when ≥50 kgP ha^{-1} (Figure III.9g). In the C:N stoichiometric ratio <10 the median estimate was the smallest with a value of ~76 Mg ha^{-1}, but with a proportion of 12.5-15 the median estimates reached their maximum (~136 Mg ha^{-1}) (Figure III.9h). In the N:P stoichiometric ratio <12.5 the AGB median estimate was ~95 Mg ha^{-1}, but with a ratio 25-37.5 the maximum median estimates were observed: (~128 Mg ha^{-1}) (Figure III.9i).

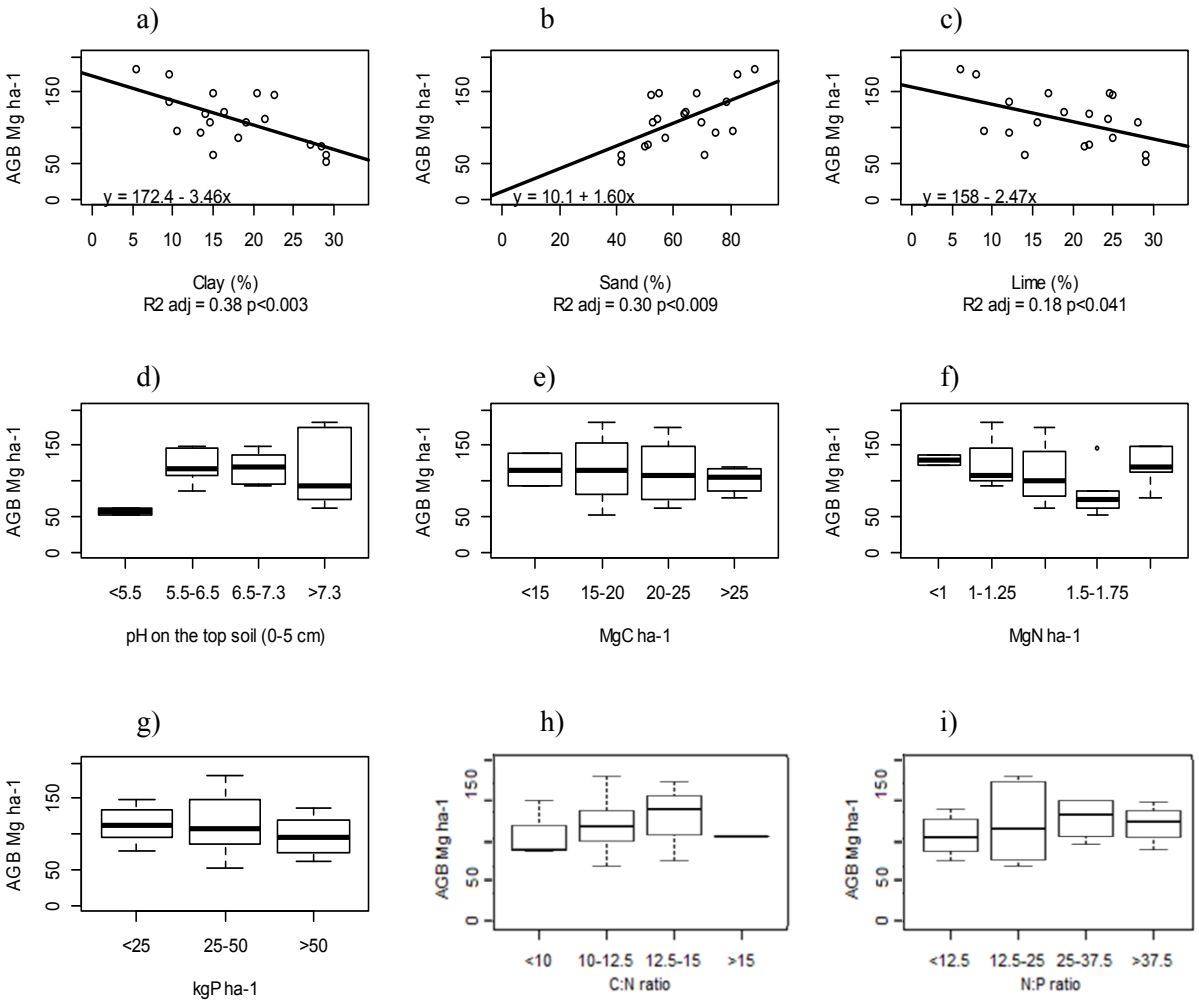

Figure III.9 Significant soil properties for the top 5 cm tested against AGB. (a) Clay, (b) Sand and (c) Silt content are presented in a linear regression to AGB. (d) The potential hydrogen (pH), (e) carbon, (f) nitrogen and (g) phosphorus stocks, and (h) C:N and (i) N:P stoichiometric ratio are presented in boxplots for highlighting general trends in the landscape.

III.4 Discussion

For a proper understanding of AGB in a mature TDF, it is necessary to perform a multi-scale and multi-factorial analysis. Information in this study such as structure and spatial heterogeneity and autocorrelation helped in generating understanding of regional dynamics, and the impact on sampling collection. From a fine scale, it was possible to identify that the main source of uncertainty of AGB is related to small trees. Small trees are highly dense and they represent an important amount of AGB. Information regarding water stress played a significant role in explaining inter-site differences in the ecosystem structure and dynamics for AGB potentials. Information such as soil physical and chemical properties, topography, and bioclimatic factors are important to understand the spatial dynamics in AGB.

III.4.1 Community assembly, spatial configuration and AGB uncertainties

Different authors (Chave *et al.*, 2003; Chave *et al.*, 2004; DeWalt and Chave, 2004; Slik *et al.*, 2010; Ruiz-Jaen and Potvin, 2011; Slik *et al.*, 2013) have shown that forest structure is necessary to explain AGB but their performance is different across sites. In this study it was possible to identify that TDF has a higher number of trees with DBH <30 cm, and it shows an inverse J-shaped tree-size distribution. This suggests that the forest is a mature natural forest with proper regeneration and continuous replacement (Hall and Bawa, 1993; Lykke, 1998; El-Sheick, 2013). Tree density seems to be highly variable across different tropical forest. For example, this site showed a higher density than another mature TDF (Gillespie *et al*., 2000), and more than a tropical moist forest (Chave *et al*., 2003) but similar to another TDF in Mexico (Jaramillo *et al.*, 2003; Gallardo-Cruz *et al.*, 2005) and to other TDFs in Latin America (Trejo, 1998; Jaramillo *et al.*, 2003; Marín *et al.*, 2005; Powers *et al.*, 2009). Nevertheless, the proportion of number of trees *per* diametric class does not differ significantly from a moist forest (Chave *et al*., 2003), in lowland Neotropical forests (DeWalt and Chave, 2004) and other TDFs (Jaramillo *et al*., 2003; Marín *et al*., 2005). This suggests that community assembly depends highly on the proportions of the individuals, rather than in the overall number of trees as might have been inferred.

The allocation of trees depends on a multi-variable inter-correlation of micro-climatic and micro-topographic conditions, and/or the result of intra-species rather than inter-species competence for light or nutrients, as has been argued by others (Hubbell, 1980; Gonzalez and Zak, 1994; Condit *et al.*, 2000). Soil properties, tree allocation (AGB and BA *per* trees ≥30 cm) did not show spatial autocorrelation. This implies that at tree level the community was spatially heterogeneous and the tree-spatial distribution did not show an assembly of patches of similar biodiversity and/or biophysical properties as was suggested by earlier authors (Hubbell, 1979; Levings, 1983; Murphy and Lugo, 1986b; Condit *et al.*, 2000). However, at the level of landscape, AGB and BA did show spatial autocorrelation. AGB was more highly influenced by water stress than BA. AGB showed a similar range of spatial autocorrelation with topographic changes, mainly in altitude and distance to streams. These factors may affect water availability and solar irradiance; as a result, the competence inter- and intra-species play an important role in mean canopy height which indirectly impact on AGB estimates (Ruiz-Jaen and Potvin, 2011). These may also result in biodiversity changing over similar ranges (He *et al.*, 1996). Based on these results we can answer Q1 by suggesting that there is not spatial autocorrelation in AGB beyond the local scale because AGB and soils' properties in the landscape are heterogeneous. Therefore, to have a proper representation of the landscape, and the variables that drive the AGB allocation, it is necessary to implement strategies to capture the range of AGB variability in space and magnitude. However, more research is needed to understand how micro-topographic changes might affect landscape AGB estimates. There are some suggestions that make us believe that AGB and tree biodiversity vary over similar spatial

ranges (He *et al.*, 1996). So it is important to begin exploring the influence of tree species diversity on spatial AGB distribution (Ruiz-Jaen and Potvin, 2011).

Mean BA and AGB proved to be similar to other reports (Gillespie *et al.*, 2000; Jaramillo *et al.*, 2003). BA distribution across diametric classes was similar to those reported for others' TDF (Jaramillo *et al.*, 2003; Marín *et al.*, 2005), where most of the BA (67%) is measured in trees with DBH <30 cm. However, trees with a DBH ≥50 cm represent almost double the amount of BA than that reported by Marín *et al*., (2005) and Jaramillo *et al*., (2003). The mean AGB fell within the reported range for this type of forest (Brown and Lugo, 1982; Brown and Lugo, 1990; Murphy and Lugo, 1986a). It was however higher than others reported for a TDF in Puerto Rico (Murphy and Lugo, 1986b) and Mexico (Jaramillo *et al.*, 2003; Martínez-Yrízar *et al*., 1992).

Forest inventories and allometric equations may drive significant changes in the understanding of this ecosystem with major implications for AGB. On the one hand, forest inventories have focused mainly on classes with DBH ≥10cm (Brown, 1997; Keller *et al.*, 2001), because smaller stems are considered principally important in young and secondary forests. On the other hand, allometric equations produce different AGB estimates *per* tree. These can lead to substantial differences in the understanding of the community assembly and AGB estimations at the landscape scales. At tree level, different allometric equations have shown that large trees (DBH ≥75 cm) were the most uncertain AGB estimates, as other authors have suggested (Baker *et al.*, 2004; Chave *et al.*, 2004). However, large trees (DBH ≥60 and 75 cm) are scarce in the TDF landscape which means that they have little impact on mean AGB estimates at the landscape scale (~20 and 11%, respectively). Similar observations have been reported in other tropical ecosystems (Keller *et al.*, 2001; Chaturvedi *et al.*, 2011), and our number is slightly higher than the 13% reported by Nascimento and Laurance (2002) for trees DBH ≥60. Whereas small to medium-sized trees (DBH <30 cm) are important, because their high abundance may contribute to the greatest biomass (>60% of the AGB) - as found in other reports (Baker *et al.*, 2004) and up to ~80% (Jaramillo *et al.*, 2003; Chaturvedi *et al.*, 2011). This has led to the conclusion that it is little differences across different allometric equations on small to medium-sized trees which have the greatest impact on a landscape scale, as they also do on the uncertainty (Keller *et al.*, 2001). Finally, the underestimation of small-sized trees may represent an important AGB loss (Keller *et al.*, 2001). They can represent about 15% loss, or 8% for trees under 10 or 5 cm in DBH, respectively, similar to proportions reported for another mature TDF in Mexico (Jaramillo *et al.,* 2003) and smaller than that reported by Read and Lawrence (2003). Based on these, the results for the Q2 is that large stems are not the major contributors in AGB estimates. Most of the TDF biomass is allocated to trees with a DBH<30 cm. Moreover, to reduce the uncertainty on AGB estimations at landscape scale, forest inventories should implement a full sampling collection for every stem, and allometric equations should be improved for small to medium-sized trees (<50 cm in DBH).

III.4.2 Little can be extrapolated from soil nutrients to understand AGB

Mature forest AGB shows fewer linear regressions to soil properties as could be inferred from studies done under different secondary forest or chronosequences (Christensen and Peet, 1984; de Castilho *et al.*, 2006). In this study different soil properties were similar to other TDFs, for example, pH (Lugo and Murphy, 1986; García-Oliva *et al.*, 1994; Wick *et al.*, 2000; García-Oliva *et al.*, 2006), soil textures (García-Oliva *et al.*, 1994), N and P (Lugo and Murphy, 1986; Campo *et al.*, 1998), and C:N and N:P ratios (Cleveland and Liptzin, 2007). However, in contrast with other studies a higher C concentration was identified for the topsoil, though similar figures for the first 20 cm. These differences were the result of the sampling collection that took place during the dry season when all micro nutrients accumulate (Jaramillo *et al.*, 2011). Moreover, this study did not find any evidence to suggest that N or P play an important role in AGB, in contrast with some other studies in secondary and chronosequences (Elser *et al.*, 2007; LeBauer and Treseder, 2008), while the C:N and N:P ratios were shown to be important to explain AGB, similar results to other authors (Mirmanto *et al.*, 1999; Slik *et al.*, 2010; Wright *et al.*, 2011; Alvarez-Clare *et al.*, 2013). This can be understood on the basis that mature forest is not as highly nutrient demanding as a secondary forest; and these results accord with those reported by Wright *et al.*,(2011) and Mirmanto *et al.*,(1999). Moreover, Ruiz-Jaen and Potvin (2011) found that the proportion of nitrogen fixer species play a major role in explaining AGB in N-limited forest. This can suggest that this forest, dominated by N-fixers (Salas-Morales *et al.*, 2007), establishes important symbiotic nitrogen fixation processes that help it overcome N-limitations.

III.4.3 Water stress is the main driver of AGB allocation at different scales

At various spatial scales, the important predictor variables were directly or indirectly correlated to water stress with implications for AGB, endorsing similar results reported for another arid region (Snyder and Tartowski, 2006).

At the local scale, soil texture actively mediates water availability (Sperry *et al.*, 1998; Sperry and Hacke, 2002). In particular, in the TDF sandy loam textures have good drainage, good water-holding capacity and the right amount of movement of soil air, helping the development of plants during the rainy season, and to overcome the dry season when water uptake is hydraulically limited (Hultine *et al.*, 2005). Trees in these textures are highly sensitive to small precipitation pulses which reflect on the carbon sequestration (Fravolini *et al.*, 2005) with significant implications for local and regional AGB.

At sub-regional scale, topographic variables also played an important role in explaining water stress. For example at higher altitudes less potential evaporation happened due to a reduction in

temperature and an increase in precipitation (SMN, 2014). This study showed that higher AGB estimates were measured at higher altitudes as a result of a reduction of water stress and not because of higher restrictions for anthropogenic disturbances, as had been suggested from landscapes dominated by disturbed forests (de Castilho *et al.*, 2006; Alves *et al.*, 2010; Woollen *et al.*, 2012). On the contrary, at lower altitudes precipitation is significantly reduced with an increase in evaporation. Some other topographical variables correlated indirectly to bring shelter to plants against water and nutrient stress, such as terrain curvature (Cusack *et al.*, 1997; Gessler *et al.*, 2000) and aspect (Galicia *et al.*, 1999; Bijalwan, 2012). Distance to streams showed an inverse correlation to AGB (Cusack *et al.*, 1997; Rango *et al.*, 2006), but to a degree only valid in the first hundred meters; this can be related to root systems which catch lateral distribution of water. While some authors (de Castilho *et al.*, 2006; Alves *et al.*, 2010) found that slope plays an important role in AGB distribution, we did not find any clear pattern, but this can be related because those studies may be allocated to different disturbance processes.

At the landscape scale, climatic variables correlated more strongly to AGB. On the one hand, temperature correlated inversely to AGB, mean annual temperature and intra-seasonal temperatures' variability. This suggests that in sites where temperature does not vary significantly during the rainy season plants tend to be more water stressed than in those areas with more variability, among which are mainly great differences during day and night when in the latter, plants re-hydrate themselves (Reich and Borchert, 1984). On the other hand, rainfall and precipitation:temperature ratio correlated positively to AGB. Where sites with higher precipitation or higher ratio of precipitation *per* °C shows less water stress and as a result, higher AGB, as other studies suggested (Murphy and Lugo, 1986b; Martínez-Yrízar *et al.*, 1992; Jaramillo *et al.*, 2003; Read and Lawrence, 2003).

It is important to highlight that water stress did play its part as the major driver on AGB and SOC. For example, this site is among the highest SOC reports for the first 50 cm, and this is in contrast to other TDFs in Mexico. This region shows a higher precipitation than other TDFs in Mexico, promoting faster soil mineralization, and as a result, higher SOC.

Finally, mean and seasonal LAI were capable of capturing the seasonal water availability by leaf expression and senescence (Reich and Borchert, 1984). Sites with a higher mean LAI or with less inter-seasonality correlated to sites with less water stress, and they also showed higher AGB estimates. These processes can be related to the cycles of carbon up-take, suggesting that sites with less inter-seasonality have a longer growing period and as a result, higher AGB estimates, which follows similar observations done by Kenzo *et al.*, (2010). LAI did not correlate to forest structure (number of trees) as might have been expected. However, the major limitation of using MODIS-LAI is that some pixels might display a mixture of signals of natural vegetation and anthropogenic disturbances and the observations may not fully represent the LAI.

III.4.4 A multi-scale conceptual integration

Mature forest AGB is the expression of multiple factors which co-evolve over different spatial and temporal scales, as similarly observed by Poisot *et al*., (2011). Our results suggest that at the local and landscape scale water availability is the major variable constraining AGB estimates. However, our variables are not capable of explaining AGB estimates >300 Mg ha^{-1}. In those sites at least three colossal trees with DBH≥45 cm were recorded. This failure in reproducing very high AGB estimates could be the result of the spatial resolution of our data sets, which is similar to results reported by de Castilho *et al*., (2006). The understanding of large-sized tree allocation on a local scale is not simple because of the complex interaction of biotic and abiotic elements. Some authors argue that large-sized tree allocation is the result of biotic interactions which modify the competitive ability of plants (Yeaton *et al.*, 1977; Hubbell, 1979, 1980; Gonzalez and Zak, 1994; Condit *et al.*, 2000; Lucero *et al.*, 2006). Also Korner (2007) suggested that it is the result of gradients in light availability mediated by local topography, soil and air temperature, which creates different types of light microhabitats. However, Arriaga *et al*., (1993) found that soil nutrient content and shade-sun conditions do not seem to explain the patchy distribution of perennial plants. In any case, such information is difficult to acquire on a landscape scale with such a degree of detail, and the most conclusive studies were done on continental or global scales (Slik *et al.*, 2013), where climatic variables explain AGB and density of large-sized trees. This study answers Q3 by showing that water availability is a key limiting factor for AGB across different scales in a TDF, but it is not the only one. Soil properties, topographic and climatic variables explain AGB trends and capture mean estimates across the landscape. Leaf deciduousness correlated to AGB due to water availability, mainly during the dry season. At the local scale, it also explained AGB estimates by topographic and soil properties. However, some AGB estimates cannot be understood, particularly explaining the presence of very large-sized trees. This suggests that there are other factors that are influencing AGB estimates and that they can only be captured with a finer spatial resolution and/or a multi-variable approach that could improve the understanding of such large AGB estimates.

III.5 Conclusion

TDF is highly heterogeneous not only in landscape structure but also in tree species, resulting in AGB distributed in patches. In a landscape like TDF, which is dominated by small stems, with a fine scale sampling collection, the landscape is not over simplified, and primary variables that drive AGB at local and landscape scales are captured. In this chapter, by excluding the outliers, the mean AGB estimates followed a normal distribution and fell between the reported ranges for similar vegetation type and rainfall, with no statistical differences between different sampling designs. The community structure was mainly driven by small trees, which account for much of the AGB estimates, contrasting with results reported for other tropical forests. Small-medium-sized trees (DBH ≤30 cm) induced the highest

uncertainty in AGB estimates. While possibly a significant source of uncertainty could be tackled using a local allometric equation for trees within 5-40 cm in DBH, the high uncertainty that those equations can provide may not reduce it significantly, in contrast to the current Pantropical equation. In a mature TDF, water availability plays the major role as far as explaining AGB in a local, sub-regional and landscape scale is concerned. Plants stressed for water availability may be affected directly and indirectly by climate, topography and soil physical properties. LAI was shown to be a useful index for AGB estimates across large spatial scales. From these results, it is possible to suggest that there are other underlying variables that could not be captured, thus misleading the AGB estimates, mainly where large-sized trees were present. Soil nutrients play an important role in regeneration processes, but how they link into AGB estimates in a mature forest is not well documented. Therefore, future models should look into how fine-scale patch dynamics may be coupled on broader scales to make a better representation of AGB and its potential implications for climate change risks. Moreover, more research is necessary to understand how nutrients are distributed and how they may correlate with climatic factors and how they correlate with AGB in mature forest, rather than focus the studies under regeneration processes and extrapolate the outcome to mature forest, which may influence the understanding of the ecosystem dynamics.

Chapter IV. The spatial heterogeneity of carbon sequestration potential in a tropical deciduous forest can be driven by model selection

IV.1 Abstract

Information regarding how non-human disturbed (potential) AGB is spatially distributed in the landscape and what factors may affect it is of importance for prioritize areas for the implementation of REDD+ projects and for understanding the ecological constraints that limit the magnitude and the allocation of carbon stocks. The aim of this chapter is to identify the factors that influence the reconstruction of the spatial heterogeneity of potential AGB that could be expected under current climate trends and without human disturbances. Here a survey of 83 field plots was applied, with an area of 300-400 m^2 and eight plots of 1 ha each. The plots were allocated in mature, undisturbed forest across major landscape gradients to investigate the AGB spatial constraints. To reconstruct the spatial heterogeneity of carbon sequestration potential, the potential AGB was reconstructed by 7 statistical techniques. This is the first study to test the performance of various techniques in predicting potential AGB from field observations and biophysical variables. The results suggest that GLM and GAM performed similarly and outperformed other more complex models. By re-scaling the information into coarser resolutions, the model also has a significant predictive power against independent data. The next 2 best models were automated neural networks (NN) and simple regression tree (RT). The models that performed with the lowest accuracy against independent data were Generalized Linear Mixed Models via Penalized Quasi-Likelihood, MaxEnt and Random Forest. The GLM, NN and RT models returned comparable mean AGB predictions to field AGB, suggesting that the potential carbon stock in the 215,687 ha evaluated is between 11,000 and 13,000 GgC. The spatial heterogeneity across AGB estimates coming from the different models shows that NN and RT tend to be biased, and estimations tend to be clustered while the GLM model was capable of reproducing the spatial patterns of observations.

IV.2 Introduction

The deforestation in the tropics has been considered an important source of carbon emissions and as a consequence a great driver of climate change (Houghton, 2005a). However, the uncertainty of such estimations is large. To estimate current carbon stock and the rate of loss (flux) some authors have estimated the loss of biomass by considering a mean deforestation rate and a mean of biomass (Achard *et al.*, 2002; DeFries *et al.*, 2002; Achard *et al.*, 2004; Houghton, 2005a). Others have estimated AGB over different time steps (Harris *et al.*, 2012; Ryan *et al.*, 2012; Collins and Mitchard, 2015). However, these losses are not able to estimate the total AGB that has been lost and they can mislead understanding of where the major AGB losses occurred, mainly as a result of the saturation point of modeled AGB. Current human disturbance may bias the understanding of deforestation and carbon losses. These differences can lead to higher AGB estimate uncertainties than the measured AGB losses. Nevertheless, these methodologies are useful for implementing conservation strategies to reduce the impacts of deforestation on carbon stocks.

To mitigate climate change and to reduce the impacts on ecological processes, both REDD+ and CDM projects should take into consideration the potential biomass that can be reached in the landscape and to understand its spatial heterogeneity (Mason *et al.*, 2012). With the assessment of potential AGB it is possible to estimate the total carbon emissions that took place in the past which cannot be estimated by other means, for example in agricultural fields (Exbrayat and Williams, 2015) or cities (Doko *et al.*, 2014; Lentz *et al.*, 2014). In any case, the understanding of the potential carbon sequestration will enable to estimate the total losses due to anthropogenic activities. Moreover, it will be possible to evaluate if a particular place has lower AGB than expected as a result of disturbances or as a result of natural constraints. And, it will help in to prioritize the implementation of restoration programs and/or land management.

AGB allocation can be understood as a multi-factor expression over multiple spatial scales, as explained in Chapter III. However, these factors interplay along the landscape, and they impact the expression of potential AGB (AGB_{pot}). Models capture the multiple responses differently and interactions among the variables; as a result, they may represent the AGB contrastingly. Thus, the critical question to be addressed of this chapter is, what are the main responsible factors to drive and to bias the AGB allocation in the landscape? To be able to answer this general question, this chapter was focus in four specific questions:

Q1. Are contrasting models returning similar mean estimates at broader scales?

Q2. Does more complex algorithms have a better performance to fit non-linear relationships when there are data limitations in observations and predictor variables?

Q3. What are the different sources of uncertainty in the models predictions?

Q4. Does the models performance are similar over different spatial scales?

IV.3 Results

Simple bivariate correlations to predict AGB are not enough to explain AGB>175 Mg ha^{-1} (Chapter III). However, with the proper model and variables it is possible to improve the accuracy of predicting AGB. This would contribute to better understanding of the factors that drive the allocation of AGB and make it possible to explore the spatial heterogeneity of potential AGB. Diverse variables, mainly those related to water stress have the capability to predict AGB. However, climatic variables exhibit high sensitivity, which drove the highest discrepancies in reproducing AGB. Model selection played a significant role in variables selection, as well as AGB spatial representation. However, not all the models have the capability to improve the null model. The scale of analysis is essential to understand the execution of the models and to explore the spatial heterogeneity of AGB. The top three best models display major contrasts in a local scale while the total AGB estimates were congruent at a landscape scale. These phenomena can be related to the sensitivity of the proportions of the selected observations during the calibration process and/or the capability of the models to predict across the extent of its calibration range. Because most of the landscape is dominated by low AGB estimates, models showed good ability to reproduce them. However, this is not true for high AGB estimates which have led to great variations in the spatial representation. Moreover, each model with its own algorithm was able to expose different forms of bias towards some biophysical variables, mainly to explain middle and high AGB estimates, and so producing significant changes to the previously perceived spatial heterogeneity of AGB.

IV.3.1 Multi-variable correlation to AGB

The most meaningful predictor variables identified across the models were: altitude (A); aspect via folded transformation (As); compound topographic index (CTI); distance to streams (DS); probability of deciduousness (PD); solar irradiance (SI); mean annual temperature (MT); and total precipitation (TP). However, climatic variables were excluded from further analysis because they make a great impact on the potential AGB. In Figure IV.1 can be seen that under a MC simulation all the selected variables predict the potential AGB close to the observations, in range and mean. On the one hand, MC model is the result of the Monte Carlo simulations when the different predictor variables are included under the MC analysis. The result shows similar distribution and range as the observations. On the other hand, when all the predictors are static and only one factor is variable, the sensitivity test shows that SI was the most significant to impact on AGB predictions but the predictions fall within the range of the observations. Contrary to the same test when using climatic information. When climatic information was used, the AGB prediction range exceeded over two orders of magnitude the maximum AGB that the ecosystem may reach. With the Spearman's correlation, it is possible to notice that SI had the strongest negative

correlation to AGB, followed by As and CTI. On the contrary, A, DRs and PD returned a positive correlation to AGB (Figure IV.1).

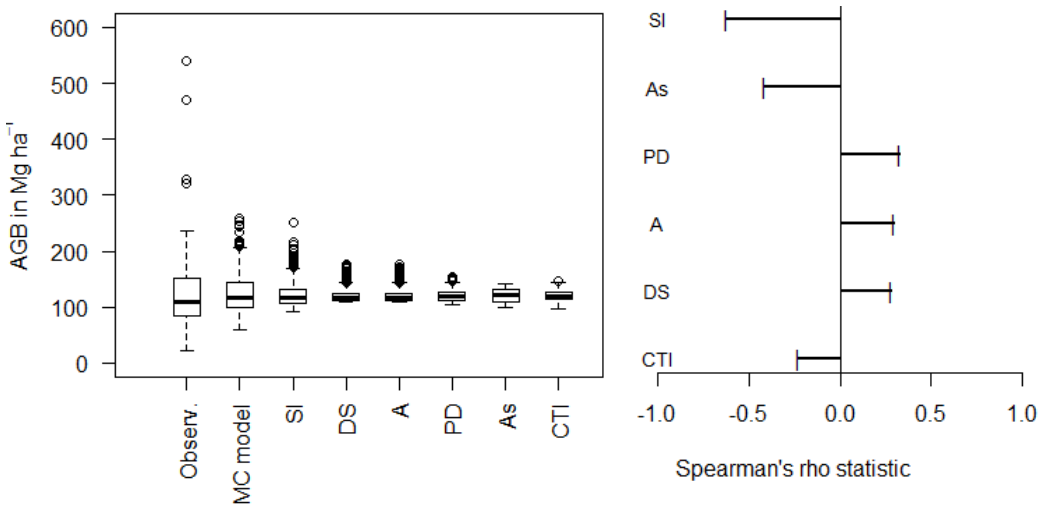

Figure IV.1 The figure on the left shows the Monte Carlo simulation for sensitivity test for the predictor variables. The panel at the right-hand size shows the Spearman's correlation between predictor variables and observed AGB under MC simulations.

IV.3.2 Models validation

The tested models exhibit diverse performance in predicting AGB_{pot} (Figure IV.2). Different statistical methods that reproduce significantly to AGB_{pot} are: GLM (RMSE=38.8 Mg ha^{-1} and bias=1.3 Mg ha^{-1}); GAM (RMSE=38.5 Mg ha^{-1} and bias=1.2 Mg ha^{-1}); NN (RMSE=54.8 Mg ha^{-1} and bias=13.4 Mg ha^{-1}); RT (RMSE=59.0 Mg ha^{-1} and bias=5.9 Mg ha^{-1}); and RF (RMSE=66.4 Mg ha^{-1} and bias=2.6 Mg ha^{-1}). Four models were excluded from further analysis: two of them showed low accuracy to reproduce observed AGB (MaxEnt and GLMM); the other two (RF and GAM) because their predictions did not improve the achievement of a simpler model. RF achieved more similar predictions than RT. However, the latter revealed more precision across the predictions, and the model was less complex. Moreover, RF reproduced the calibration samples accurately, but predictions against the independent validation samples displayed a reduction in accuracy to reproduce observation with AGB >200 Mg ha^{-1}. Though GAM produced almost identical predictions to GLM, it was excluded from being a more complex model. To ensure that the lack of predictability of RF and MaxEnt models was not related to the limitation caused by the low number of employed variables, the models were re-tested with all the other predictor variables. The predictions did not however significantly improve in contrast with the original parsimonious model.

Only GLM, GAM and NN models produced a 95% CI for predictions over the perfect fit, which suggests that validation samples fall in between the 95% CI. Also, these models showed a more

constrained uncertainty in estimates <300 Mg ha^{-1}. Though the RT model offered a constrained 95% CI across predictions, the mean predictions produced a good match for AGB <300 Mg ha^{-1} against independent validation samples (Figure IV.2).

Most of the modelled AGB_{pot} estimates performed better than the null model (RMSE 77.9 Mg ha^{-1} and bias of 22.8 Mg ha^{-1}). For example, there was a reduction of 50% of the RMSE for GLM, 24% for RT and 30% for NN. Regarding the bias, an analogous reduction trend was observed (in 95% for GLM, 74% for RT and 41% for NN).

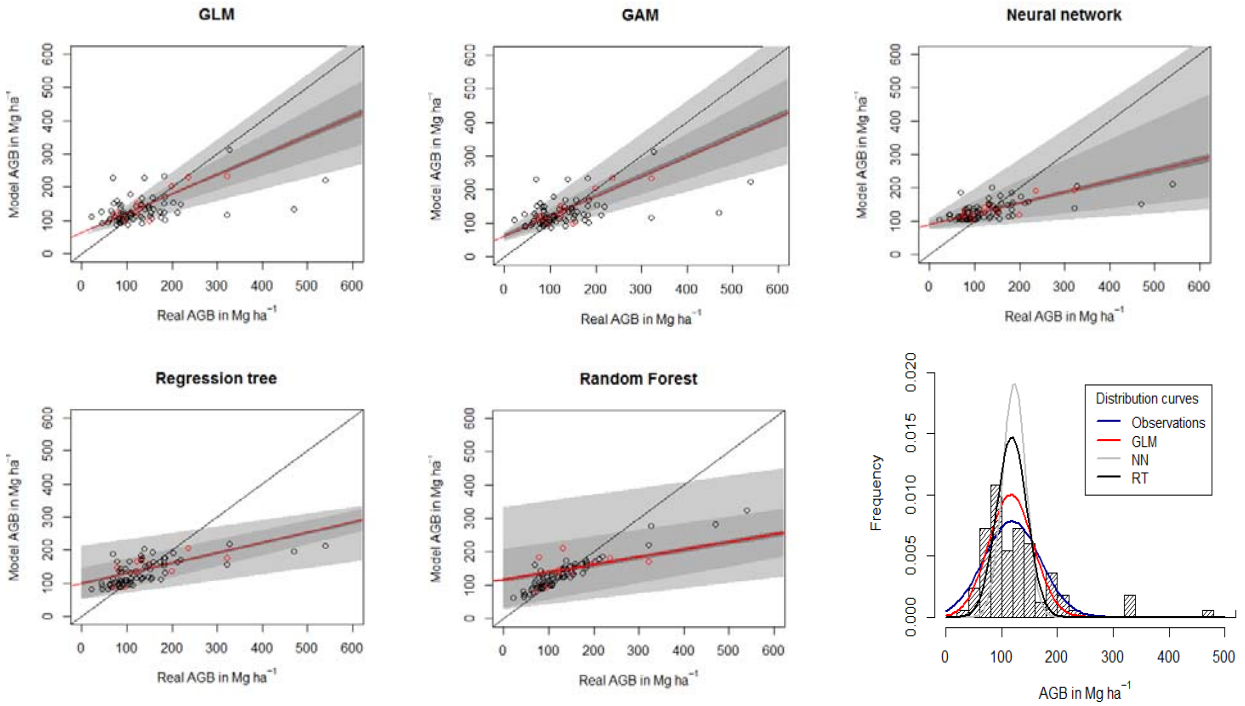

Figure IV.2 Scatter plots for observations and predictions. Black circles refer to calibration, and red circles refer to validation. Light grey shade represents the 95% CI for predictions, darker grey represents the standard deviation, and the darkest grey corresponds to the 95% CI around the fitted line. The histogram bars refers to field observations. Different lines express the distribution of the predictions in the landscape. The blue curve is the normal distribution of the observations. The red, grey and black curves represent the models' prediction, GLM, NN and RT, respectively.

At finer resolution (300-400 m^2) the GLM, RT and NN mean estimations were statistically similar to the observations. The mean AGB for the observations was 132.8±83.4 Mg ha^{-1} (STD), while GLM produced a mean estimate of 133.0±40.8 Mg ha^{-1} (W=1,372 *p-value*=0.09), RT of 132.1±37.1 Mg ha^{-1} (W=1,347 *p-value*=0.07) and NN of 131.5±26.9 Mg ha^{-1} (W=1,373 *p-value*=0.09) (Figure IV.2). When the predictions were up-scaled into plots measuring a quarter of a hectare and 1 hectare and contrasted against independent observations (N=32 and N=8, respectively), overall GLM was the best model in reproducing the mean estimates. When the mean prediction failed, the observed AGB fell in between the 95% CI for predictions. The CI in GLM tended to be wider (low precision) in sites where mean estimates differed to those observed, but the CI was constrained (high precision and high accuracy) when the mean

estimates were close to the perfect fit. RT and NN revealed lower precision in the modelled AGB estimates. The mean predictions were comparable to the mean AGB used during the calibration, suggesting that the models were not able to restrict the AGB predictions (Figure IV.3). This mechanism produced reduced RMSE and bias. For example, NN was the model with the smallest figures (RMSE 26.2 Mg ha^{-1} and bias -19.3 Mg ha^{-1}). GLM was the model with the highest bias and RMSE (RMSE 33.4 Mg ha^{-1} and bias -20.3 Mg ha^{-1}) and RT fell in the middle of both (RMSE 29.7 Mg ha^{-1} and bias -21.0 Mg ha^{-1}). Particularly for GLM, solar irradiation was the main driver to explain the bias in AGB. Places with a reduced solar irradiation (<450 W m^{-2}) overestimated AGB.

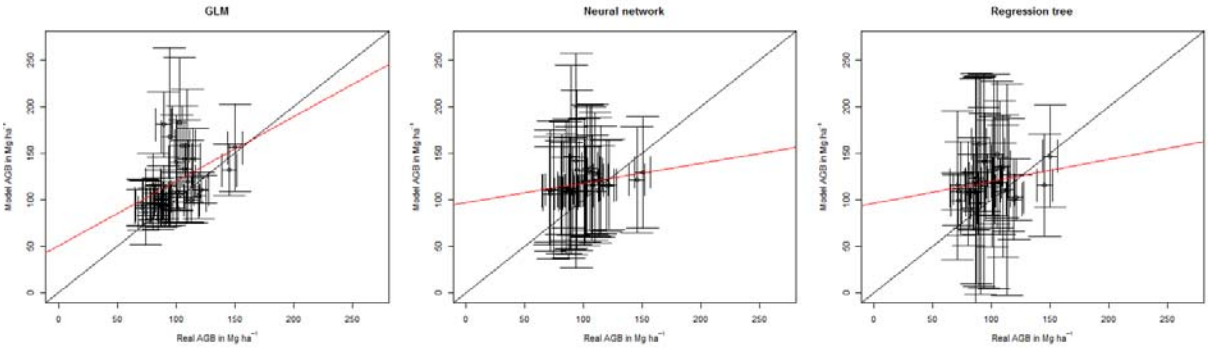

Figure IV.3 Scatter plots for 2,500 m^2 and 1 ha observations and predictions. The bars in axis X refers to the 95% CI for observations, while the bars in the axis Y correspond to the 95% CI for the predictions. The red line refers to linear regression between observed and modelled; the black line refers to the perfect fit.

IV.3.3 Models' uncertainty

There are major differences in the precision and accuracy of the models to estimate the AGB across the landscape. The CI and CV across the models exhibit different performances and patterns. For example, the GLM model showed the highest precision in the estimates with higher accuracy among the other models, with a mean CV of 11±4%. The lowest CV figures were related to AGB estimates <200 Mg ha^{-1}, wherein most of the cases the CV was <10%, representing 96% of the landscape. The highest CV was identified for high AGB estimates (≥500 Mg ha^{-1}) with a mean of 43% (ranging in between 20 and 80%). However, this only represents 0.05% of the landscape. The RT model restricted the AGB estimates which promoted a higher precision over the various bootstraps. This model demonstrated the most constrained CI along the models, but the mean CV was higher than GLM (26±9%). The lowest CV was spotted for predictions ≥160 Mg ha^{-1} with a mean of 20%, but this only represents a limited area of the landscape (11%). However, the highest CV (mean of 25% and ranging in between 15 a 70%) is dominantly represented across the landscape (60% of the area) where AGB estimates are <115 Mg ha^{-1}. Of the three models the NN model performed most poorly. Overall its mean estimates were akin to the observations, but the CI and the CV showed poor performance. The lower limit of the CI tended to be

roughly constant around 100 Mg ha^{-1}, while the upper boundary reached figures over 600 Mg ha^{-1}. The low precision and accuracy of this model tells us that NN has a very wide CI, and the mean CV tend to be the highest (35±14%), where <12% of the landscape has a CV under 20% (Figure IV.4).

At landscape scale, the total above ground carbon (AGC) stocks are comparable between models and the extrapolation from field observations. This suggests that at this scale models and observations present similar mean AGB (Figure IV.5), suggesting that AGC in the landscape is between 11,000 and 13,000 GgC (Figure IV.4 and Figure IV.5).

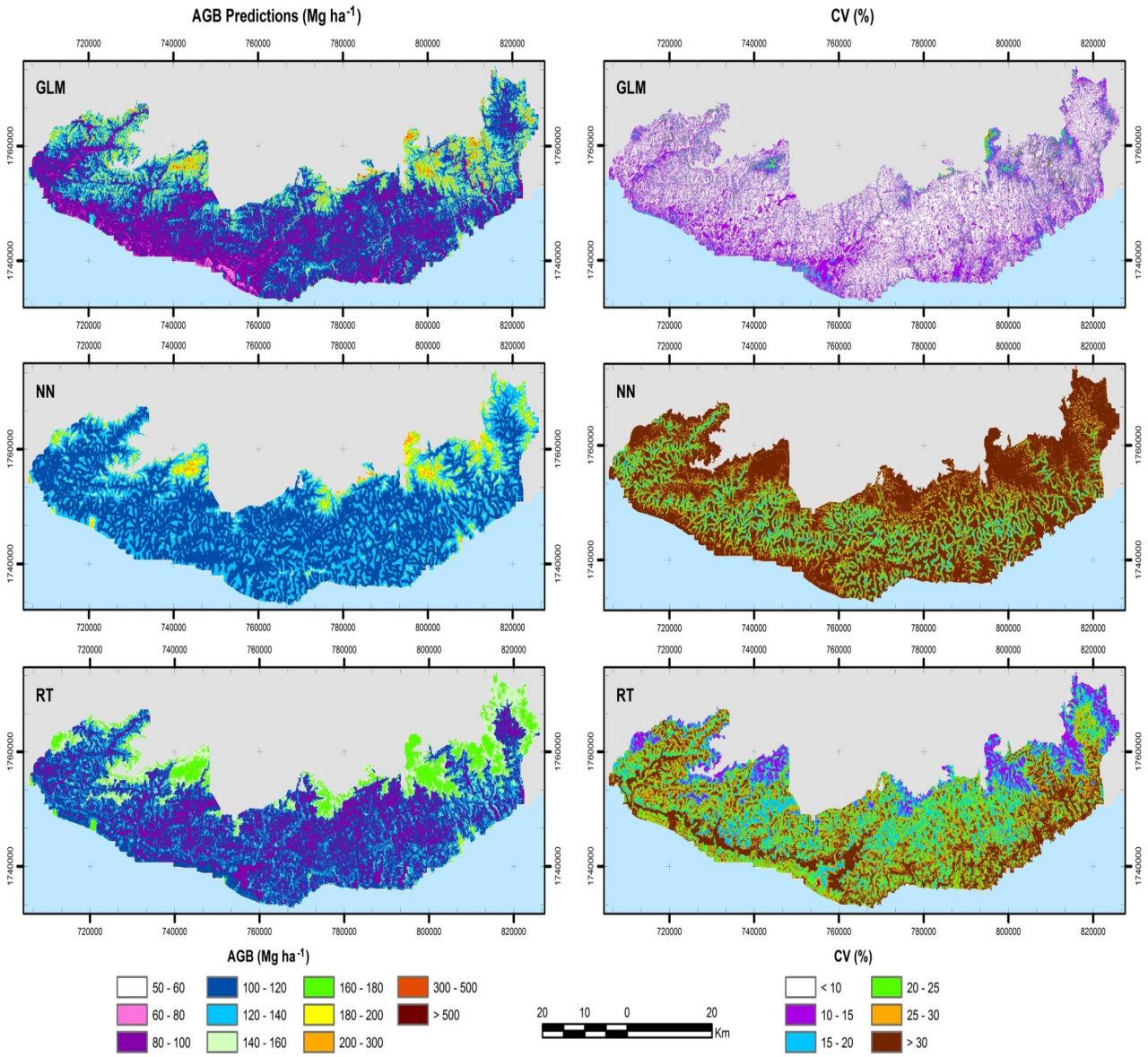

Figure IV.4 Potential biomass (Mg ha^{-1}) and CV (%) distribution for GLM, NN and RT.

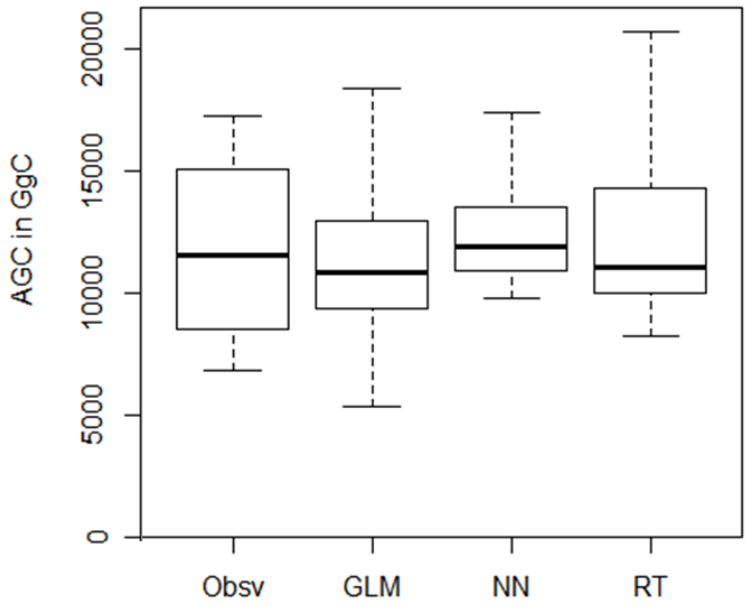

Figure IV.5 Boxplots of different extrapolations for potential carbon stock in the landscape. The total area used for the landscape is 215,687 ha and the carbon content in wood is 47.25% (Chapter III).

IV.3.4 Spatial heterogeneity across the models

Major contrasts in the AGB estimates are at the local scale. The models showed divergent magnitudes (Figure IV.6) in about 50% of the landscape when the mean estimates were over the mean AGB recorded in the field. NN and RT models produced the most similar spatial distribution of the AGB (r^2=0.58, Figure IV.6). Main similarities across the models were for AGB under 120 Mg ha^{-1}. The largest discrepancies were the result of the limitations of NN and RT to make extrapolations over the upper calibration limit. In both cases, when GLM predictions were over 250 Mg ha^{-1}, NN and RT predictions were highly imprecise (grey shades in Figure IV.6).

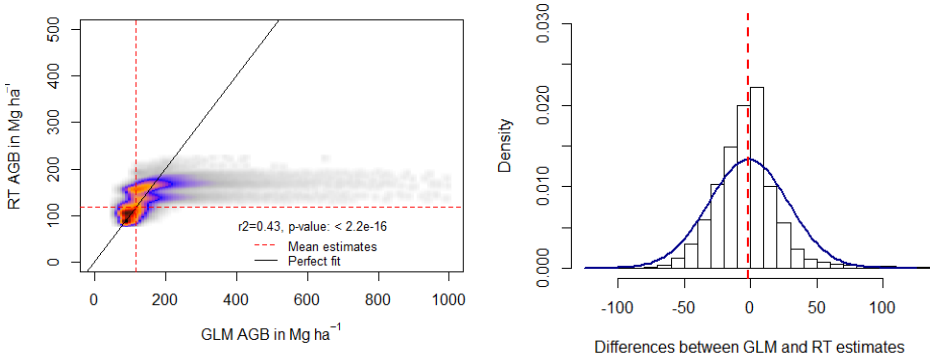

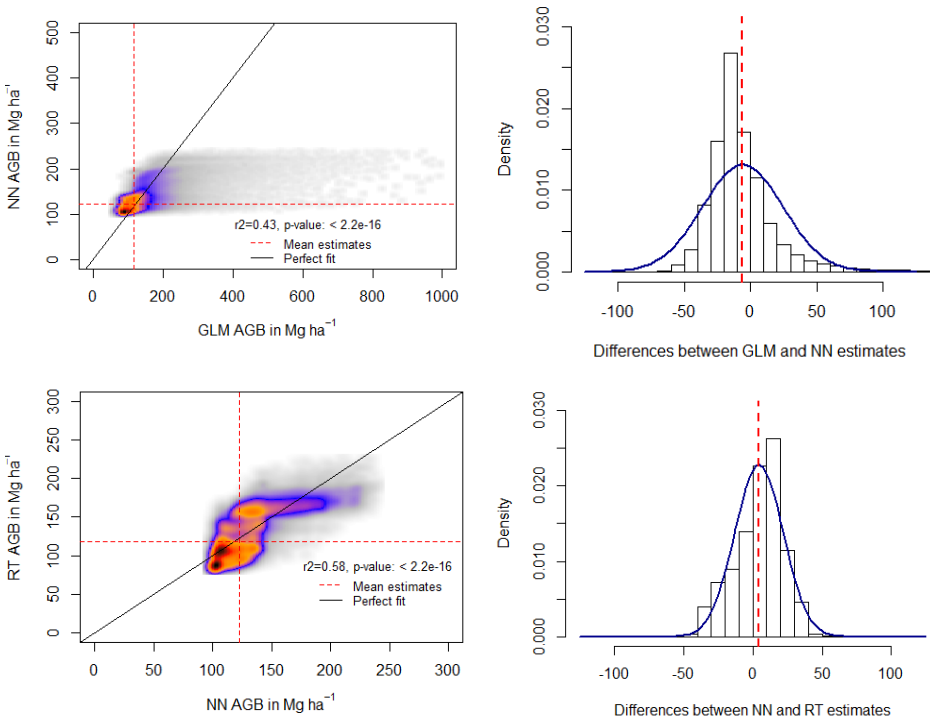

Figure IV.6 The smoothed scatter plots present the correlation across models' predictions. The colors represent the density observations for a certain pair of AGB estimates. Grey light shades represent a couple of observations, changing into dark grey, blue, orange, red and black for the highest density of observations around the same value. The histograms represent the paired difference between models. The blue line represents the normal distribution of such discrepancies, and the red dotted line represents the mean difference.

The capability of GLM to identify areas prone to extreme AGB estimates is of great importance at the local scale in contrast to the other models. GLM predictions at 400m^2 resolution expose that the landscape can have as little as 52.2 Mg ha^{-1}, comparable to results measured in the field. Moreover, it can reach values as high as 1,250 Mg ha^{-1}, typically as the result of one or more very large trees, similar to another tropical ecosystem (Hansen *et al.*, 2015). However, when the resolution is up-scaled into a hectare, the minimum value does not change significantly (67.6 Mg ha^{-1}). The AGB aggregation meant that high AGB estimates were reduced to 450 Mg ha^{-1}, congruent to field observations and other tropical ecosystems (Réjou-Méchain *et al.*, 2015).

When the AGB estimates were contrasted against each other, the disparity across the models presented diverse spatial patterns. GLM differences against NN and RT showed corresponding trends along the various predictor variables. However, there were disparities in how the variables can bias the AGB differences. The most influential variable to explain such discrepancies is solar irradiance, followed by altitude, distance to streams and CTI. Aspect and probability of deciduousness did not bias the AGB divergence for any of the

models (Annex 3, 4 and 5). Solar irradiance biased the AGB predictions: in places with lower solar irradiance the GLM predictions were higher than NN or RT (<500 Wm^{-2} in contrast to NN and <450 Wm^{-2} for RT). NN predicted higher AGB estimates than RT in places with >520 Wm^{-2}, but RT produced higher AGB estimates in the range of 450-500 Wm^{-2}. Altitude was important to explain the contrast between GLM and NN, but not for RT. The trend suggests that at higher altitudes, the discrepancies in AGB between GLM and NN increase. Distance to streams and CTI is essential to explain the differences between GLM and NN. The greater the values in either of both variables, the smaller would be the variation in AGB estimates. In more protected terrains (high CTI values) or larger distances to the streams, NN tended to produce bigger AGB estimates than GLM.

Finally, regarding the AGB spatial autocorrelation, GLM estimates had a pattern analogous with those of the observations (Chapter III). For example, the spatial autocorrelation for GLM revealed a range <850 m, while RT and NN showed larger ranges (7.2 km and >20 km, respectively), with NN estimates producing the highest clustering (Annex 6). For all models, the spatial dependence was estimated as moderate (0.5) nugget-to-sill ratio.

IV.4 Discussions

Multi-variable analysis revealed better capacity to explain potential AGB than bivariate correlations, as seen in Chapter III. However, the spatial heterogeneity of potential AGB are directly influenced by variables and model selection. MC analysis revealed that influential predictor variables can over- or under-predict potential AGB. The sensitivity of potential AGB towards some variables would have impacted on the spatial heterogeneity of AGB. While variables selection could be solved by sensitivity analysis, models selection is not straightforward. Models selection displayed contrasting performances depending on the scale under analysis. Most of the models performed better than a null model and 4 out of the 7 tested models captured the mean AGB used during the calibration. Only one model was capable of reproducing the spatial heterogeneity in higher spatial resolutions.

IV.4.1 Models' performance

This study presented the proposition that GLM outperforms other models to reproduce independent AGB estimates at contrasting spatial scales. GLM models had the capability to reproduce the distribution of the observations, the spatial correlation and the range of

observed AGB estimates. The CI developed from multiple iterations captured the high variability of observed AGB estimates with low uncertainty for estimates under 300 Mg ha^{-1}, which represents the major proportion of the landscape. There were some other models that improved the predictions against a null model, apart from MaxEnt and GLMM which performed worst. However, some characteristics appeared differently depending on the scale of analysis. For example, for the mean AGB at a landscape level the models GLM, GAM, NN and RT showed a close approximation. On a local scale, NN and RT were not reliable to reproduce AGB estimates, mainly when the expected AGB was over the range used during the calibration. This led to the underestimation of large AGB locations across the landscape. Moreover, NN and RT AGB estimates were similar. GAM offered a good approximation to predict AGB, and it is important not to underestimate its applicability when GLM performs with low reliability. Consequently, answer to Q1 shows that while most of the models were capable of reproducing mean estimates at the landscape scale, others (MaxEnt and GLMM) were not.

Learning machines like NN and RF predict accurately the AGB estimates used during the calibration. Particularly for NN, the optimization produced a great predictability level for calibration values, but they misled for independent samples. These models were capable of selecting the best explicative variables. However, the interpretation of the multi-variable inter-relationship and how they connect to AGB is complex and not straightforward (Saatchi *et al.*, 2007). Possibly NN and RF could improve their prediction level by allowing the selection across a larger set of predictor variables and a larger data set of observations. However, in this study for comparison purposes and to build a parsimonious model, it was decided to use the minimum number and the same variables for all the models. Further studies could explore the impact of a free variable selection and the use of a larger set of observations to reproduce AGB observations.

Other authors had suggested that RF outperforms the RT (Breiman, 2001; Baccini, 2008) and had demonstrated the applicability of using it for AGB predictions (Baccini, 2008). However, in those studies it is not clear to what extent the predictability level improves against independent data, limited observations and with limited predictor variables, in agreement with Saatchi *et al.,* (2007). While RF is a great tool for making predictions, there are still some insights needed to make it the first choice for AGB prediction with data limitation, as has been faced in this study.

According to Saatchi *et al.,* (2011b) in all cases, MaxEnt outperformed other methods in modelling the spatial distribution of AGB and in providing significantly better accuracy compared with an independent dataset. However, they reported that at least 100 observations

were necessary to build each class of AGB. Felicísimo *et al.*,(2013) found that MaxEnt predictions matched MLR, MARS and RT with a limited number of observations (N=90); they did use a higher number of explicative variables (N=20). In this research, as for many others who would like to reproduce potential AGB from the mature forest, the lack of field observations and predictor variables are a decisive constraint. In this study each class did not have more than six observations. Which in any case will limit the applicability of MaxEnt to test the reliability of AGB prediction.

Moreover, in this study other sources of limitations of MaxEnt and Random Forest could be related to their poor performance: (1) the scale of analysis is much finer than any other studies before. This finer scale may have great impact on spatial variability of biophysical properties, reducing the large variability that can be reported from sub-national to global studies. (2) The landscape under study is represented by only one ecosystem. With this approximation the variability of AGB estimates is reduced, and so in turn the various classes built to run the model in MaxEnt are likewise limited. This stands in contrast to other studies where other ecosystems featuring contrasting mean AGBs were the subject (Baccini, 2008; Saatchi *et al.*, 2011b). (3) Another factor that limited the applicability of these models was the use of only mature forest, and by not taking into consideration different degradation processes; as a consequence, the range of AGB was constrained. All of these elements may have had significant effects on MaxEnt and Random Forest models, and possibly on NN, impeding their ability to identify the signals that correlate multiple biophysical variables and AGB. These could also explain why the results in MaxEnt and RF models had little variability and why most of them fell around the mean AGB of the landscape. While the predictions done by RF and NN during the calibration were comparable, the applicability to extrapolate over a wider region was limited, with high uncertainty attached to their predictions. This performance has impact on the spatial heterogeneity of potential AGB, resulting in more homogeneous landscapes which may mislead studies of carbon stocks.

In light of the present findings, it can be said that there are some other models that could play important roles in predicting AGB but there is a need to test them. For example, Yang *et al.*,(2012) found that the geographically weighted regression performed better than ordinary least squares when predicting spatially a disease. However, others (Czarnota *et al.*, 2015) have suggested that this model has a great impact on collinearity effects, including reversal paradox, which plays a crucial role in reducing its applicability. Also, other authors have suggested that multi-variate adaptative regression splines (MARS) could be another useful tool (Lu *et al.*, 2012). However, other authors (Leathwick *et al.*, 2006; Austin, 2007) suggested that it produced almost identical predictions to GAM and did not improve

significantly on the multiple linear regressions (MLR) or other models such as RT and NN (Moisen and Frescino, 2002). In any case, what can be seen is that contrasting modelling approaches were tested, and there is not full agreement whether one model performs better than another. However, most of the studies agree that MLR, in this study GLM, is an important tool to keep using to explore geographical relationships. Moreover, further new models should be analyzed in the light of the level of improvement against an MLR, such as computational speed, user-friendliness, and transparency of fitted relations. Based on what was presented before, the Q2 is answered. And thus, more complex algorithms were affected by data limitations in observations, meaning simpler models are more robust for reconstructing potential AGB. Not all the models have the same capability to reproduce the mean estimates at landscape scales. However, it is not entirely clear to what extent lack of reliability is the result of the limitation of observations or because the landscape is constrained into only one ecosystem. Finally, there are some other groups of models that simulate the steady state of carbon stocks from dynamic ecosystem models. Those models are built on a contrasting platform and are dynamically constrained. Moreover, they use different predictor variables. Because of that, it could be a good opportunity to contrast these approaches in order diagnose strengths and weaknesses across differences in predicting AGB estimates (Cramer *et al.*, 2001; Moorcroft *et al.*, 2001; Friend *et al.*, 2014).

IV.4.2 Accuracy on AGB reconstruction

The models were capable of estimating mean AGB over large areas with precision and accuracy. However, at a local scale, the models have divergent performances not only in the allocation of the AGB estimates, but also in their range of values (low precision). These have led to changes in the AGB_{pot} estimation across the landscape. The uncertainty in the predictions was contrastingly wide across the models. GLM minimized uncertainty in the predictions, while RT and NN were more uncertain. The precision and the accuracy of modelled AGB by GLM had divergent performances. There is smaller uncertainty in the prediction for low AGB_{pot} estimates and when the mean predictions were close to the observations. Higher uncertainties were related mainly when the mean predictions failed to be close to the observations. On the contrary, though NN and RT mean differences between predictions were smaller, the total mean residuals were reduced by estimating a mean AGB_{pot} at the observations level, rather than by getting a closer approximation to each observation. Also, the uncertainty in the NN and RT predictions was consistently wider than GLM. By multi-model integration, it was possible to comprehend that the main discrepancies in the

allocation of AGB_{pot} predictions were related to the poor execution in reproducing the observations, and the bias along biophysical properties. Models revealed that some variables impacted more than others to over- or under-predict AGB_{pot} with impact on its uncertainty. In some cases spatial anomalies along the models were of great concern, coincident with other observations (Houghton *et al.*, 2001; Saatchi *et al.*, 2007; Ometto *et al.*, 2015). Consequently we can conclude to Q3 that the uncertainty in the models is induced by the bias that various predictor variables promote in the models which make those models fail in the reproducibility of observations. These processes are crucial to understand the achievement of the models and to re-direct future efforts to reduce such bias with object direct sampling collection, which will depend on more accurate prediction of AGB estimates and with better spatial representation.

A reconstruction of spatial AGB_{pot} patterns was possible only by using GLM. This results can be understood on the basis that this model produced the closest estimations to real AGB at contrasting scales, similar distribution and spatial autocorrelation. Moreover, the GLM model was capable of predicting areas with very large AGB estimates at a very fine resolution. Some may argue that very large AGB estimates (>1,000 Mg ha^{-1}) are an error in the model. However, when the pixel was up-scaled, the maximum AGB estimates fell under expected ranges, suggesting that those fine resolution pixels are the most promising places to have larger trees (Hansen *et al.*, 2015; Réjou-Méchain *et al.*, 2015). There is a need to set field campaigns to visit those sites and evaluate the performance of the model in predicting very large AGB estimates, or a selective bias in over-estimation AGB induced by a biophysical property. In any case, it is of great concern to describe the benefit of using this type of model, or to understand the lack of accuracy in very high AGB estimates. Based on what was presented it is possible to answer Q4. Accordingly, models selection has impact on the spatial heterogeneity of the potential AGB. In this study, only GLM was capable of reproducing such patterns over contrasting spatial scales. However, it is more common to find models capable of capturing the mean AGB at the landscape scale with better performance than a null model, with reduced bias and RMSE, but failing to capture AGB's true spatial heterogeneity. As a result, the models perform differently over different spatial scales. Therefore, testing models is recommended for the spatial representation of potential or current AGB estimates at fine scales.

IV.4.3 Models' applicability

The applicability and extrapolation of the methodology is feasible to implement in other regions. This study demonstrates that it is possible to reconstruct the spatial heterogeneity of the potential AGB with widely available biophysical variables, in contrast to other studies that tend to use information that normally is unknown in such as basal area, community tree density, species composition or soil properties (Slik *et al.*, 2010; Ruiz-Jaen and Potvin, 2011).

The estimation of spatial heterogeneity of potential AGB in the landscape is of importance when measuring carbon emissions and ecological dynamics. They serve as a baseline for determining loss or gain for biomass (Slik *et al.*, 2010). The spatial variation of potential AGB will help in a better assessment and understanding of impacts of deforestation and forest degradation in carbon emissions and climate change as well as biological niches for biodiversity or food supply for diverse species. It would be the basis for building informed decisions when restoring or managing an ecosystem and to prioritize areas for implementing REDD+ projects. It can guide and describe rare elements in the landscape which in most studies tend to be avoided or minimized by changing the sampling design. This would turn into the major role in landscape ecology and population analysis.

IV.5 Conclusions

This is the first study to test the performance of different techniques in estimating the spatial heterogeneity of potential AGB from field observations and biophysical variables on contrasting scales; also in simulating potential AGB estimates with high resolution over a broad region. These types of study are necessary to make net estimates of carbon emissions due to deforestation and forest degradation. Moreover, they can help in reducing the uncertainty of spatial variation of carbon stocks, and in the understanding of ecological constraints on carbon stocks as well as other ecological processes.

Models selection and climatic variables play an important role to drive contrasting differences in AGB allocation and magnitude. At regional scales GLM, GAM, NN and RT had comparable performance in reconstructing potential mean estimates. The estimates were tested by various means to ensure their reliability and their uncertainty. A simpler model like GLM not only outperformed others in predicting and allocating AGB, and reproducing similar spatial patterns as the observations, but also it showed other great advantages. These included transparency of fitted relationships, efficiency in computational speed and the possibility of building automated models. GLM should be used even when other ranges of

techniques are tested. By doing this, the results will provide large insights into both the relative strengths of new models, and the weakness of GLM. Because it remains to be seen whether new algorithms (support vector machines, multi-variate adaptative regression splines, spatial simultaneous autoregressive models) can produce improvements in the predictions with transparency and computational efficiency. With these in mind the reader will be able to trade-off flexibility, simplification in the model and reliability of predictions coming from simpler models such as GLM, NN and RT, against more complex newer algorithms that often do not have a proper evaluation of their applicability on AGB estimates or spatial studies, despite recent publications tending to bias the perception of their application.

Chapter V. Driving forces of net carbon losses in a tropical dry forest, Oaxaca, México

V.1 Abstract

The Tropical Dry Forest is not only one of the most important tropical ecosystems in terms of area, but is also one of the most degraded ecosystems. Little is known about the impacts on carbon stocks, therefore carbon emissions. There are different studies which explain deforestation dynamics, but there is still a lack of understanding of how they correlate to carbon losses. Recently different authors have built current biomass maps for the tropics and México. However, it is not clear how well they predict at the local scale, and how they can be used to estimate carbon emissions. This chapter evaluates the performance of different maps in representing the biomass spatial heterogeneity, and integrates different socio-ecological variables to understand the bias in their predictions. The results shows that there are important differences in the current biomass maps without a clear consensus. However, a general pattern of biomass distribution can be inferred and the forces driving carbon emissions can be identified. Finally, it is possible to estimate the net carbon emissions due to deforestation and forest degradation. This study estimated that currently ~44% of the potential carbon stock estimated for the region is still present. A total of 6,764 GgC has been emitted due to deforestation and degradation of the forest. Most carbon losses were identified in places suitable for agriculture, close to rural areas and to roads. The lowest losses were found in places with high water stress and within the boundaries of the National Protected Area. Moreover, places not suitable for agriculture, but close to the coast showed carbon losses as a result of urban settlements.

V.2 Introduction

TDF is now recognized to be of great conservation importance due to high deforestation rates (Trejo and Dirzo, 2000; Maass *et al.*, 2005; Dirzo *et al.*, 2011) and the high risk of release of its existing carbon as a result of LUCC (Skutsch *et al.*, 2009). This forest is considered one of the most endangered (Janzen, 1986; Janzen, 1998), but one of the least studied ecosystems in the tropics (Dirzo *et al.*, 2011). For example, in Mexico TDF has shrunk from its natural primary forested area to a remaining proportion of 25-36%, giving place to secondary forest (Rzedowski, 1998; Portillo-Quintero and Sánchez-Azofeifa, 2010;

Dirzo *et al.*, 2011). In Mexico TDF is mainly transformed into grassland for cattle raising, shifting cultivation for self consumption and, in a less significant proportion, to irrigated agriculture (Maass, 1995; Noble and Dirzo, 1997; Janzen, 1998; Trejo and Dirzo, 2000; Corona, 2012). However, fuel wood extraction may represent the most important carbon emission source (Gaston *et al.*, 1998).

In recent years different authors (Baccini, 2008; Goetz *et al.*, 2009; Mitchard *et al.*, 2011; Baccini *et al.*, 2012b; Mitchard *et al.*, 2013; Cartus *et al.*, 2014; Avitabile *et al.*, 2016; Rodriguez-Veiga, 2016) have worked on developing tools for understanding, validating and/or measuring current AGB estimates over pan-tropical regions. Despite their validations, there is no independent validation of these maps at the scale of their applicability and currently there is still high uncertainty across these predictions, and it is unknown to what extent they can be used for better decision making at regional scales (Saatchi *et al.*, 2007). Therefore, the total carbon forest losses due to anthropogenic actions by deforestation and forest degradation processes is unknown.

LUCC is considered the main driving force leading to environmental degradation, land fragmentation, loss of global biodiversity (Lambin *et al.*, 2001) and carbon emissions at local scales (Corona, 2012). However, local drivers such as demographic and biophysical factors play a major role in explaining spatial patterns of LUCC across the landscape (Bürgi *et al.*, 2004; Pan *et al.*, 2004). Analysis of local deforestation should ideally focus on the forest ecosystem and its uses, the landscape dynamics and the local demographic, cultural, social, economical and political characteristics that drive deforestation (McConnell *et al.*, 2004). Therefore, the systems have to be evaluated under a socio-ecological perspective (Lambin and Meyfroidt, 2010). To understand forest carbon losses due to deforestation and forest degradation, models should look into these drivers as important sources of information to explain current AGB estimates and their potential to produce more reliable local AGB estimates. To improve accuracy in predictions on current AGB maps, it is necessary to understand the socio-ecological constraints that drive the spatial distribution of AGB. Because of that the main objective of this chapter is to address the question: how much AGB has been lost in a tropical deciduous forest and what are the main drivers of such losses? To be able to answer this question I set different questions:

Q1. Do the different maps show similar total AGB estimates at landscape scales?

Q2. Does ground truth highly heterogeneous AGB sites, promote that the diverse AGB prediction models show differences in their AGB estimates?

Q3. Are the ground truth low AGB estimates related to anthropogenic drivers, particularly to agricultural activities, rather than biophysical factors?

V.3 Results

V.3.1 Current biomass estimates and uncertainties among the maps

The 95% CI range of each different AGB map encompasses the range of the field observations (Figure V.1). However, none of the maps (N=5) showed significantly similar mean estimates to the field observations (N=47) (t-test on paired samples and Wilcoxon rank-sum test, *p*-value <0.005). The Baccini and Saatchi maps showed a higher mean estimate than the field observations, while all other maps showed a lower mean estimate (*p*-value <0.001). Comparison of the median AGB between the maps also showed significant differences at the 5% level (See notches on Figure V.1). However, Saatchi's is the only map that produced the median closest to field observations. The map with the lowest mean estimates is Avitabile (2016) followed by Cartus (Figure V.1). Aggregating all the input maps (AGB_{maps}) produced a mean AGB estimate at the landscape scale of 59.6 ± 18.4 Mg ha^{-1}, ranging between 15-125 Mg ha^{-1} (Figure V.2a). Mean AGB_{maps} showed similar distribution at pixel (N=43) and landscape scale (N=1,764) than the field observations (N=43) (*p*-value=0.07 and *p*-value=0.59, t-test on paired samples and Wilcoxon rank-sum test, respectively). Higher estimates are constrained mainly in the northern boundary, while the lowest estimates are constrained in the southwestern section of the landscape.

The variability across the input maps showed a mean CV_{maps} of 57.8 ± 17.8%, with a maximum figure of 138.7% and minimum of 13.2% (Figure V.2b). Comparing CV_{maps} to the CV measured from the AGB field observations showed a weak correlation at finer scales (r =-0.11, *p*-value=0.009). However, CV_{maps} was shown to be significantly correlated (*p*-value <0.002) with different biophysical variables. For example, CV_{maps} showed a positive correlation with: potential AGB (r = 0.10), AGB loss (r = 0.20), altitude (r = 0.23) and total precipitation (r = 0.25); and Precipitation of Driest Quarter (r = 0.26). In contrast, CV_{maps} showed a negative correlation with: temperature (maximum temperature during rainy season (r =-0.19); mean temperature (r = -0.19); Isothermality (r = -0.23) and less importantly to distance to agriculture fields (r = -0.08) (Figure V.3).

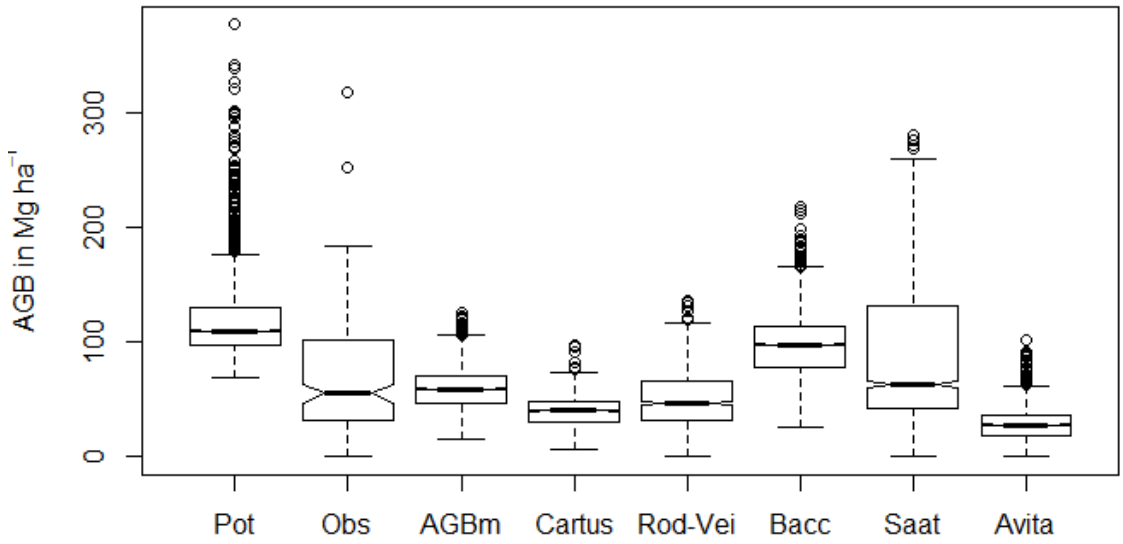

Figure V.1 Boxplots for potential and current AGB estimates produced by different maps at the landscape scale. Notches highlight the median estimate from each map. Acronyms are: Pot - potential AGB; Obs - Field AGB scaled into 1km^2 with at least 3 observations within the pixel; AGBm - Mean AGB of the different AGB maps; Rod-Vei - Rodriguez-Veiga map; Bacc – Baccini map; Saat – Saatchi map; and Avita – Avitabile map.

From a multivariable perspective it is possible to identify that 32% of the landscape showed a mean CV_{maps} of 60% distributed in regions with a total precipitation >975 mm. Moreover, 51% of the landscape showed a mean CV_{maps} of 49% in places with reduced precipitation (<975 mm), with a maximum temperature during rainy season <35°C and altitudes under 270 m asl. The highest mean CV_{maps} of 71% is identified in about 2% of the landscape where total precipitation is under 975 mm, maximum temperature during rainy season is >35°C and there are AGB losses of 70%. Finally, 1% of the landscape showed the lowest mean CV_{maps} of 39% located in places at lower altitudes (<10 m asl) with limited precipitation and high maximum temperatures during rainy season.

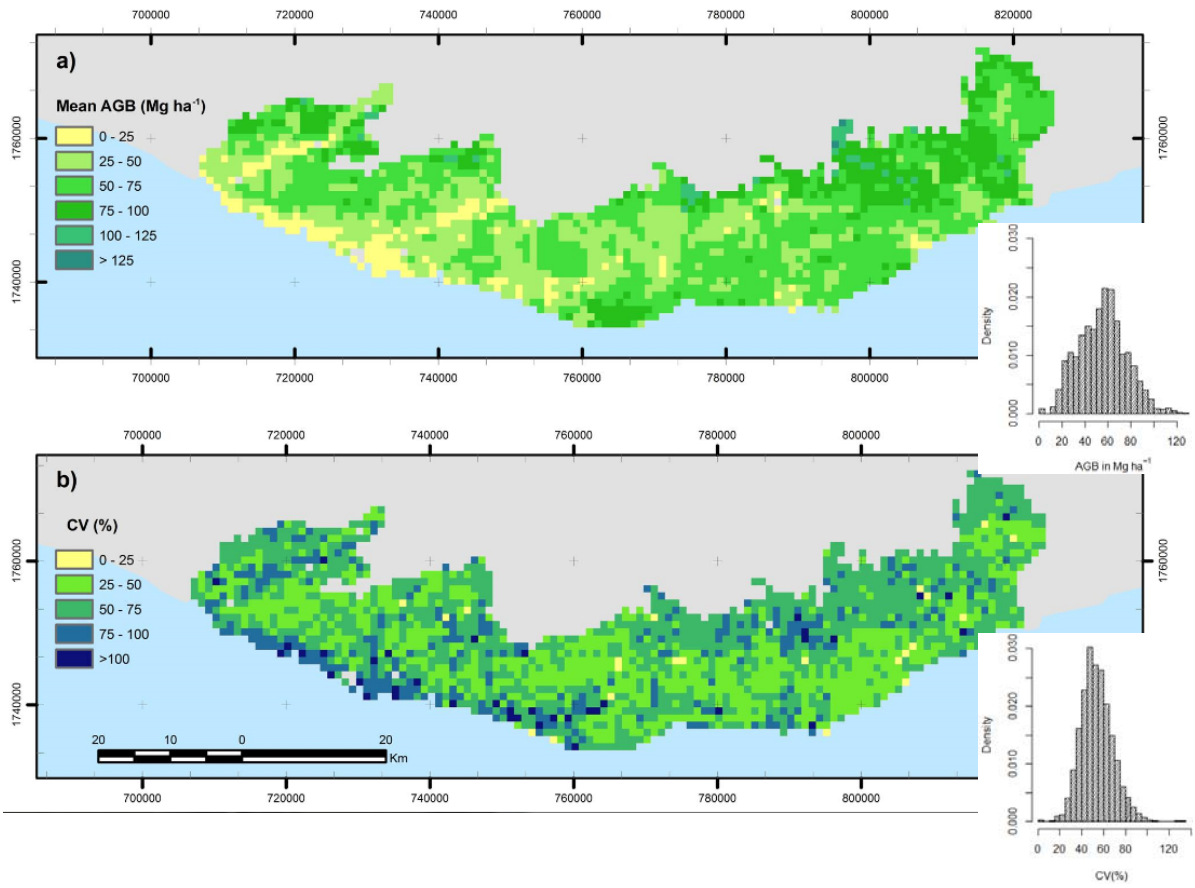

Figure V.2 Current mean AGB (Mg ha^{-1}) and CV_{maps} (%) estimates across different input maps.

V.3.2 Landscape biomass losses and their spatial distribution

The landscape has an AGB_{pot} of 25,578 Gg with a total AGB_{loss} of 56% (6,764 GgC). However, the maps showed differences in their predictions. The Saatchi and Baccini maps showed the most conservative losses of ~8,000 Gg AGB lost. The Cartus and Rodriguez-Veiga maps fell in the mid range at ~17,500 Gg AGB lost. The Avitabile map suggested losses that exceed 20,000 Gg AGB (Figure V.4 and Table V.1). The mean AGB_{loss} was restricted between 0-400 Mg ha^{-1}, with the majority concentrated between 20-100 Mg ha^{-1}. By the epoch 2006 about 22% of the landscape was transformed into an anthropogenic land-cover representing a total AGB_{def} of 5,464 Gg (38.2% of the total losses)

.

Regarding the current AGB distribution reported by the models for the different municipalities under study, in Table V.1 shows that all the models share similar trends in the AGB ranking. The municipalities with the highest AGB losses are San Pedro Pochutla and San Miguel del Puerto. Interestingly, the latter also showed the highest AGBpot

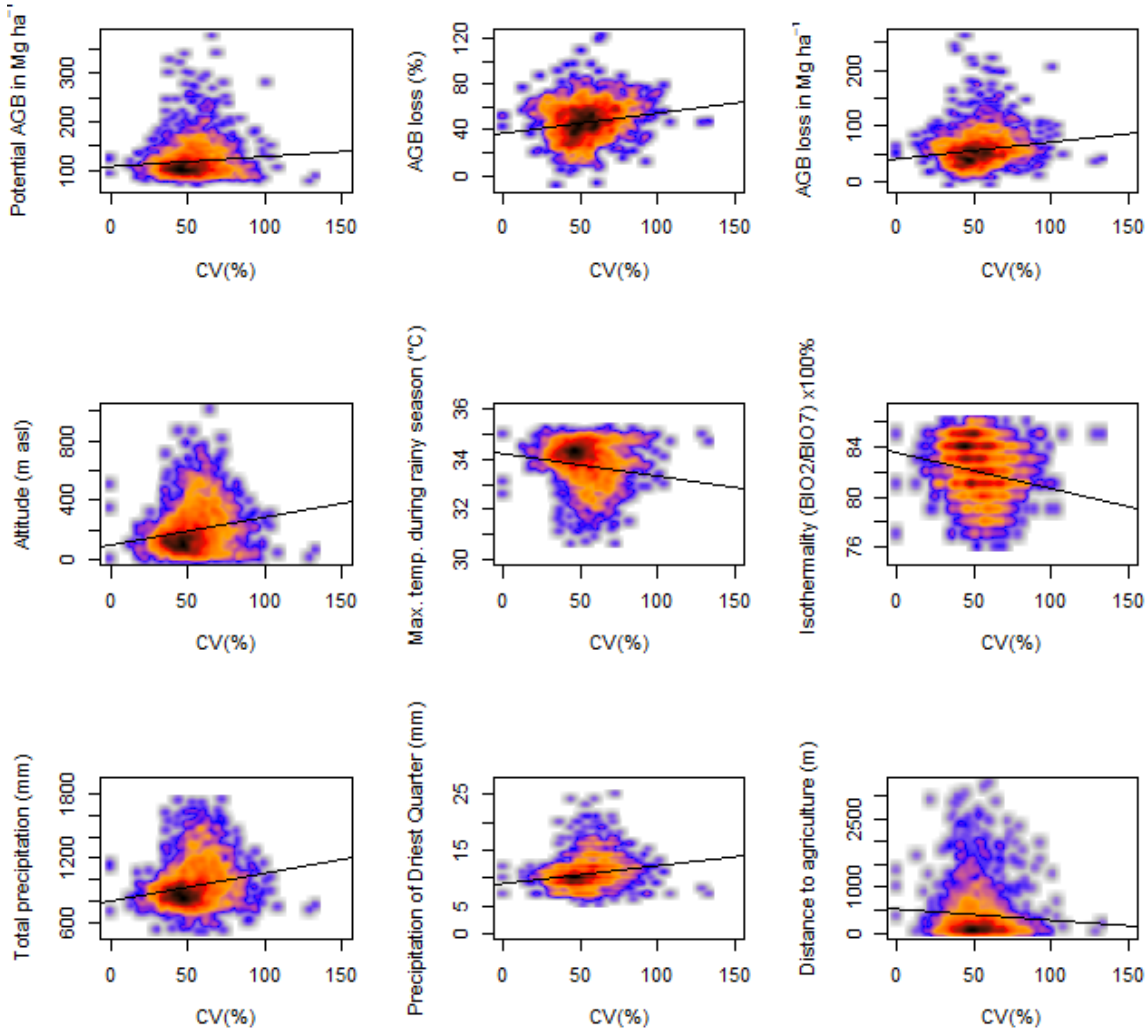

Figure V.3 Spatial explanatory variables that correlate with CV(%) across the maps. Colours represent the number of observations for a certain pair of CV_{maps} and predictor variable. Light grey shades represent a pair of observations, changing into dark grey, blue, orange, red and black for the highest density of observations around the same value (N=1,764).

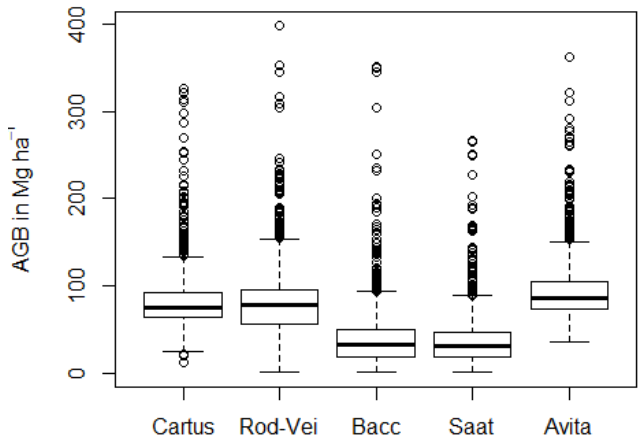

Figure V.4 Total and relative AGB_{loss} at a landscape scale (potential minus current estimates). Acronyms are : Rod-Vei - Rodriguez-Veiga map; Bacc – Baccini map; Saat – Saatchi map; and Avita – Avitabile map.

Table V.1 Total and relative AGB_{loss} at a landscape scale (potential minus current estimates), mean AGB (potential and current) and mean loss in percentage per municipality. Acronyms are : Rod-Vei - Rodriguez-Veiga map; Bacc – Baccini map; Saat – Saatchi map; and Avita – Avitabile map. The total area under study is 215,687 ha.

	Gg	**Mean AGB per Municipalities (Mg ha^{-1})**				
Maps	**Total AGB loss**	**Santa María Huatulco**	**Santa María Colotepec**	**San Miguel del Puerto**	**San Pedro Pochutla**	**Santa María Tonameca**
Potential	25,578	115.6+/-26.0	113.4+/-21.4	140.0+/-32.4	111.1+/-21.6	105.8+/-22.4
Cartus	17,847	41.5+/-9.3	33.6+/-12.8	44.7+/-8.9	39.2+/-9.3	32.6+/-12.4
Rodriguez-Veiga	17,260	54.4+/-24.8	32.5+/-19.8	47.1+/-15.8	42.5+/-23.0	39.9+/-26.7
Baccini	8,322	94.7+/-25.0	84.7+/-27.4	111.0+/-28.1	100.2+/-25.6	83.5+/-24.4
Saatchi	7,912	92.7+/-53.0	64.8+/-46.1	126.7+/-48.3	73.3+/-44.2	47.9+/-26.0
Avitabile	20,155	27.2 +/- 11.4	25.7+/-11.0	34.1+/-14.0	29.8+/-13.5	24.4+/-10.8
Mean		89.6+/-23.4	88.5+/-19.9	106.5+/-30.7	82.0+/-20.6	81.3+/-19.0
Mean loss	**14,299 +/- 7,399**	22.5%	22.0%	23.9%	26.2%	23.2%

Above ground carbon (AGC) losses are not evenly distributed in the landscape and show spatial patterns (Figure V.5). The main factors that explain forest carbon losses are related to socio-economic drivers (Figure V.6a) and less importantly, climatic and topographic variables (Figure V.6b). In both cases, the regression tree explains over 31% of the variance of the estimated carbon losses, respectively. Mean AGB losses of 65% were identified in regions close to agricultural fields (<100 m), paved roads (<1,700 m) and human settlements (<1,350 m). In places >100 m from agricultural fields, close to dirt roads (<600 m), and close to human settlements (<1,000 m) the AGC loss averaged 61%. Minor

losses (~35%) are found in sites >770 m from agricultural fields and >600m from dirt roads. However, places that fall between the range of 100-770 m from agricultural fields have a mean loss of 32% and up to 39% when the same sites are close to human settlements (<500 m). Interestingly socio-economic drivers performed differently in regions with water stress (Figure V.6b). For example, low AGC losses (31%) were identified in regions close to agricultural fields (<250 m) with limited precipitation during driest quarter (<11 mm) and isothermality <82.5%. In contrast, higher mean AGC losses (65%) were observed in areas close to agricultural fields (<100 m), with a maximum temperature during rainy season of 35°C and <900 m to paved roads. Places with distances >100 m from agricultural fields, isothermality >82%, close to paved roads (<1,000 m) and at lower altitudes (<25 m asl) showed an AGC loss of 65%. However, under similar allocations with mean diurnal range< 14°C reduced AGC loss was reduced to 35%.

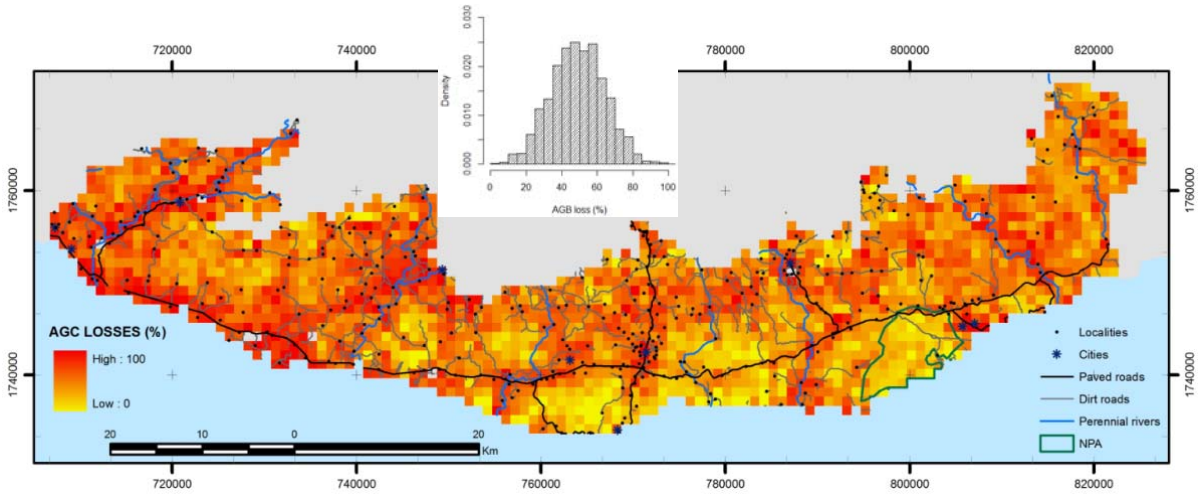

Figure V.5 Spatial distribution of mean AGC losses in percentage (deforestation and degradation)

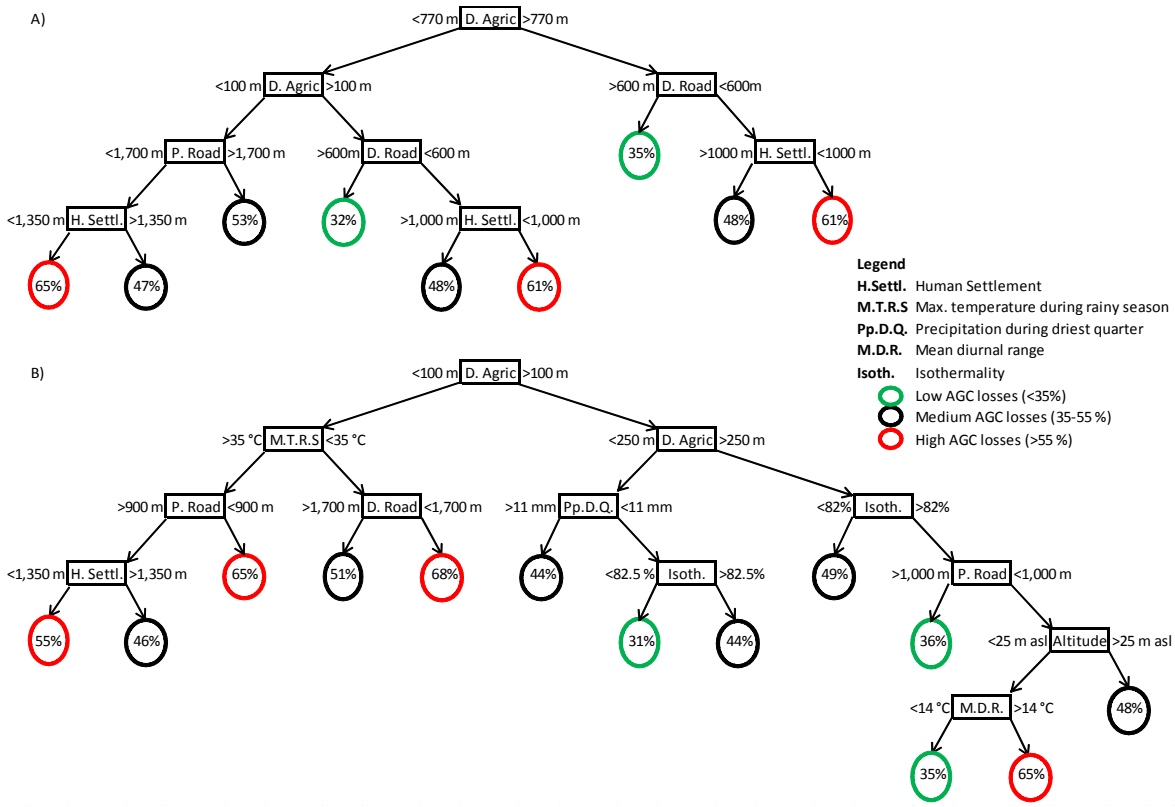

Figure V.6 Regression trees for socio-economic and biophysical spatial patterns of AGC losses (%). (A) includes socio-economic drivers and (B) includes socio-economic drivers in addition to topographical and climatic variables. The regression tree A explains 31% of the variance, while B explains 33%, both in contrast to the estimated AGC losses (Figure V.5).

The maps in Figure V.7 present variation in AGC losses from Figure V.5 and those estimated from Figure V.6. In both models (with and without biophysical variables from Figure V.6) ~50% of the landscape showed discrepancies under 10%. Differences up to 20% between models can be seen in 78% and 83% of the landscape for the model only socio-economic variables, and socio-economic and biophysical variables, respectively. Medium variations (20-50%) were observed in areas with anthropogenic covers. And major variations (>50%) are distributed without a clear patterns. The regression tree models overestimated AGC losses in anthropogenic covers, this is because factors such as green belts, urban parks and the use of green buffers in agricultural areas are not properly represented in the regression tree model.

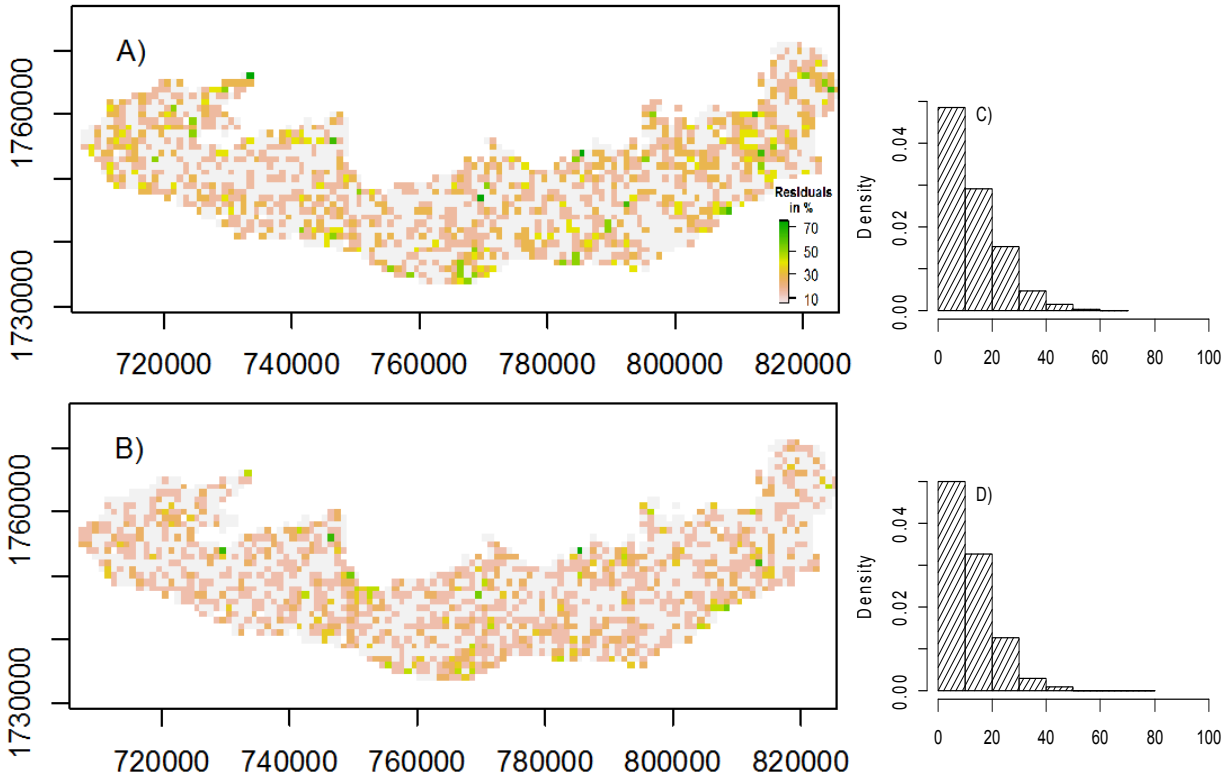

Figure V.7 Residuals estimated from the regression tree of AGC losses. Figure A shows the residuals for the model derived from socio-economic factors. Figure B presents the residuals of the socio-economic and biophysical model. Figures C and D show the histogram of the residuals for model A and B, respectively.

V.4 Discussion

V.4.1 Map performance in estimating current AGB

Field observations and maps fall within the expected range of AGB estimates for TDF in Mexico and Central America (Brown *et al.*, 1989; Brown and Lugo, 1990; Holly *et al.*, 2007; Becknell *et al.*, 2012). The AGB estimates for the landscape suggests a degraded forest. However, the range of values observed suggests a mature forest matrix among secondary forest and anthropogenic cover. For example, this region included estimates over the 210 Mg ha^{-1} (field observations, Baccini and Saatchi maps) maximum reported by Powers *et al*., (2009). Interestingly, while it is known that a larger pixel size reduces the range of AGB values due to spatial averaging and the exclusion of very high AGB values, in this study it was possible to identify that the input maps with higher spatial resolution

showed the lowest estimated AGB range, which suggests that signal saturation may have resulted in an underestimation of AGB.

By integrating multiple input maps and comparing estimates to potential biomass total carbon emissions due to deforestation and forest degradation can be monitored. There are, however, important differences among the maps, as a result of total AGB losses, which suggests that results are not yet accurate enough to give exact values. For example, at the extreme, total AGB loss can differ by>100% (Avitabile and Saatchi maps). Nevertheless, these results allow a general picture of potentially how much AGB has been lost overtime, and set a benchmark for landscape management. This means that a multi-map comparison should not be used in isolation to quantify carbon emissions at a fine scale, but can be used for coarse scale monitoring, in particular to detect deforestation and/or forest degradation, similar to the results reported by Mitchard *et al.,* (2013) and Rodriguez-Veiga *et al.,* (2016). Based on these results, the answer to Q1 is that at the landscape scale these maps are not capable of reproducing AGB estimates but they can give a broad idea of how much AGB has been lost. Nevertheless, a multi model agreement performed better than any of the other maps and statically similar to field observations.

The maximum predicted values of AGB among the maps are also different: all of them are lower than the mean estimate for mature forest (~400 Mg ha^{-1}) although the cause remains unclear. All the models used to build the maps included different combination of remote sensing layers and all included altitude from SRTM. For example, the Saatchi map showed the highest AGB predictions per unit of area (~280 Mg ha^{-1}), followed by Baccini (~225 Mg ha^{-1}). Rodriguez-Veiga produced a maximum prediction of ~150 Mg ha^{-1} while the Cartus and Avitabile maps reached up to ~100 Mg ha^{-1}. Model selection (MaxEnt vs RandomForest) did not show any pattern that could explain why models over-/under-estimated AGB.

Though Cartus and Rodriguez-Veiga, and Avitabile used the NFI from Mexico to calibrate the models and build the AGB maps, they showed different saturation of AGB estimates. This could be the result of using a combination of different remote sensing layers. This suggests that for other regions of Mexico the saturation point of these maps may differ, similar to observations from other regions and vegetation covers (Le Toan *et al.*, 2004; Mitchard *et al.*, 2009; Mutanga *et al.*, 2012). According to Cartus (2014) their map of AGB for Mexico showed a tendency towards overestimation for those areas with the lowest AGB (<100 Mg ha^{-1}). Conversely, at higher AGB predictions the map showed a tendency towards underestimation, similar to the Avitabile map. This suggests that the input maps for this region significantly underestimate AGB, which can explain much of the difference when

comparing extreme total AGB estimates across the input maps. Moreover, Cartus (2014) showed that their map predicted the AGB of TDF better in contrast to other ecosystems, nevertheless, the performance for this region was limited. It is important to consider that their model only included trees with a DBH of >7.5 which suggests an under estimation of ~15% of the total AGB (Chapter IV). Finally, to build the Avitabile map the Cartus map was used in combination with the data from 4,296 field plots as the 'true' ground AGB estimates, where possibly high-biomass estimates were under- represented in the training data (Avitabile, pers. comm). This may explain why this map showed similar estimates to Cartus map and produced the lowest total AGB estimates.

The CV_{maps} showed that at the landscape scale the AGB maps compare reasonably well to the figure reported for Mexico and Central America (Avitabile *et al.*, 2016). Nevertheless, locally CV_{maps} showed some local trends, suggesting that CV_{maps} are spatially clustered. It was found that CV_{maps} related weakly to CV from local field AGB estimates, but did relate to biophysical variables. This is important to notice because it may be possible to make future adjustments and reduce such variability enabling more accurate AGB predictions to be made. Interestingly CV_{maps} tended to produce higher figures in places where AGB_{loss} was estimated, similar to the results from Avitabile (2016). However, the relation with AGB_{pot} was reduced. This suggests that maps tend to have greater disagreement in AGB reduction regardless of the AGB_{pot} at certain locations. Moreover, although at global and sub-regional scales tropical forest is known to be correlated with climatic variables (Brown and Lugo, 1982; Larjavaara and Muller-Landau, 2012; Girardin *et al.*, 2014) (and Chaper IV) none of the maps included such information, and only the Baccini map considered land surface temperature which could act as a proxy for solar irradiation and/or mean temperature. This may explain why CV_{maps} showed the strongest correlation with climatic variables. Altitude also showed an important correlation to CV_{maps}, this could be related with the remote sensing saturation point and how different maps calculated the AGB estimates. This is mostly evident at higher altitudes where more AGB tends to be located (Chapter IV and V). Also, it could be the result that the altitude map used in this study has a much finer resolution, which may perform better in capturing small altitudinal changes, which may be more representative over broader scales. Finally, socio-economic variables did not show a relation with CV_{maps}, which may suggest that a general pattern of human disturbance was captured by the maps. Based on these findings we concluded (Q2) that major differences across the current AGB maps are not the result of the high heterogeneity of AGB across sites. Differences in maps are likely the result of how the different models predict AGB and

how they overcome the saturation point, mainly as a result of the lack of predictor variables such as temperature and precipitation.

V.4.2 Total aboveground carbon emissions due to deforestation and degradation

While Corona (2012) and Mendoza (2015) found that in this region the proximate drivers of deforestation are grassland for cattle raising, agriculture and urban developments, it was unknown how much of the AGB has been lost as a result of the LUCC and forest degradation. This study estimated that currently ~ 44% of the potential carbon estimated for the region (5,335 GgC) is still present which suggests a degraded forest (Asner *et al.*, 2010). This is similar to the proportion of the landscape that has intact forest with no LUCC processes recorded for the period 1985-2006 and only minor modifications between 1995-2006 (Corona, 2012). The input maps do not differ importantly in the epoch they represent and little differences across the maps are expected as a result of LUCC, less than 2.3% in a period of 5 years (2006-2011) (PSIG, 2015). Therefore, differences in current AGB maps cannot be regarded the epoch they represent. And their AGB estimations could be considered as they represent the same epoch. However, the main source of uncertainty can be related to forest degradation, which no other study had evaluated, and there is not enough information to understand this process fully.

The input maps fall within the field observation range, however, there is not a clear consensus among them, this explains why the mean CV_{maps} in the landscape is 58%. For example, Mitchard *et al.,* (2013) found that the Baccini and Saatchi maps produced similar AGB estimates over larger areas, similar to the results observed in this study. However, from all the maps tested the Baccini and Saatchi maps produced the highest AGB estimates for the landscape, including the mean field observations. Cartus and Avitabile produced similar results and fell within the lowest estimates. While the Rodriguez-Veiga map displayed estimates in the middle range of these two groups of estimates. When the information is analysis at municipality level all the models showed contrasting mean AGB estimates, and only the ranking of the AGB is comparable across the models. Finally, while all the input maps had a validation process and all showed a fairly good performance, in this study at the landscape scale, it is not clear which of all of these maps, if any, accurately predicts AGB.

Different studies have reported differences across the AGB maps which may drive significant impacts on total AGB carbon. Avitabile *et al.,* (2016) suggest that the Baccini and Saatchi maps produced an over estimation in AGB, similar to that reported for other regions (Mitchard *et al.*, 2011; Baccini and Asner, 2013; Mitchard *et al.*, 2013). However, based on

our findings it is difficult to identify to what extent the Baccini and Saatchi maps over estimate AGB. This is mainly because Avitabile and Cartus tend to suggest much lower AGB estimates than those observed in the field, as well as the inherent errors in the models such as considering trees ≥7.5 cm in DBH and by excluding plots with high AGB estimates from the analysis. According to Avitabile *et al.,* (2016) their map predicted 9-18% lower than the Saatchi and Baccini estimates with much lower figures in Central America and Mexico, and in dry vegetation. However, in this study it was possible to notice that such differences are significantly much higher than their findings. According to field measurements and the expert knowledge this could mean at least a 30% under estimation of AGB at lower altitudes and more than 100% for higher altitudes. At the landscape scale this could represent ~50% of total AGB. If the two extreme input maps are not taken into account (Avitabile and Saatchi) it can be suggested that the current AGC for the landscape would fall in between a minimum of 3,657 (Cartus *et al.*, 2014) and a maximum of 8,162 GgC (Baccini *et al.*, 2012b).

Skutsch (2009) suggested that dry forest carbon emissions are important because of continued carbon losses although their carbon content is considerably lower per hectare than other tropical forests. In the landscape under study a total of 6,764 GgC has been emitted due to deforestation and degradation of the forest. Because of the scale of analysis (1 km^2), emissions from deforestation and degradation cannot be quantified individually and both are masked as disturbance. However, based on others ~67% of the total carbon emissions can be regarded as being due to forest degradation (Gaston *et al.*, 1998; Ryan *et al.*, 2012) under similar land use management as the landscape in this study. However, more research at finer scales is needed in order to estimate the amount of carbon that has been released due to forest degradation and to understand the factors that drive such activities. This will lead to better forest management for climate change mitigation action plans.

V.4.3 Patterns and processes of carbon emissions

Forest AGC loss is not evenly distributed in the landscape and is related mainly to socio-economic pressures. Ryan *et al.,* (2012) found that AGB loss in a region in Africa is primarily the result of clearance for small-scale agriculture and charcoal production by selective removal of medium size stems. Corona (2012) and Ryan *et al.,* (2012) found that cleared areas are the result of small expansions in the boundaries of already cleared land, similar processes observed for AGB losses. Ryan *et al.,* (2012) hypothesized that woodland

clearances would target high biomass areas, however, in this study we did not find evidence to suggest such a process. This is because the labor required to remove forest or extract wood in high AGB areas is much more time consuming and the return rate per hour is much smaller because access to those areas would require a much higher effort in terms of fuel wood transportation. This is supported by the results and where higher AGB losses happen closer to current agricultural lands, human settlements and roads, rather that AGB gains.

Climatic variables and altitude were significant variables to explain the spatial variability of AGC reductions, however, they act as underlying explanatory variables of LUCC processes. For example, places with high water stress are less suitable for agriculture, as a result less AGC was lost. In contrast, accessible regions and those climatically suitable for agriculture showed the highest transformations in AGC. Interestingly, at lower altitudes (close to the coast) places limited for agricultural activities but close to urban establishments and paved roads showed high AGC reductions, this can be understood as a result of urban expansion and establishment of tourist resorts along the coast (Corona, 2012). Finally, regions isolated from human land cover change within the boundaries of the National Protected Area have shown a reduced pressure on forest, similar to observations made by Corona (2012), Mendoza (2015) and Corona *et al.,* (2016).

Forest degradation processes are difficult to measure at the spatial resolution of this study, however, it can be argued that degradation happens close to dirt roads, human settlements and agricultural fields. According to Corona (2012) and Corona *et al.,* (2016) the process of shifting cultivation in the region takes place up to 4 km from the previous agriculture plot, suggesting within this spatial range the population may play an important role for forest degradation. Where sites closer to rural settlements are preferable for shifting cultivation (<1 km) and cattle raising (<3 km), similar ranges identified in this study for carbon losses. Finally, it is important to notice that topographical variables such as slope, aspect, distance to river, terrain curvature, compound topographic index and solar irradiation did not play any role in the understanding of AGC reductions. Based on the findings of this chapter, it is possible to say for Q3 that anthropogenic drivers (agricultural activities) play the major role in predicting low AGC due to deforestation and forest degradation. However, it is important to note that there are some other drivers such as urban expansion, that colonized sites that are not suitable for agriculture and play an important role in explaining low AGB estimates. Moreover, biophysical factors played and underplaying role to drive the deforestation dynamics, rather that influencing current low AGB estimates. My results shows that while more research is needed to understand the impacts of error propagation among the

models, I consider that the allocation and drivers of carbon emissions will not change significantly.

V.5 Conclusion

This is the first study to attempt to understand the spatial differences in AGB estimates across the different current AGB maps at the landscape scale. In addition this study explores the total carbon emissions due to disturbances and processes that have lead to AGB losses. This study shows that there are important differences in the current AGB maps, that there is not a clear consensus among them and that their AGB can be under or overestimated, with no clear evidence to suggest which is more reliable for local land management or decision making. However, this could be solved by taking into consideration the understanding of the socio-ecological systems and using it in the models with a bottom-up perspective. This study showed that climatic variables play a major role in the spatial bias across the different maps, and the socio-economic variables played an important role in explaining AGB losses. So it is possible that high CV measurements and AGB map biases can be reduced when taking into consideration such regional conditions. By including socio-economic variables and not only relying on remote sensing information, the models that predict current AGB can be improved significantly and the impact of remote sensing signal saturation can be minimized. As a result, maps that are built from the bottom-up may have more explicative power to reproduce current field based AGB estimates, inform where the landscape has been severely degraded or identify promising places for carbon conservation, among other uses. Moreover, these types of maps will be capable of dealing with the high uncertainty in current AGB maps and they will be capable of capturing the high AGB spatial heterogeneity, characteristic of tropical dry ecosystems. Finally, carbon emissions due to disturbance are expected to increase in the coming years. The role of population in driving deforestation is complex, and characterized by spatial and temporal impacts. The growing rural population will have larger demands for wood and food, so while remote or protected areas may have the potential for storing high AGB, forest near settlements and access routes are likely to continue being disturbed unless affordable alternatives are available for the sustainable use of the forest.

Chapter VI. General discussion

Land-use and land-cover changes and selective logging have led to losses in the carbon storage of diverse tropical ecosystems (Houghton, 2005a). Tropical deciduous forest has been one of the most impacted of these (Janzen, 1998), but the outcomes have been poorly quantified. Various elements impact directly and indirectly on the response of AGB. Little is known of ecological processes of AGB distribution over various spatial scales in natural and non-human disturbed ecosystems, as most studies have been focused on disturbed vegetation. The lack of integrity across scales, variables, and models selection plays a major role in understanding the spatial representation of AGB. The multiple responses and interactions among the variables may divergently represent the AGB magnitude and allocation. Therefore, it is important to explore the AGB allocation as a multi-factor expression over multiple spatial scales and methodological approaches.

This study has the following major aims: to improve the accuracy of predictions of net carbon losses, it is necessary to understand the socio-ecological constraints that drive the spatial distribution of natural and current AGB. This study took a multi-scale approach with a multi-model testing process to identify factors that drive AGB magnitude and allocation in a mature forest. As a starting point, forest structure and biophysical variables were explored. Next, a multi-variable integration was applied because AGB is a multi-factor expression over distinct spatial scales. A multi-model inter-comparison was used to identify the best model(s) that could reproduce AGB estimates as well as its spatial configuration. Finally, an estimation was made of net carbon emissions caused by deforestation and forest degradation along with the socio-ecological drivers.

The structure followed in this section can be summarized: firstly, mature forest properties were explored and explained over contrasting spatial scales. Variables that correlated to AGB were explained in light of current knowledge and how they interact with other factors to predict AGB. Secondly, various sources of uncertainty in this study were presented. Critical errors were examined to find out the impact on AGB. Finally, drivers of carbon emissions due to deforestation and degradation were identified, highlighting their importance for the construction of future AGB maps.

VI.1 AGB assembly in a mature forest

A TDF forest community shows an inverse J-shaped tree-size distribution. The forest can be considered mature natural forest with proper regeneration and continuous replacement (Hall and Bawa, 1993; Lykke, 1998; El-Sheick, 2013). Tree density and community assembly suggest that the proportions of the individuals *per* diametric class is less variable in

TDF than the tree density alone suggests. TDF forest community is dominated by a great number of trees with DBH <30 cm with a limited number of large-sized trees (DBH ≥60 cm), with a mean AGB of 118.1±44.0 Mg ha^{-1}. Mean BA and AGB are similar to other reports (Brown and Lugo, 1982; Murphy and Lugo, 1986b; Brown and Lugo, 1990; Gillespie *et al.*, 2000; Jaramillo *et al.*, 2003; Marín *et al.*, 2005). But they are higher than other TDF in Puerto Rico (Murphy and Lugo, 1986b) and Mexico (Jaramillo *et al.*, 2003; Martínez-Yrízar *et al*., 1992).

The results advocate that the AGB heterogeneity for mature forest can be captured with a multi-scale and multi-factorial analysis (Poisot *et al.*, 2011), but it fails for very high AGB. AGB allocation varies in the landscape as a consequence of processes over diverse scales. Despite this, most of the variables are directly or indirectly related to water stress. In other arid regions, water availability is the major limitation for AGB (Snyder and Tartowski, 2006).

At the local scale, soil texture actively mediates water availability (Sperry *et al.*, 1998; Sperry and Hacke, 2002) while soil nutrients play a reduced role in explaining AGB. Particularly, in the TDF sandy loam textures have good drainage in the under storage, good water-holding capacity and the right amount of movement of soil air, helping the development of plants during the rainy season, and to overcome the dry season when water uptake is hydraulically limited (Hultine *et al.*, 2005). Trees allocated in these soil textural classes are highly sensitive to small precipitation pulses reflecting on the carbon sequestration (Fravolini *et al.*, 2005) with significant implications for local and regional AGB. Soil nutrients (C, N and P) have little correlation to AGB as could be inferred from studies done on secondary forest or chronosequences which are highly nutrient demanding (Christensen and Peet, 1984; Mirmanto *et al.*, 1999; de Castilho *et al.*, 2006; Wright *et al.*, 2011). However, C:N and N:P ratios were important to explain AGB (Mirmanto *et al.*, 1999; Slik *et al.*, 2010; Wright *et al.*, 2011; Alvarez-Clare *et al.*, 2013). Ruiz-Jaen and Potvin (2011) found that the proportion of N-fixer species plays a major role in explaining AGB in N-limited forest. So forests dominated by N-fixers (Salas-Morales *et al.*, 2007) establish important symbiotic nitrogen fixation processes which help them overcome N-limitations.

Soil properties and tree allocation did not show spatial autocorrelation. Thus at tree level, the community was spatially heterogeneous and the tree-spatial distribution did not show an assembly of patches of comparable biodiversity and/or biophysical properties, as had been proposed by other authors (Hubbell, 1979; Levings, 1983; Murphy and Lugo, 1986b; Condit *et al.*, 2000). Some authors argue that large sized-tree allocation is the result of biotic interactions which modify the competitive ability of plants (Yeaton *et al.*, 1977;

Hubbell, 1979, 1980; Gonzalez and Zak, 1994; Condit *et al.*, 2000; Lucero *et al.*, 2006). Also Korner (2007) proposed that it is the result of gradients in light availability mediated by local topography, soil and air temperature by creating distinct types of light microhabitats. Consequently, large tree allocation depends on a multi-variable inter-correlation of micro-climatic and micro-topographic conditions, rather than intra- or inter- species for light or nutrients (Hubbell, 1980; Gonzalez and Zak, 1994; Condit *et al.*, 2000). Nonetheless, Arriaga *et al*., (1993) found that soil nutrient content and shade-sun conditions do not seem to explain the patchy distribution of perennial plants. Particularly for this study, some plots with very high AGB estimates could not entirely be understood without considering the presence of large-sized trees. Consequently, it is necessary to explore the drivers of allocation of colossal trees to be able to make a proper representation of the AGB, mainly for those outlier sites (de Castilho *et al.*, 2006). The representation of local site conditions, as well as sub-regional and landscape factors are positively influences to promote the development of individual trees over the average. The major limitation in this type of study is that such information is difficult to acquire on a landscape scale with such a degree of detail. Therefore, the most conclusive studies were done at continental or global scales (Slik *et al.*, 2013), where climatic variables explain the density of large-sized trees.

In a sub-regional scale, altitudes promote differences in potential evaporation by changes in the temperature and precipitation regime (SMN, 2014). This study finds that larger AGB estimates were measured at higher altitudes, as a consequence of water stress reduction. On the contrary, at lower altitudes precipitation is significantly reduced with an increase in potential evaporation. Other topographical variables indirectly correlate to bring shelter to plants against water and nutrient stress such as terrain curvature (Cusack *et al.*, 1997; Gessler *et al.*, 2000) and aspect (Galicia *et al.*, 1999; Bijalwan, 2012). Distance to streams is a direct force of water availability over longer periods (Cusack *et al.*, 1997; Rango *et al.*, 2006), but only in the first hundred meters, because of the root systems which catch lateral distribution of water. Other authors (de Castilho *et al.*, 2006; Alves *et al.*, 2010) found that slope plays a critical role in AGB distribution. However, in this study it was found that there is not a clear pattern, but this does not necessarily contradict the others because those studies may have been allocated to forest under different disturbance processes. Finally, high leaf expression (eg. LAI) played an important role in determining sites with lower water limitation, mainly during the dry season (Reich and Borchert, 1984). Sites with a higher mean of LAI or with less inter-seasonality were correlated to sites with less water stress, displaying larger AGB estimates. These processes can be related to the cycles of carbon up-take, where sites with less inter-seasonality have a longer growing period and as a result,

larger AGB estimates, similarly to observations done by Kenzo *et al*., (2010). The major limitation of using MODIS-LAI is that some pixels maybe have a mixture of signals of natural vegetation and anthropogenic disturbances.

At the landscape scale, climatic variables correlated more strongly to AGB. On the one hand, temperature correlated inversely to AGB, mean annual temperature and intra-seasonal temperature variability. Then in sites where plants tend to be more water stressed, temperature does not vary significantly during the rainy season. This is in contrast to areas with more variability, where there are mainly great differences, including at night, when plants re-hydrate (Reich and Borchert, 1984). On the other hand, rainfall and precipitation:temperature ratio correlate positively to AGB (Murphy and Lugo, 1986b; Martínez-Yrízar *et al.*, 1992; Jaramillo *et al.*, 2003; Read and Lawrence, 2003).

VI.2 Uncertainties in AGB reconstruction

According to Chave *et al.,* (2004) the main sources of uncertainty are tree measurements, plot size and selection of allometric equations. However, if the aim is to explain the spatial distribution of AGB, the selection of predictor variables and model play a compelling role. Moreover, depending on the model's validation approach the uncertainty could be underestimated.

(1) Tree measurements have random errors due to personal data collection (DBH and tree-height measurements) or the nature of the tree (differences in wood density and/or carbon concentration). For the former error it is assumed that the measurements are independent and follow a normal distribution. Positive and negative errors of the same size would happen with analogous frequency of DBH and height measurements. Because of the large number of samples it is possible to offset random errors. Gross errors, such as double counting or missing trees are considered absent due to the fact trees were marked during the data collection. However, gross errors during data collection in the field are impossible to estimate without re-measuring the trees. According to these results, forest inventories that look into trees larger than DBH>10 cm may drive serious changes in the perception of this ecosystem with major implications on AGB (Keller *et al.*, 2001). In this study, it was possible to account for at least 15% of AGB underestimation, analogous with proportions reported for another mature TDF in Mexico (Jaramillo *et al.,* 2003) and less than that reported by Read and Lawrence (2003). This contrasts with the results reported for other tropical ecosystems (~3%) showing a much greater precipitation (~2,500 mm) (Chave *et al.*, 2004). Consequently, tropical dry forest should be analyzed and sampled differently from tropical rain forests where large-sized trees are more common, and small-sized trees have a

reduced representation (Turner, 2001). Finally, the latter type of error was minimized by including local wood density and wood and litter carbon content.

(2) The plots sized 10x30 and 10x40m are the right size to capture a normal distribution of AGB in a mature TDF, and produce comparable results to plots of 1 ha. The numbers of trees for small and large sampling approaches have similar distribution, including large-sized trees. The advantages of this sampling approach are: (a) a higher number of repetitions at lower costs; (b) easily comparable results because of its popularity (Chapter I); (c) the possibility to discern species' composition (Giliba *et al.*, 2011); and (d) their impact on AGB (Kirby and Potvin, 2007); (e) exploration of the processes that drive large-sized tree allocation on a local scale; (f) the landscape is not over-simplified by the final result; and (g) better interpretation of disturbances and natural regeneration processes are possible. Therefore, patterns and processes are better understood, mainly in very complex topographic conditions.

(3) The selection of the allometric equation reveals a great impact on AGB prediction. For the region there is not a local allometric equation. Hence, it was necessary to use equations built for other regions. Therefore, intrinsically any allometric equation shows a high uncertainty. Nevertheless, with a multi-model integration of the most approachable allometric equations, it was possible to account for the uncertainty of AGB, and to identify the main source of error. At the tree level, large-sized trees (DBH ≥75 cm) were shown to create the most uncertain AGB estimates, as other authors have proposed (Baker *et al.*, 2004; Chave *et al.*, 2004). Nonetheless, large-sized trees (DBH ≥60 cm) are scarce in the TDF which limits their impact on mean AGB (~20%). The same observations done to other tropical ecosystems (Keller *et al.*, 2001; Chaturvedi *et al.*, 2011) produced slightly greater than the 13% reported by Nascimento and Laurance (2002). Small to medium-sized trees (DBH <30 cm) are important because they are abundant and they contribute to the greatest biomass (>60% of the AGB) (Jaramillo *et al.*, 2003; Baker *et al.*, 2004; Chaturvedi *et al.*, 2011). At tree level there are little differences across diverse allometric equations on estimating AGB for small to medium-sized trees. However, because of their high density they have the greatest impact on a landscape scale, as they do on the uncertainty (Keller *et al.*, 2001). Therefore to reduce the uncertainty of AGB estimations at landscape scales, forest inventories should implement a full sampling collection for every stem, and allometric equations should be improved for small to medium-sized trees (<50 cm in DBH). Finally, a significant source of uncertainty can be tackled using a local allometric equation for trees within 5-40 cm in DBH.

(4) Selection of predictor variables and modelling provided possibly the most critical source of uncertainty to reproduce AGB. On the one hand, predictor variables that correlate to AGB exhibit divergent explicative power to reproduce AGB. In some cases, the variable exposes great sensitivity with the capability of over or under estimating AGB. Over-fitting models with predictor variables increased the model fit, but decreased the predictive performance. In this study, both elements were taken into consideration. Firstly, with the exploration of how the ecosystem is assembled it was possible to select the most significant predictor variables and test their sensitivity in the models. Climatic variables played an important role in predicting AGB. However, AGB predictions were variable. On the other hand, model selection was significant in predicting AGB. Most of the models were capable of predicting AGB over large areas with accuracy, capturing mean AGB estimate for the landscape. Nonetheless, at a local scale, the models showed divergent performances, not only in the allocation of the AGB estimates, but also in the range of predicted values. These have led differences in the predictability of AGB across the landscape. Independent validation demonstrates that the uncertainty in the predictions was contrastingly different across the models. GLM produced a constrained uncertainty in the predictions, while RT and NN showed a much wider uncertainty. GLM offers a smaller uncertainty in the prediction for low AGB estimates and when the mean predictions were close to the observations. But larger uncertainties were generated mainly when the mean predictions failed to be close to the observations. On the contrary, though NN and RT kept differences between predictions small, the total mean residuals were reduced because they reproduced precisely the mean landscape AGB, failing to produce accurate estimations. Also, the uncertainty in the predictions was consistently wider than with GLM. Spatial differences in the models were of great concern, similar to observations done for other studies (Houghton *et al.*, 2001; Saatchi *et al.*, 2007; Ometto *et al.*, 2015). The observed spatial AGB patterns were only possible to reconstruct with GLM. When contrasting the various models' predictions against a null model, MaxEnt and GLMM performed worst. Thus, it is recommended to test contrasting models for the spatial representation of AGB estimates at fine scales.

Finally, (5) while the model validation approach does not influence directly the uncertainty of the predictions, it may underestimate the level of uncertainty. Independent validation reveals that models performed worse than Jackknife (MaxEnt) or bootstrapping techniques (Harrell, 2015). The same models tested against independent data display a serious reduction in their ability to predict AGB (Hill *et al.*, 2013). Models such as RF and NN can be easily over-fitted. In particular with RF and NN, the bootstrapping technique reported better performance in reproducing AGB estimates used during the calibration.

Notably for NN, the optimization produced excellent model fitting, but a poor prediction capability for independent samples. Techniques such as bootstrapping or Jackknife may mislead the results and underestimate uncertainty in AGB predictions (Harrell, 2015). Therefore, it is recommended that an independent validation should be implemented to validate the performance of the models (Hill *et al.*, 2013) and when possible models should be tested over various spatial scales.

VI.3 Deforestation and degradation processes

The carbon emissions due to deforestation and forest degradation can be estimated through the integration and comparison of multiple input maps. In this study a net carbon emission was derived, by contrasting the potential carbon stocks map with the diverse current carbon stock maps. In the study it was considered that the input maps did not differ importantly in the epoch they represent, and little differences across the maps are expected as a result of LUCC. The LUCC during the period 2006-2011 for the same region was reported in <2.3% of the landscape (PSIG, 2015). The potential total carbon stock in the region is between 11,000 and 13,000 GgC (Chapter IV). About 44% of the potential carbon estimated for the region is still present, which represents a degraded forest (Asner *et al.*, 2010), characterized by a mature forest matrix among secondary forest and anthropogenic covers. During the period 1985-2006, an analogous proportion of the landscape did not show any LUCC process (Corona, 2012). It is estimated that about 7,000 GgC has been emitted due to deforestation and degradation of the forest (Chapter V). The scale of analysis (1 km^2) does not enable counting of emissions from deforestation and degradation individually, and both processes are masked as disturbance. Nevertheless, this study considers that ~62% of the total carbon emissions can be regarded as being due to forest degradation. This is comparable to estimates from other studies undertaken at finer resolutions which reported that forest degradation accounts for ~67% of net losses of AGB (Gaston *et al.*, 1998; Ryan *et al.*, 2012) under similar land-use management as the landscape in this study. These results allow a general picture of potentially how much AGB has been lost over time, and set a benchmark for landscape management.

In this region Corona (2012) and Mendoza (2015) found that the proximate drivers of deforestation are grassland for cattle raising, agriculture and urban development. However, it was unknown how much of the AGB has been lost because of LUCC and forest degradation. Nevertheless, Skutsch (2009) reported that dry forest carbon emissions are important because of continued carbon losses. Forest AGB loss is not evenly distributed in the landscape and is related mainly to socio-economic pressures. Corona (2012) and Ryan *et al.*,

(2012) found that cleared areas are the result of small expansions in the boundaries of already cleared land, congruent with processes observed for AGB losses. Greater AGB losses were observed closer to current agricultural lands, human settlements and roads. Climatic variables and altitude were significant variables to explain the spatial variability of AGC reductions. And they act as underlying explanatory variables of LUCC processes. For example, places with high water stress are less suitable for agriculture, consequently, less AGC was lost. In contrast, accessible regions and those climatically suitable for agriculture have the highest transformations in AGC. Interestingly, at lower altitudes (close to the coast) places limited for agricultural activities but close to urban establishments and paved roads exhibit high AGC reductions. This can be related to urban expansion and the establishment of tourist resorts along the coast (Corona, 2012). Finally, regions isolated from human land-cover change within the boundaries of the National Protected Area have shown a reduced pressure on the forest (Figure V.5); analogous observations have been reported by Corona (2012) and Mendoza (2015). Forest degradation processes are difficult to measure at the spatial resolution of this study. However, it can be argued that degradation happens close to dirt roads, human settlements, and agricultural fields. According to Corona (2012) and Corona *et al.*, (2016), the process of shifting cultivation in the region takes place up to 4 km from the previous agriculture plot, suggesting within this spatial range the population may play a critical role in forest degradation. Where sites closer to rural settlements are preferable for shifting cultivation (<1 km) and cattle raising (<3 km), similar ranges were identified in this study for carbon losses.

Finally, future models with the aim to quantify current AGB maps should take into consideration socio-ecological factors. The selection of those variables would depend not only on the ecosystem studied, but also in the spatial resolution of the outcome. For example, finer resolution maps, with pixels under $1km^2$, should include topographic information with a much finer resolution than that provided by the SRTM. Also, socio-economic variables, and LULC maps should be built accordingly. Deforestation in Mexican TDF is mainly driven by agricultural activities and land cleared in small patches, which are underestimated and misplaced in national LULC maps. A comparable situation may happen in other tropical-dry regions in the world. Coarser resolution maps, with pixels over $1km^2$, can include among their predictor variables national LULC maps, as well as SRTM as an altitude variable, alongside climatic variables. This shows the great importance of taking a bottom-up approach when the aim is to develop a high resolution AGB map.

Chapter VII. General conclusion

In spite of what is often reported about AGB in other tropical forests, AGB in the TDF shows significant differences. Among the tropical forest, the TDF has relevant differences in its structure with important implications for AGB. It was generally assumed that large-sized trees represented the greatest proportion of AGB in tropical forests. However, this study shows that this is not generally true for all tropical forests. Tree density and AGB allocation in TDF are dominated by small to medium-sized trees, and large-sized trees have little representation. This has serious implications for how the field information can be collected. This study also proves that there are not significant differences in small and large sampling design. It finds that TDF is a characteristic ecosystem to which generalist conclusions built from studies in tropical forest, including savannas, do not apply, or should be taken with more caution.

The estimation of spatial heterogeneity of AGB in the landscape is of great importance when measuring carbon stocks and ecological dynamics. It will serve as a baseline for determining changes in AGB. Consequently, the scale of data collection is crucial. The sampling collection used in this thesis allowed the identification, clarification and understanding of the main drivers of AGB allocation in the mature TDF. Also, it was viable to test differences in the spatial pattern of AGB that come up from diverse sources of data and model selection. On one hand, various multi-variable models support the belief that water availability plays the major role in explaining AGB on a local, sub-regional and landscape scale. On the other hand, model selection produced contrasting AGB estimates and patterns. Not all the models were capable of improving a null model and/or reproducing the spatial patterns of AGB. Also, it was demonstrated that an independent validation is mandatory to account for the uncertainty of the predictions. The models showed reduced predictability power for independent data than bootstrapping or Jacknife techniques. Most of the models were capable of reproducing a mean AGB estimate at the landscape scale. Only the GLM model reproduced similar spatial AGB magnitudes and patterns as the observations. However, it is not clear if these prediction capabilities could be extrapolated to other regions. Therefore, it is necessary to explore in more detail how different models can be fitted to reproduce AGB in places beyond their current spatial calibration range.

Various elements influence the AGB allocation in the mature forest. Among all of them water availability played the most decisive part of various spatial scales. In this study, soil nutrients did not correlate to AGB in the mature forest. However, it is not well documented if similar patterns were observed in other mature forests, because most studies have focused on secondary forests. Water availability promoted stress to the plant and with

it, its carbon uptake. Water availability is directly and indirectly affected by climate, topography and soil physical properties. Consequently, AGB in relation to water availability should be analyzed over various spatial scales. Also, more research regarding AGB allocation in mature forest and nutrients is needed.

Some observations were always underestimated by all the models. This suggests that there are other underlying variables that were not identified in this study and require more analysis. Those observations were characterized as showing very-high AGB with more than one large-sized tree. In that case it is of primary concern to identify factors that promote the clustering of those large-sized trees. Other studies have suggested that to minimize these effects, the data collection should be done in larger plots. This would be difficult, considering that sampling collection must not be compromised; the chosen sampling strategy would have critical impacts on the outcome of that analysis. Firstly, the spatial representation of AGB maps would never be smaller than the sampling collection. Secondly, the understanding of AGB allocation would be simplified, and information such as nutrient availability, micro-climate and species composition would be biased or minimized. Thirdly, the highly heterogeneous TDF landscape would be oversimplified. Therefore, spatial patterns such as AGB allocation about aspect, slope, altitude and solar irradiation would be highly uncertain. Finally, socio-economic pressures would be minimized and difficult to measure and model. Consequently, with the approach implemented in this study fine resolution AGB maps can be improved. Moreover, future models should look into how fine-scale patch dynamics may be coupled at broader scales to make a better representation of AGB and its potential implication for climate change risks. Accordingly, an accurate representation of the spatial variation of potential AGB will help in a better assessment and understanding of impacts of deforestation and forest degradation in carbon emissions and climate change as well as biological niches for biodiversity or food supply for diverse species.

The results of this study tell us that there is not a clear consensus among various current AGB maps. However, they also show that with a multi-model comparison it is possible to identify carbon emissions drivers and calculate total carbon emissions due to forest disturbances. Socio-economic variables played the major role in explaining AGB losses. Climatic variables were only significant to understand the spatial bias across the diverse maps. Models should not only rely on remote sensing information as a proxy of socio-ecological drivers. Therefore, current AGB maps should consider a bottom-up perspective for AGB allocation from a socio-ecological perspective. AGB maps built from this approach will have more explicative power to reproduce current field-based AGB

estimates. Consequently, an important source of uncertainty can be minimized. Nevertheless, it is expected that carbon emissions due to disturbance will increase in the coming years. The role of population in driving deforestation is complex and characterized by spatial and temporal impacts. The growing rural population will have larger demands for wood and food, so while remote or protected areas may have the potential for storing high AGB, forest near settlements and access routes are likely to continue being disturbed unless affordable alternatives are available for the sustainable use of the forest.

Finally, these outputs are useful to support informed decisions when restoring or managing an ecosystem. The results obtained in this study can guide and identify rare elements in the landscape which in most studies tend to be avoided or minimized by changing the sampling design. Also, they can help in the understanding of patterns and processes in landscape ecology and population analysis. It should be said that the scale of field sampling collection and the pixel size of the raster variables should be accordingly evaluated to the spatial resolution of the AGB representation.

Chapter VIII. Further work

VIII.1 How accurate are the models of Chapter IV to reproduce AGB in other regions of Mexico?

Models built in Chapter IV showed great capabilities to reproduce mean AGB at the landscape scale, but only GLM in a local scale. Therefore, it would be important to test these same models in other regions of Mexico with similar vegetation types. A complete independent validation is needed over the spatial range where the models show the capacity to extrapolate information over greater spatial scales. Failure in the models can also shed light on the limitations of possible variables, helping in the identification of new alternatives to overcome this situation. With these new and adjusted models we can expect improvement in estimations of AGB over larger spatial scales, and the representation of key factors to understand AGB spatial distribution.

VIII.2 Identify and account for other biological restraints to AGB accumulation.

AGB in a mature TDF is mainly driven by water stress. Various sources of information have suggested that nutrients are also important. However, this study did not find such correlation in mature forest. Nevertheless, it is possible to explore how nutrients could drive different AGB stock for successional stages. This information is crucial to understand the mechanism for carbon sequestration over successional stages and the impact of future warmer and drier conditions on TDF carbon sequestration.

Leaf Mass Area (LMA) is a significant variable that correlates with photosynthetic activities and traits in the plant growth and therefore on carbon sequestration rates. Strategies in leaf physiology (LMA & chemical composition) may be explored to see their effect on the growth rates of woody tissue, changes over successional stages and climatic conditions and species composition. Therefore, this analysis should explore soil classification and nutrients (Na, K, Mg, Ca, $N\text{-}NO_3$, $N\text{-}NH_4$) and cationic exchange capacity (CEC) to AGB for successional stages and mature forest. Finally, biodiversity has been shown to be a functional trait in carbon sequestration. Nitrogen sequester plants may induce contrasting paths in carbon sequestration processes, as well as the local total AGB.

VIII.3 How do N, P, and water stress affect growth rates and canopy structure in a mature forest?

Based on the results in Chapter III and Chapter IV it was possible to identify that N and P alone did not present an important factor in explaining AGB in a mature forest. However, there is still a lack of understanding of how these micro-nutrients may affect carbon sequestration (biomass and/or soil). Water stress was the most significant variable to explain AGB. Also, reduced water stress turned in higher LAI and AGB. However, the mechanism of how water stress, N and P may intervene in the forest canopy structure in a mature forest is not entirely clear. Therefore, it is important to test how the enrichment of N, P and watering may drive contrasting carbon stock and forest structure in a mature forest over multiple years.

To test this approach it is necessary to establish diverse sampling plots with contrasting altitudes but similar topography (slope, aspect and distance to streams). Within each of the plots four independent sub-plots should be delimited. One plot will work as validation, and the other three for testing the model. The first test would be watered the whole year, the second would be watered and N enriched, and finally, the last plot would be watered and N and P enriched.

Diverse information should be collected to understanding the effects of these modifications. First of all, all the trees should be classified to specie, geotagged and coded in the field. DBH and height measurements should be recorded for every tree, shrub and seedling. This process should be done at least 3 times per year. With this process it will be possible to monitor DBH changes over time as well as changes in measuring the height. To reduce error in measurements, all plants should be marked where previous measurement was done and changes in height and DBH recorded. Flowering seasonality for each tree should be evaluated, and the starting and ending day of leaves falling. Litterfall tramps should be considered *per* tree to establish the influence for each specie or correlation to woody biomass. Litter on the ground would have to be weighed to contrast changes over time. Fine roots production and LMA changes need to be recorded. Finally, ideally, each site would have instruments to record soil and atmospheric temperature, soil wetness and atmospheric relative humidity.

Chapter IX. References

.

Achard, F., Eva, H.D., Mayaux, P., Stibig, H.J., Belward, A., 2004. Improved estimates of net carbon emissions from land cover change in the tropics for the 1990s. Global Biogeochemical Cycles 18, GB2008.

Achard, F., Eva, H.D., Stibig, H.J., 2002. Determination of deforestation rates of the world's humid tropical forests. Science 297, 999–1002.

Altmann, A., Tolosi, L., Sander, O., Lengauer, T., 2010. Permutation importance: a corrected feature importance measure. Bioinformatics 26, 1340-1347.

Alvarez-Clare, S., Mack, M.C., Brooks, M., 2013. A direct test of nitrogen and phosphorus limitation to net primary productivity in a lowland tropical wet forest. Ecology 94, 1540-1551.

Alves, L.F., Vieira, S.A., Scaranello, M.A., Camargo, P.B., Santos, F.A.M., Joly, C.A., Martinelli, L.A., 2010. Forest structure and live aboveground biomass variation along an elevational gradient of tropical Atlantic moist forest (Brazil). Forest Ecology and Management 260, 679-691.

Allen, T.F.J., Hoekstra, T.W., 1990. The confusion between scale-defined levels and conventional levels of organization in ecology. Journal of Vegetation Science 1, 5-12.

Anav, A., Friedlingstein, P., Beer, C., Ciais, P., Harper, A., Jones, C.D., Murray-Tortarolo, G., Papale, D., Parazoo, N.C., Peylin, P., Piao, S., Sitch, S., Viovy, N., Wiltshire, A., Zhao, M., 2015. Spatiotemporal patterns of terrestrial gross primary production: A review. Reviews of Geophysics 53, 785-818.

Anaya, C.A., García-Oliva, F., Jaramillo, V.J., 2007. Rainfall and labile carbon availability control litter nitrogen dynamics in a tropical dry forest. Oecologia 150, 602-610.

Arora, V.K., Boer, G.J., Friedlingstein, P., Eby, M., Jones, C.D., Christian, J.R., Bonan, G., Bopp, L., Brovkin, V., Cadule, P., Hajima, T., Ilyina, T., Lindsay, K., Tjiputra, J.F., Wu, T., 2013. Carbon–Concentration and Carbon–Climate Feedbacks in CMIP5 Earth System Models. Journal of Climate 26, 5289-5314.

Arriaga, L., Maya, Y., Diaz, S., Cancino, J., 1993. Association between cacti and nurse perennials in a heterogeneous tropical dry forest in northwestern Mexico. Journal of Vegetation Science 4, 349-356.

Asner, G.P., Powell, G.V.N., Mascaro, J., Knapp, D.E., Clark, J.K., Jacobson, J., Kennedy-Bowdoin, T., Balaji, A., Paez-Acosta, G., Victoria, E., Secada, L., Valqui, M., Hughes, R.F., 2010. High-resolution forest carbon stocks and emissions in the Amazon. Proceedings of the National Academy of Sciences 107, 16738-16742.

Aukland, A., Sohngen, B., Hall, M., Brown, S., 2002. 2001 Analysis of leakage, baselines and carbon benefits for the Noel Kempff Climate Action Project. Winrock International, 1621 N. Kent St., Arlington, VA 22209.

Austin, P.C., 2007. A comparison of regression trees, logistic regression, generalized additive models, and multivariate adaptive regression splines for predicting AMI mortality. Statistics in Medicine 26, 2937-2957.

Avitabile, V., Herold, M., Heuvelink, G., Lewis, S.L., Phillips, O.L., Asner, G.P., al., e., 2016. An integrated pan-tropical biomass maps using multiple reference datasets. Global Change Biology 22, 1406-1420.

Baccini, A., Asner, G.P., 2013. Improving pantropical forest carbon maps with airborne LiDAR sampling. Carbon Management 4, 591-600.

Baccini, A., Goetz, S.J., Walker, W.S., Laporte, N.T., Sun, M., Sulla-Menashe, D., Hackler, J., Beck, P.S.A., Dubayah, R., Friedl, M.A., 2012a. Estimated carbon dioxide emissions from tropical deforestation improved by carbon-density maps. Nature Clim Change 2.

Baccini, A., Goetz, S.J., Walker, W.S., Laporte, N.T., Sun, M., Sulla-Menashe, D., Hackler, J., Beck, P.S.A., Dubayah, R., Friedl, M.A., Samanta, S., Houghton, R.A., 2012b.

Estimated carbon dioxide emissions from tropical deforestation improved by carbon-density maps. Nature Clim. Change 2, 182-185.
Baccini, A., Laporte, N., Goetz, S.J., Sun, M., and Dong, H., 2008. A first map of tropical Africa's above-ground biomass derived from satellite imagery. Environmental Research Letters 3, 9.
Bachelet, D., Neilson, R.P., Hickler, T., Drapek, R.J., Lenihan, J.M., Sykes, M.T., Smith, B., Sitch, S., Thonicke, K., 2003. Simulating past and future dynamics of natural ecosystems in the United States. Global Biogeochemical Cycles 17, 1045.
Baker, T.R., Phillips, O.L., Malhi, Y., Almeida, S., Arroyo, L., Di Fiore, A., Erwin, T., Killeen, T.J., Laurance, S.G., Laurance, W.F., Lewis, S.L., Lloyd, J., Monteagudo, A., Neill, D.A., Patiño, S., Pitman, N.C.A., M. Silva, J.N., Vásquez Martínez, R., 2004. Variation in wood density determines spatial patterns in Amazonian forest biomass. Global Change Biology 10, 545-562.
Barlow, J., Peres, C.A., Lagan, B.O., Haugaasen, T., 2003. Large tree mortality and the decline of forest biomass following Amazonian wildfires. Ecology Letters 6, 6-8.
Bauer, M., Loeffelholz, B., Wilson, B., 2005. Estimation, mapping and change analysis of impervious surface area by Landsat remote sensing. In: Conference, P. (Ed.), American Society of Photogrammetry and Remote Sensing, Sioux Falls, South Dakota, USA, p. 9.
Becknell, J.M., Kissing Kucek, L., Powers, J.S., 2012. Aboveground biomass in mature and secondary seasonally dry tropical forests: A literature review and global synthesis. Forest Ecology and Management 276, 88-95.
Beder, S., 2006. Environmental Principles and Policies. Earthscan, London, UK.
Beder, S., 2007. Carbon offsets are not sustainable. Green 22, 16-17.
Bennie, J., Huntley, B., Wiltshire, A., Hill, M.O., Baxter, R., 2008. Slope, aspect and climate: Spatially explicit and implicit models of topographic microclimate in chalk grassland. Ecological Modelling 216, 47-59.
Berdanier, A.B., Klein, J.A., 2011. Growing Season Length and Soil Moisture Interactively Constrain High Elevation Aboveground Net Primary Production. Ecosystems 14, 963-974.
Beven, K.J., 1977. Distributed Hydrological Modelling: Applications of the TOPMODEL Concept. Wiley & Sons, Chichester.
Bijalwan, A., 2012. Land use and vegetation analysis of dry tropical forest. Using remote sensing & GIS. Lambert, Academic Publishing, UK.
Bijalwan, A., Swamy, S., Sharma, C., Sharma, N., Tiwari, A., 2010. Land-use, biomass and carbon estimation in dry tropical forest of Chhattisgarh region in India using satellite remote sensing and GIS. Journal of Forestry Research 21, 161-170.
Bishop, C., 1995. Neural networks for pattern recognition. Oxford University Press, Oxford.
Bolin, B., Sukumar, R., Ciais, P., Cramer, W., Jarvis, P., Kheshgi, H., Nobre, C., Semenov, S., Steffen, W., 2000. IPCC special report on land use, land-use change and forestry. Cambridge University Press, Cambridge, UK.
Bolovo, F., Bruzzone, L., Carlin, L., 2010. A Novel Technique for Subpixel Image Classification Based on Support Vector Machine. IEEE TRANSACTIONS ON IMAGE PROCESSING 19, 2983-2999.
Bray, R., Kurtz, L., 1945. Determination of total, organic and available forms of phosphorus in soil. Soil Sci 59, 39-45.
Breiman, L., 1996. Bagging Predictors Machine Learning 24, 123-140.
Breiman, L., 2001. Random Forest. Machine Learning 45, 5-32.
Brown, S., 1997. Estimating biomass and biomass change of tropical forests: a Primer. *FAO Forestry Paper* FAO - Food and Agriculture Organization of the United Nations.
Brown, S., 2002. Measuring carbon in forest: current status and future challenges. Environmental Pollution 116, 363-372.

Brown, S., Gillespie, A.J.R., Lugo, A.E., 1989. Biomass Estimation Methods for Tropical Forests with Applications to Forest Inventory Data. Forest Science 35, 881-902.
Brown, S., Lugo, A., 1984. Biomass of tropical tree plantations and its implications for the global carbon budget. Canadian Journal of Forestry Research 16, 390-394.
Brown, S., Lugo, A.E., 1982. The storage and production of organic matter in tropical forests and their role in the global carbon cycle. Biotropica 14, 161-187.
Brown, S., Lugo, A.E., 1990. Tropical secondary forests. Journal of Tropical Ecology 6, 1-32.
Bürgi, M., Hersperger, A.M., Schneeberger, N., 2004. Driving forces of landscape change — current and new directions. Landscape Ecol 19, 857-868.
Burgos, A., Maass, J.M., 2004. Vegetation change associated with land-use in tropical dry forest areas of Western Mexico. Agriculture, Ecosystems & Environment 104, 475-481.
Burquez, A., Martínez-Yrizar, A., 2010. Accuracy and bias on the estimation of aboveground biomass in the woody vegetation of the Sonoran Desert. Botany 89.
Burrough, P.A., McDonnell, R., Burrough, P.A., 1998. Principles of Geographical Information Systems. Oxford University Press, Oxford, UK.
Bushnell, 2016. Technical Specs. Bushnell.
Cairns, M., Olmsted, I., Granados, J., Argaez, J., 2003. Composition and aboveground tree biomass of a dry semi-evergreen forest on Mexico's Yucatan Peninsula. Forest Ecology and Management 186, 125-132.
Campo, J., Jaramillo, V., Maass, J.M., 1998. Pulses of soil phosphorus availability in a Mexican tropical dry forest: effects of seasonality and level of wetting. Oecologia 115, 167-172.
Canadell, J.G., Le Quere, C., Raupach, M.R., Field, C.B., E.T, B., Ciais, P., Conway, T.J., Gillett, N.P., Houghton, R.A., Marland, G., 2007. Contributions to accelerating atmospheric CO(2) growth from economic activity, carbon intensity, and efficiency of natural sinks. Proceedings of the National Academy of Sciences of the United States of America. National Academy of Sciences, USA, pp. 18866-18870.
Cao, M., Woodward, F.I., 1998. Dynamic responses of terrestrial ecosystem carbon cycling to global climate change. Nature 393, 249-252.
Carpenter, S., DeFries, R., Dietz, T., Mooney, A., Polasky, S., Reid, V., Scholes, J., 2006. Millennium ecosystem assessment: research needs. Science 314, 257-258.
Cartus, O., Kellndorfer, J., Walker, W., Franco, C., Bishop, J., Santos, L., Fuentes, J., 2014. A National, Detailed Map of Forest Aboveground Carbon Stocks in Mexico. Remote Sensing 6, 5559.
Castellanos, J., Maass, M., Kummerow, J., 1991. Root biomass of a dry deciduous tropical forest in Mexico. Plant Soil 131, 225-228.
Castillo-Campos, G., Halffter, G., Moreno, C.E., 2008. Primary and secondary vegetation patches as contributors to floristic diversity in a tropical deciduous forest landscape. Biodiversity and Conservation 17, 1701-1714.
Castillo, A., Magaña, A., Pujadas, A., Martínez, L., Godínez, C., 2005. Understanding the Interaction of Rural People with Ecosystems: A Case Study in a Tropical Dry Forest of Mexico. Ecosystems 8, 630-643.
CCSP, 2003. Strategic Plan for the U.S. Climate Change Science Program. A Report by the Climate Change Science Program and the Subcommittee on Global Change Research. In: Office, C.C.S.P. (Ed.). U.S. Climate Change Science Program, Washington, DC, USA, p. 211.
Céspedes-Flores, Moreno-Sánchez, 2010. Estimación del valor de la pérdida de recurso forestal y su relación con la reforestación en las entidades federativas de México. Investigación Ambiental 2, 5-13.
CIEDD, 2012. Carpeta Regional: Costa. In: Desarrollo, C.d.I.E.y.D.p.e. (Ed.), Información estadística y geografía básica. Estado de Oaxaca.

Civco, D.L., Hurd, J.D., 1997. Impervious surface mapping for the state of Connecticut. American Society for Photogrammetry and Remote Sensing Seattle, Washington, Missouri,, pp. 124-135.
Civco, D.L., Hurd, J.D., Wilson, E.H., Arnold, C.L., Prisloe Jr, M.P., 2002. Quantifying and describing landscapes in the northeast United States. Photogrammetric Engineering and Remote Sensing 68, 1083-1090.
Clark, M., 2013. Generalized Additive Models. Getting started with additive models in R. Centre for Social Reseach. University of Notre Dame.
Cleveland, C., Liptzin, D., 2007. C:N:P stoichiometry in soil: is there a "Redfield ratio" for the microbial biomass? Biogeochemistry 85, 235-252.
Cochran, W.G., 1977. Sampling Techniques. New York. Wiley.
Collins, M.B., Mitchard, E.T.A., 2015. Integrated radar and lidar analysis reveals extensive loss of remaining intact forest on Sumatra 2007–2010. Biogeosciences 12, 6637-6653.
CONAFOR, 2007. Manual y procedimientos para el muestreo de campo del Inventario Nacional Forestal y de Suelos 2004-2009. In: Forestal, C.N. (Ed.). CONAFOR, Zapopan, Jalisco, Mexico.
CONAFOR, 2012. Inventario Nacional Forestal y de Suelos. Informe 2004-2009. In: Geomática, G.d.I.F.y. (Ed.). Coordinación General de Planeación e Información, Zapopan, Jalisco, Mexico.
Condit, R., Ashton, P.S., Baker, P., Bunyavejchewin, S., Gunatilleke, S., Gunatilleke, N., Hubbell, S.P., Foster, R.B., Itoh, A., LaFrankie, J.V., Lee, H.S., Losos, E., Manokaran, N., Sukumar, R., Yamakura, T., 2000. Spatial Patterns in the Distribution of Tropical Tree Species. Science 288, 1414-1418.
Corona, R., 2009. Programa de Manejo Forestal Sostenible y Aseguramiento de los Servicios Ambientales en Bahías de Huatulco, Oaxaca. FONATUR-PSIG, Mexico City.
Corona, R., 2012. Conductores de la deforestación: Estudio de Caso en el Bosque Tropical Caducifolio en Oaxaca. Editorial Académica Española.
Corona, R., Galicia, L., Palacio, J., Bürgi, M., Hersperger, A.M., 2016. Local deforestation patterns and their driving forces of tropical dry forest in two municipalities in Southern Oaxaca, Mexico (1985-2006). Investigaciones Geográficas, Boletín del Instituto de Geografía, UNAM.
Cox, P., Harris, P., Huntingford, C., Betts, R., Collins, M., Jones, C., Jupp, T., Marengo, J., Nobre, C., 2008. Increasing risk of Amazonian drought due to decreasing aerosol pollution. Nature 453, 210-215.
Cramer, W., Bondeau, A., Schaphoff, S., Lucht, W., Smith, B., Sitch, S., 2004. Tropical forests and the global carbon cycle: impacts of atmospheric carbon dioxide, climate change and rate of deforestation. Philosophical Transactions of the Royal Society B: Biological Sciences 359, 331-343.
Cramer, W., Bondeau, A., Woodward, I., Prentice, C., Betts, R., Broykin, V., Cox, P., Fisher, V., Foley, J., Friend, A., Kucharik, Lomas, M., Ramankutty, N., Sitch, S., Smith, B., White, A., Young-Molling, 2001. Global response of terrestrial ecosystem structure and function to CO2and climate change: results from six dynamic global vegetation models. Global Change Biology 7, 357-373.
Crawley, M.J., 2013. The R Book. Wiley.
Cressie, N.A.C., 1985. Fitting variogram models by weighted least squares. Journal of the International Association for Mathematical Geology 17, 563-586.
Cressie, N.A.C., 1993. Statistics for Spatial Data, Revised Edition. Wiley, New York.
Currie, W.S., 2011. Units of nature or processes across scales? The ecosystem concept at age 75. New Phytologist 190, 21-34.
Cusack, G.A., Hutchinson, M.P., Kalma, J.D., 1997. Relating Biomass and Land Surface Reflectance to Primary Terrain Attributes in a Small Catchment. In: Zerger, A., Argent, R.M. (Eds.), MODSIM 1997. International Congress on Modelling and

Simulation. Modelling and Simulation Society of Australia and New Zealand, University of Tasmania, Hobart.
Czarnota, J., Wheeler, D.C., Gennings, C., 2015. Evaluating Geographically Weighted Regression Models for Environmental Chemical Risk Analysis. Cancer Informatics, 117-127.
Chaturvedi, R.K., Raghubanshi, A.S., Singh, J.S., 2011. Carbon density and accumulation in woody species of tropical dry forest in India. Forest Ecology and Management 262, 1576-1588.
Chave, J., Andalo, C., Brown, S., Cairns, M.A., Chambers, J.Q., Eamus, D., Fölster, H., Fromard, F., Higuchi, N., Kira, T., Lescure, J.P., Nelson, B.W., Ogawa, H., Puig, H., Riéra, B., Yamakura, T., 2005. Tree allometry and improved estimation of carbon stocks and balance in tropical forests. Oecologia 145, 87-99.
Chave, J., Condit, R., Aguilar, S., Hernandez, A., Lao, S., Perez, R., 2004. Error propagation and scaling for tropical forest biomass estimates. Phil. Trans. R. Soc. Lond. B 359, 409–420.
Chave, J., Condit, R., Lao, S., Caspersen, J.P., Foster, R.B., Hubbell, S.P., 2003. Spatial and temporal variation of biomass in a tropical forest: results from a large census plot in Panama. Journal of Ecology 91, 240-252.
Chave, J., Réjou-Méchain, M., Búrquez, A., Chidumayo, E., Colgan, M.S., Delitti, W.B.C., Duque, A., Eid, T., Fearnside, P.M., Goodman, R.C., Henry, M., Martínez-Yrízar, A., Mugasha, W.A., Muller-Landau, H.C., Mencuccini, M., Nelson, B.W., Ngomanda, A., Nogueira, E.M., Ortiz-Malavassi, E., Pélissier, R., Ploton, P., Ryan, C.M., Saldarriaga, J.G., Vieilledent, G., 2014. Improved allometric models to estimate the aboveground biomass of tropical trees. Global Change Biology 20, 3177-3190.
Chomitz, K.M., Buys, P., De Luca, G., Thomas, T.S., Wertz-Kanounnikoff, S., 2007. ¿Realidades antagónicas? Expansión agrícola, reducción de la pobreza y medio ambiente en los bosques tropicales. Mayol Ediciones S.A.
Christensen, N.L., Peet, R.K., 1984. Convergence during secondary forest sucession. Journal of Ecology 72, 25.
Dale, V., Joyce, L., Mcnulty, S., Neilson, R., Ayres, M., Flannigan, M., Hanson, P., Irland, L., Lugo, A., Peterson, C., Simerloff, D., Swanson, F., Stocks, B., Wotton, B., 2001. Climate Change and Forest Disturbances. BioScience 51, 723-734.
Davidson, E.A., Janssens, I.A., 2006. Temperature sensitivity of soil carbon decomposition and feedbacks to climate change. Nature 440, 165-173.
de Castilho, C.V., Magnusson, W.E., de Araújo, R.N.O., Luizão, R.C.C., Luizão, F.J., Lima, A.P., Higuchi, N., 2006. Variation in aboveground tree live biomass in a central Amazonian Forest: Effects of soil and topography. Forest Ecology and Management 234, 85-96.
DeFries, R.S., Houghton, R.A., Hansen, M.C., al., e., 2002. Carbon emissions from tropical deforestation and regrowth based on satellite observations for the 1980s and 90s. Proceedings of the National Academy of Sciences 99, 14256–14261.
Del Grosso, S., Parton, W., Stohlgren, T., Zheng, D., Bachelet, D., Prince, P., Hibbard, K., Olson, R., 2008. Globla potentila net primary production predicted from vegetation class, precipitation, and temperature. Ecology 89, 2117-2126.
Delaney, M., Brown, S., Lugo, A.E., Torres-Lezama, A., Bello-Quintero, N., 1998. The quality and turnover of dead wood in permanent forest plots in six life zones of Venezuela. Biotropica 30, 2-11.
Delaney, M., Brown, S., Lugo, A.E., Torres-Lezama, A., Quintero, N.B., 1997. The distribution of organic carbon in major components of forests located in five life zones of Venezuela. Journal of Tropical Ecology 13, 697-708.
Delignette-Muller, M.L., Dutang, C., 2015. fitdistrplus: An R Package for Fitting Distributions. Journal of Statistical Software 64, 1-34.

Denman, K., Brasseur, G., 2007. Couplings between changes in the climate system and biogeochemistry. In: al., S.e. (Ed.), The Physical Science Basis, Contribution of Working Group 1 to the Fourth Assessment Report of the IPCC. Cambridge University Press, NY, USA, pp. 499–587.
DeWalt, S.J., Chave, J., 2004. Structure and Biomass of Four Lowland Neotropical Forests. Biotropica 36, 7-19.
Diffenbaugh, N., Giorgi, F., Pal, J., 2008. Climate change hotspots in the United States. Geophysical Research Letters 35, L16709.
Dirzo, R., Young, H., Mooney, H., Ceballos, G., 2011. Seasonally dry tropical forest. Ecology and conservation. . Island Press., Washington, p. 392.
Doko, T., Chen, W., Qazi, o., Okabayashi, S., Meguro, D., Kanamori, T., Jones, M., Kawata, C., Yagasaki, T., Ichinose, T., Sasaki, K., 2014. Potential plant biomass estimation through field measurement and vegetation cover mapping using ALOS satellite imagery: Case study of Fujiyoshida City, Japan. IOP Conference Series: Earth and Environmental Science 17, 012078.
Dougherty, M., Dymond, R.L., Goetz, S.J., Jantz, C.A., Goulet, N., 2004. Evaluation of impervious surface estimates in a rapidly urbanizing watershed. Photogrammetric Engineering and Remote Sensing 70, 1275-1284.
Dreiseitl, S., and Ohno-Machado, L., 2002. Logistic regression and artificial neural network classification models: a methodology review. Journal of Biomedical Informatics 35, 352-359.
Eaton, J.M., 2005. Woody Debris and the Carbon Budget of Secondary Forests in the Southern Yucatán Peninsular Region. Department of Environmental Sciences. University of Virginia, Virginia, USA, p. 76.
Eaton, J.M., Lawrence, D., 2009. Loss of carbon sequestration potential after several decades of shifting cultivation in the Southern Yucatán. Forest Ecology and Management 258, 949-958.
El-Sheick, M.A., 2013. Population structure of woody plants in the arid cloud forests of Dhofar, southern Oman. Acta Bot. Croat 72, 97-111.
Elias, M., Potvin, C., 2003. Assessing inter- and intra-specific variation in trunk carbon concentration for 32 neotropical tree species. Canadian Journal of Forest Research 33, 1039-1045.
Elith, J., Phillips, S.J., Hastie, T., Dudík, M., Chee, Y.E., and Yates, C.J., 2011. A statistical explanation of MaxEnt for ecologists. Diversity and Distributions 17, 43-57.
Elser, J.J., Bracken, M.E.S., Cleland, E.E., Gruner, D.S., Harpole, W.S., Hillebrand, H., Ngai, J.T., Seabloom, E.W., Shurin, J.B., Smith, J.E., 2007. Global analysis of nitrogen and phosphorus limitation of primary producers in freshwater, marine and terrestrial ecosystems. Ecology Letters 10, 1135-1142.
Enquist, C.A.F., 2002. Predicted regional impacts of climate change on the geographical distribution and diversity of tropical forests in Costa Rica. Journal of Biogeography 29, 519-534.
Eva, H.D., Achard, F., Stibig, H.J., al., e., 2003. Response to comment on ‘determination of deforestation rates of the world’s humid tropical forests’. Science 299, 1015b.
Ewers, R., Laurance, W.F., Souza, C.J., 2008. Temporal fluctuations in Amazonian deforestation rates. Environmental Conservation 35, 303-310.
Exbrayat, J.F., Williams, M., 2015. Quantifying the net contribution of the historical Amazonian deforestation to climate change. Geophysical Research Letters 42, 2968-2976.
FAO, 1996. Global climate change and agricultural production. Direct and indirect effects of changing hydrological, soil and plant physiological processes. In: Bazzaz, F. (Ed.). Wim Sombroek, Rome, Italy.
FAO, 2005. Situación de los bosques del mundo 2005. FAO Forestry Paper, Rome, Italy, p. 153.

FAO, 2010. Challenges and opportunities for carbon sequestration in grassland systems. A technical report on grassland management and climate change mitigation. Integrated Crop Management. Food and Agriculture Organization of the United Nations, Rome, Italy.
Fearnside, P.M., 1997. Wood density for estimating forest biomass in Brazilian Amazonia. Forest Ecology and Management 90, 59-87.
Fearnside, P.M., Laurance, W.F., 2003. Comment on 'determination of deforestation rates of the world's humid tropical forests'. Science 299, 1015a.
Felicísimo, Á.M., Cuartero, A., Remondo, J., Quirós, E., 2013. Mapping landslide susceptibility with logistic regression, multiple adaptive regression splines, classification and regression trees, and maximum entropy methods: a comparative study. Landslides 10, 175-189.
Firdaus, M.S., Hanif, A.H.M., Safiee, A.S., Ismail, M.R., 2010. Carbon sequestration potential in soil and biomass of Jatropha curcas. World Congress of Soil Science, Soil Solutions for a Changing World, Brisbane, Australia, pp. 62-65.
Fischlin, A., Ayres, M., Karnosky, D., Kellomaki, S., Louman, B., Ong, C., Palttner, G.-K., Santoso, H., Thompson, I., 2009. Future environmental impacts and vulnerabilities. In: Seppala, R., Buck, A., Katila, P. (Eds.), Adaptation of forests and people to climate change: a global assessment report, Helsinki, pp. 53-100.
Flannigan, M., Stocks, B., Wotton, B., 2000. Climate change and forest fires. Science of the Total Environment 262, 221-229.
Flint, E.P., Richards, J.F., 1994. Trends in carbon content of vegetation in south and southeast Asia associated with changes in land use. In: V.H, D. (Ed.), Effects of Land Use Change on Atmospheric CO2 Concentrations: South and Southeast Asia as a Case Study. Springer-Verlag, New York, USA, pp. 201–299.
Foody, G.M., 2002. Status of land cover classification accuracy assessment. Remote Sensing of Environment 80, 185-201.
FRA, 2010. Global Forests Resources Assessment 2010. FAO Forestry Paper, Rome.
Fravolini, A., Hultine, K.R., Bugnoli, E., Gazal, R., English, N.B., Williams, D.G., 2005. Precipitation pulse use by an invasive woody legume: the role of soil texture and pulse size. Oecologia 144, 618-627.
Friday, L., Laskey, R., 1991. The Fragile Environmental. Cambridge University Press, Cambridge, UK.
Friedl, M.A., and Brodley, C.E., 1997. Decision tree classification of land cover from remotely sensed data. Remote Sens. Environ. 61, 399-409.
Friend, A.D., Lucht, W., Rademacher, T.T., Keribin, R., Betts, R., Cadule, P., Ciais, P., Clark, D.B., Dankers, R., Falloon, P.D., Ito, A., Kahana, R., Kleidon, A., Lomas, M.R., Nishina, K., Ostberg, S., Pavlick, R., Peylin, P., Schaphoff, S., Vuichard, N., Warszawski, L., Wiltshire, A., Woodward, F.I., 2014. Carbon residence time dominates uncertainty in terrestrial vegetation responses to future climate and atmospheric CO2. Proceedings of the National Academy of Sciences 111, 3280-3285.
Galicia, L., López-Blanco, J., Zarco-Arista, A.E., Filips, V., García-Oliva, F., 1999. The relationship between solar radiation interception and soil water content in a tropical deciduous forest in Mexico. Catena 36, 153-164.
Gallardo-Cruz, J.A., Meave, J.A., Pérez-García, E.A., 2005. Estructura, composición y diversidad de la selva baja caducifolia del Cerro Verde, Nizanda (Oaxaca), México. Boletion de la Sociedad Botánica de México 76, 19-35.
García-Oliva, F., Casar, I., Morales, P., Maass, J.M., 1994. Forest-to-pasture conversion influences on soil organic carbon dynamics in a tropical deciduous forest. Oecologia 99, 392-396.
García-Oliva, F., Gallardo, J.F., Montaño, N.M., Islas, P., 2006. Soil carbon and nitrogen dynamics followed by a forest-to-pasture conversion in western Mexico. Agroforestry Systems 66, 93-100.

García, E., 2004. Modificaciones al sistema de clasificación climatica de Köppen. Instituto de Geografía - UNAM, Mexico City.
García, R., Mendoza, I., Galicia, L., 2005. Evaluation of tropical deciduous forest landscapes, lower Papagayo river basin (Guerrero), Mexico. Investigaciones Geográficas 56, 77-100.
Gasparri, N., Parmuchi, M., Bono, J., Karszenbaum, H., Montenegro, C., 2010. Assessing multi-temporal Landsat 7 ETM+ images for estimating above-ground biomass in subtropical dry forests of Argentina. Journal of Arid Environments 74, 1262-1270.
Gaston, G., Brown, S., Lorenzini, M., Singh, K.D., 1998. State and change in carbon pools in the forests of tropical Africa. Global Change Biology 4, 97-114.
Gei, M.G., Powers, J.S., 2013. Nutrient Cycling in Tropical Dry Forests. Tropical Dry Forests in the Americas. CRC Press, pp. 141-155.
Gessler, P.E., Chadwick, O.A., Chamran, F., Althouse, L., Holmes, K., 2000. Modeling Soil–Landscape and Ecosystem Properties Using Terrain Attributes. Soil Science Society of America Journal 64, 2046-2056.
Gibbs, H., Brown, S., Niles, J., Foley, J., 2007. Monitoring and estimating tropical forest carbon stocks: making REDD a reality. Environmental Research Letters 2, 1-13.
Giliba, R., Boon, E.K., Kayombo, C.J., Musamba, E.B., Kashundye, A.M., Shayo, P.F., 2011. Species Composition, Richness and Diversity in Miombo Woodland of Bereku Forest Reserve, Tanzania. J. Biodiversity 2, 1-7.
Gillespie, T.W., Grijalva, A., Farris, C.N., 2000. Diversity, composition, and structure of tropical dry forests in Central America. Plant Ecology 147, 37-47.
Girardin, C.A.J., Espejob, J.E.S., Doughty, C.E., Huasco, W.H., Metcalfe, D.B., Durand-Baca, L., Marthews, T.R., Aragao, L.E.O.C., Farfán-Rios, W., García-Cabrera, K., Halladay, K., Fisher, J.B., Galiano-Cabrera, D.F., Huaraca-Quispe, L.P., Alzamora-Taype, I., Eguiluz-Mora, L., Revilla, N.S., Silman, M.R., Meir, P., Malhi, Y., 2014. Productivity and carbon allocation in a tropical montane cloud forest in the Peruvian Andes. Plant Ecology & Diversity 7, 107-123.
Goetz, S., Baccini, A., Laporte, N., Johns, T., Walker, W., Kellndorfer, J., Houghton, R., Sun, M., 2009. Mapping and monitoring carbon stocks with satellite observations: a comparison of methods. Carbon Bal Manag 4.
Gonzalez, O.J., Zak, D.R., 1994. Geostatistical analysis of soil properties in a secondary tropical dry forest, St. Lucia, West Indies. Plant Soil 163, 45-54.
Groppelli, B., Bocchiola, D., Rosso, R., 2011. Spatial downscaling of precipitation from GCMs for climate change projections using random cascades: A case study in Italy. Water Resources Research 47, 3.
Hall, C.A.S., Uhlig, J., 1991. Refining estimates of carbon released from tropical land-use change. Canadian Journal For. Res 21, 118-131.
Hall, P., Bawa, K., 1993. Methods to assess the impact of extraction of non-timber tropical forest products on plant populations. Economic Botany 47, 234-247.
Hansen, E.H., Gobakken, T., Bollandsås, O.M., Zahabu, E., Næsset, E., 2015. Modeling Aboveground Biomass in Dense Tropical Submontane Rainforest Using Airborne Laser Scanner Data. Remote Sensing 7, 788-807.
Hansen, M.C., DeFries, R.S., 2004. Detecting longterm global forest change using continuous fields of tree-cover maps from 8-km Advanced Very High Resolution Radiometer (AVHRR) data for the years 1982-99. Ecosystems 7, 695-716.
Harrell, F.E., 2015. Describing, Resampling, Validating, and Simplifying the Model. In: Harrell, F.E. (Ed.), Regression Modeling Strategies. With Applications to Linear Models, Logistic and Ordinal Regression, and Survival Analysis. Springer, NY, USA.
Harris, N.L., Brown, S., Hagen, S.C., Saatchi, S.S., Petrova, S., Salas, W., Hansen, M.C., Potapov, P.V., Lotsch, A., 2012. Baseline Map of Carbon Emissions from Deforestation in Tropical Regions. Science 336, 1573-1576.
Hastie, T., 2015. Package 'gam'.

He, F., Legendre, P., LaFrankie, J., 1996. Spatial pattern of diversity in a tropical rain forest in Malaysia. Journal of Biogeography 23, 57-74.
Hietel, E., Waldhardt, R., Otte, A., 2005. Linking socio-economic factors, environment and land cover in the German Highlands, 1945–1999. Journal of Environmental Management 75, 133-143.
Hijmans, R.J., Cameron, S.E., Parra, J.L., Jones, P.G., Jarvis, A., 2005. Very high resolution interpolated climate surfaces for global land areas. International Journal of Climatology 25, 1965-1978.
Hill, T.C., Williams, M., Bloom, A.A., Mitchard, E., Ryan, C., 2013. Are inventory based and remotely sensed above-ground biomass estimates consistent? PLoS One 8, e74170.
Hogberg, P., Nordgren, A., Buchmann, N., Taylor, A.F.S., Ekblad, A., Hogberg, M.N., Nyberg, G., Ottosson-Lofvenius, M., Read, D.J., 2001. Large-scale forest girdling shows that current photosynthesis drives soil respiration. Nature 411, 789-792.
Holmgren, M., Scheffer, M., Huston, M., 1997. The Interplay of Facilitation and Competition in Plant Communities. Ecology 78, 1966-1975.
Holly, K.G., Sandra, B., John, O.N., Jonathan, A.F., 2007. Monitoring and estimating tropical forest carbon stocks: making REDD a reality. Environmental Research Letters 2, 045023.
Houghton, R.A., 1995. Land-use change and the carbon cycle. Global Change Biology 1, 275-287.
Houghton, R.A., 1999. The annual net flux of carbon to the atmosphere from changes in land use 1850–1990. Tellus 51B.
Houghton, R.A., 2003. The contemporary carbon cycle. In: Schlesinger, W.H. (Ed.), Treatise on Geochemistry. Elsevier Ltd, New York, USA, pp. 473-513.
Houghton, R.A., 2005a. Aboveground forest biomass and the global carbon balance. Global Change Biology 11, 945-958.
Houghton, R.A., 2005b. Tropical deforestation as a source of greenhouse gas emissions. In: Moutinho, P., Schwartzman, S. (Eds.), Tropical Deforestation and Climate Change, Washington DC, USA.
Houghton, R.A., 2008. Carbon Flux to the Atmosphere from Land-Use Changes: 1850-2005. In: Carbon Dioxide Information Analysis Center, O.R.N.L., U.S. Department of Energy (Ed.), In TRENDS: A Compendium of Data on Global Change, Oak Ridge, Tenn., USA.
Houghton, R.A., Hackler, J.L., 1999. Carbon flux to the Atmosphere from Land-use Changes: 1850 to 1990. In: Carbon Dioxide Information Analysis Center, U.S.D.o.E. (Ed.). Oak Ridge National Laboratory, Oak Ridge, Tennessee, USA.
Houghton, R.A., Lawrence, K.T., Hackler, J.L., Brown, S., 2001. The spatial distribution of forest biomass in the Brazilian Amazon: a comparison of estimates. Global Change Biology 7, 731-746.
Houghton, R.A., Skole, D.L., 1990. Carbon. In: Turner, I.B.L., Clark, W.C., Kates, R. W, Richards, J.F., Mathew, J.T., Meyer, W.B. (Eds.), The Earth as Transformed by Human Action: Global and Regional Changes in the Biosphere over the Past 300 Years. Cambridge University Press, Cambridge, pp. 393-408.
Hubbell, S.P., 1979. Tree Dispersion, Abundance, and Diversity in a Tropical Dry Forest. Science 203, 1299-1309.
Hubbell, S.P., 1980. Seed Predation and the Coexistence of Tree Species in Tropical Forests. Oikos 35, 214-229.
Hulme, P.E., 2005. Adapting to climate change: Is there scope for ecological management in the face of a global threat? . Journal of Applied Ecology 42, 784-794.
Hultine, K.R., Koepke, D.F., Pockman, W.T., Fravolini, A., Sperry, J.S., Williams, D.G., 2005. Influence of soil texture on hydraulic properties and water relations of a dominant warm-desert phreatophyte. Tree Physiology 26, 313-323.

INEGI, 2000. Diccionario de Datos Fisiográficos 1:1,000,000 (Vectorial). In: Informática, I.N.d.E.G.e. (Ed.). Instituto Nacional de Estadística, Geografía e Informática, Aguascalientes, Mexico.
INEGI, 2001. Conjunto de Datos Vectoriales de la Carta de Uso de Suelo y Vegetación, 1:250,000, (serie II). Instituto Nacional de Estadística, Geografía e Informática, Aguascalientes, Mexico.
INEGI, 2003a. Conjunto de datos vectoriales de la carta de vegetacion primaria 1:1,000,000. In: Informática, I.N.d.E.G.e. (Ed.). INEGI, Aguascalientes, Mexico.
INEGI, 2003b. Digital topographic vectors (1995, 1999, 2000, 2001, 2002 and 2003). In: Informática, I.N.d.E.G.e. (Ed.). INEGI, Aguascalientes, Mexico.
INEGI, 2004. Síntesis de información geográfica del estado de Oaxaca. INEGI, Aguascalientes, Mexico.
INEGI, 2005. Conjunto de Datos Vectoriales de Uso del suelo y Vegetación, escala 1:250,000 (serie III). Instituto Nacional de Estadística, Geografía e Informática, Aguascalientes, Mexico.
INEGI, 2008. Conjunto de Datos Vectoriales de Uso del suelo y Vegetación, escala 1:250,000 (serie IV). Instituto Nacional de Estadística, Geografía e Informática, Aguascalientes, Mexico.
IPCC, 2003. Good Practice Guidance for Land Use, Land-Use Change and Forestry. In: Penman, J., Gytarsky, M., Hiraishi, T., Krug, T., Kruger, D., Pipatti, R., Buendia, L., Miwa, K., Ngara, T., Tanabe, K., Wagner, F. (Eds.). Intergovernmental Panel on Climate Change (IPCC), IPCC/IGES, Hayama, Japan.
IPCC, 2006. IPCC Guidelines for National Greenhouse Gas Inventories. In: Eggleston, H.S., Buendia, L., Miwa, K., Ngara, T., Tanabe, K. (Eds.), National Greenhouse Gas Inventories Programme. Institute For Global Environmental Strategies, Japan.
IPCC, 2007. Contribution of Working Group I to the Fourth Assessment Report of the Intergovernmental Panel on Climate Change. Cambridge University Press, Cambridge.
Iverson, L., Brown, S., Prasad, A., Mitasova, H., Gillespie, A.J.R., Lugo, A.E., 1994. Use of GIS for estimating potential and actual forest biomass for continental South and Southeast Asia. In: V.H, D. (Ed.), Effects of Land Use Change on Atmospheric CO2 Concentrations: South and Southeast Asia as a Case Study. Springer-Verlag, NY, USA, pp. 67–116.
Janzen, D., 1986. Tropical Dry Forest: The Most Endangered Major Tropical Ecosystem. In: Wilson, E.O., Peter, F.M. (Eds.), Biodiversity. National Academies Press (US), Washington (DC), USA.
Janzen, D.H., 1998. Tropical dry forests: the most endangered major tropical ecosystem. In: Wilson, E.O. (Ed.), Biodiversity. Natural Academy, Washington DC, USA, pp. 130-137.
Jaramillo, V., Martínez-Yrízar, A., Sanford, R.L., 2011. Primary Productivity and Biogeochemistry of Seasonally Dry Tropical Forests. In: Dirzo, R., Young, H., Mooney, H., Ceballos, G. (Eds.), Seasonally Dry Tropical Forests: Ecology and Conservation. Island Press, Washington, pp. 109-128.
Jaramillo, V.J., Kauffman, J.B., Rentería-Rodríguez, L., Cummings, D.L., Ellingson, L.J., 2003. Biomass, Carbon, and Nitrogen Pools in Mexican Tropical Dry Forest Landscapes. Ecosystems 6, 609-629.
Jha, C., Singh, J., 1990. Composition and dynamics of dry tropical forest in relation to soil texture. Journal of Vegetation Science 1, 609-614.
Journel, A.G., Froidevaux, R., 1982. Anisotropic hole-effect modeling. Mathematical Geology 14, 217-239.
Keller, M., Palace, M., Hurtt, G., 2001. Biomass estimation in the Tapajos National Forest, Brazil: Examination of sampling and allometric uncertainties. Forest Ecology and Management 154, 371-382.

Kirby, K.R., Potvin, C., 2007. Variation in carbon storage among tree species: Implications for the management of a small-scale carbon sink project. Forest Ecology and Management 246, 208-221.
Korner, C., 2007. The use of "altitude" in ecological research. Trends Ecol. Evol 22, 569–574.
Kuhn, M., 2015. A shor introduction to the caret Package.
Kumar, L., Skidmore, A.K., Knowles, E., 1997. Modelling topographic variation in solar radiation in a GIS environment. International Journal of Geographical Information Science 11, 475-497.
Kyrklund, B., 1990. Cómo pueden contribuir los bosques y las industrias forestales a reducir el exceso de anhídrido carbónico en el atmósfera. Unasylva 43, 12-14.
Lambin, E.F., Geist, H.J., Lepers, E., 2003. Dynamics of land-use and land-cover change in tropical regions. Annual Review of Environment and Resources 28, 205-241.
Lambin, E.F., Meyfroidt, P., 2010. Land use transitions: Socio-ecological feedback versus socio-economic change. Land Use Policy 27, 108-118.
Lambin, E.F., Turner, B.L., Geist, H.J., Agbola, S.B., Angelsen, A., Bruce, J.W., Coomes, O.T., Dirzo, R., Fischer, G., Folke, C., George, P.S., Homewood, K., Imbernon, J., Leemans, R., Li, X., Moran, E.F., Mortimore, M., Ramakrishnan, P.S., Richards, J.F., Skånes, H., Steffen, W., Stone, G.D., Svedin, U., Veldkamp, T.A., Vogel, C., Xu, J., 2001. The causes of land-use and land-cover change: moving beyond the myths. Global Environmental Change 11, 261-269.
Larjavaara, M., Muller-Landau, H.C., 2012. Temperature explains global variation in biomass among humid old-growth forests. Global Ecology and Biogeography 21, 998-1006.
Laurance, W.F., Delamônica, P., Laurance, S.G., Vasconcelos, H.L., Lovejoy, T.E., 2000. Rainforest fragmentation kills big trees. Nature 404, 836.
Laurance, W.F., Laurance, S.G., Delamônica, P., 1998. Tropical forest fragmentation and greenhouse gas emissions. Forest Ecology and Management 110, 173-180.
Le Toan, T., Quegan, S., Woodward, I., Lomas, M., Delbart, N., Picard, G., 2004. Relating Radar Remote Sensing of Biomass to Modelling of Forest Carbon Bugets. Climatic Change 379-402.
Leathwick, J.R., Elith, J., Hastie, T., 2006. Comparative performance of generalized additive models and multivariate adaptive regression splines for statistical modelling of species distributions. Ecological Modelling 199, 188-196.
LeBauer, D.S., Treseder, K.K., 2008. Nitrogen limitation of net primary productivity in terrestrial ecosystems is globally distributed. Ecology 89, 371-379.
Leitner, L.A., 1987. Plant cmmunities of a large arroyo at Punta Cirio, Sonora. The Southwestern Naturalist 32, 21-28.
Lentz, D.L., Dunning, N.P., Scarborough, V.L., Magee, K.S., Thompson, K.M., Weaver, E., Carr, C., Terry, R.E., Islebe, G., Tankersley, K.B., Grazioso Sierra, L., Jones, J.G., Buttles, P., Valdez, F., Ramos Hernandez, C.E., 2014. Forests, fields, and the edge of sustainability at the ancient Maya city of Tikal. Proceedings of the National Academy of Sciences of the United States of America 111, 18513-18518.
Levings, S.C., 1983. Seasonal, Annual, and Among-site Variation in the Ground Ant Community of a Deciduous Tropical Forest: Some Causes of Patchy Species Distributions. Ecological Monographs 53, 435-455.
Lewis, S., Brando, P., Phillips, O., van der Heijden, G., Nepstad, D., 2011. The 2010 Amazon Drought. Science, 331-554.
Lira, I., Ceballos, G., 2010. Huatulco, Oaxaca. In: Ceballos, G., Martínez, L., García, A., Espinoza, E., Bezaury, J., Dirzo, R. (Eds.), Diversidad, Amenazas y Áreas Prioritarias para la Conservación de las Selvas Secas del Pacífico de México. CONABIO & Fondo de Cultura Económica, Mexico City.

Lu, C.-J., Lee, T.-S., Lian, C.-M., 2012. Sales forecasting for computer wholesalers: A comparison of multivariate adaptive regression splines and artificial neural networks. Decision Support Systems 54, 584-596.
Lu, D., Batistella, M., Moran, E., 2005. Satellite Estimation of Aboveground Biomass and Impacts of Forest Stand Structure. Photogrammetric Engineering & Remote Sensing 71, 967-974.
Lucero, M.E., Barrow, J.R., Osuna, P., Reyes, I., 2006. Plant–fungal interactions in arid and semi-arid ecosystems: Large-scale impacts from microscale processes. Journal of Arid Environments 65, 276-284.
Lugo, A., Brown, S., 1980. Los bosques tropicales: ¿fuentes o sumideros de carbono atmosférico? Unasylva 32, 9-13.
Lugo, A.E., Murphy, P.G., 1986. Nutrient dynamics of a Puerto Rican subtropical dry forest. Journal of Tropical Ecology 2, 55-72.
Lykke, A.M., 1998. Assessment of species composition change in savanna vegetation by means of woody plant's size class distributions and local information. Biodiversity and Conservation Biology 7, 1261-1275.
Maass, J.M., 1995. Tropical deciduous forest conversion to pasture and agriculture. In: Bullock, S.H., Mooney, H. (Eds.), Seasonally Dry Tropical Forests. Cambridge University Press, Cambridge, UK., pp. 399-422.
Maass, J.M., Balvanera, P., Castillo, A., Daily, G.C., Mooney, H.A., Ehrlich, P., Quesada, M., Miranda, A., Jaramillo, V., García-Oliva, F., Martínez-Yrizar, A., Cotler, H., López-Blanco, J., Pérez-Jiménez, A., Búrquez, A., Tinoco, C., Ceballos, G., Barraza, L., Ayala, R., Sarukhán, J., 2005. Ecosystem services delivered by tropical dry forests: a case study from the Pacific Coast of Mexico. Ecology and Society 10, 1-23.
Maestre, F., Salguero-Gómez, R., Quero, J., 2012. It is getting hotter here: determining and projecting the impacts of global environmental change on drylands. Philosophical Transactions of the Royal Society B: Biological Sciences 367, 3032-3075.
Malhi, Y., Roberts, J.T., Betts, R.A., Killeen, T.J., Li, W.H., Nobre, C.A., 2008. Climate change, deforestation, and the fate of the Amazon. Science 319, 169-172.
Mann, M.E., Bradley, R.S., Hughes, M.K., 1998. Global-scale temperature patterns and climate forcing over the past six centuries. Nature 392, 779-787.
Marín, G.C., Nygård, R., Rivas, B.G., Oden, P.C., 2005. Stand dynamics and basal area change in a tropical dry forest reserve in Nicaragua. Forest Ecology and Management 208, 63-75.
Martínez-Yrízar, A., 1995. Biomass distribution and primary productivity of tropical dry forests. In: Bullock, S.H., Mooney, H.A., Medina, E. (Eds.), Seasonally Dry Tropical Forests. Cambridge University Press, Cambridge, pp. 326-345.
Martínez-Yrízar, A., Sarukhan, J., Perez-Jimenez, A., Rincon, E., Maass, J.M., Solis-Magallanes, J.A., Cervantes, L., 1992. Above-ground phytomass of a tropical deciduous forest on the coast of Jalisco, Mexico. Journal of Tropical Ecology 8, 87-96.
Martínez, J., Fernández.-Bremauntz, A., Osnaya, P., 2004. Cambio climático: una visión desde México. In: (INE), I.N.d.E. (Ed.). INE, Mexico, DF, p. 525.
Mason, N.W.H., Carswell, F.E., Overton, J.M., Briggs, C.M., Hall, G.M.J., 2012. Estimation of current and potential carbon stocks and Kyoto-compliant carbon gain on conservation land. Publishing Team, New Zealand Department of Conservation (DOC), PO Box 10420, The Terrace, Wellington 6143, New Zealand.
McConnell, W.J., Sweeney, S.P., Mulley, B., 2004. Physical and social access to land: spatio-temporal patterns of agricultural expansion in Madagascar. Agriculture, Ecosystems & Environment 101, 171-184.
McCullagh, P., and Nelder, J.A., 1989. Generalized Linear Models. London, UK., Chapman & Hall/CRC.

Medeiros, A.S., Drezner, T.D., 2012. Vegetation, climate, and soil relationships across the Sonoran Desert. Écoscience 19, 148-160.
Meir, P., Pennington, T., 2011. Climatic change and Seasonally Dry Tropical Forest. In: Dirzo, R., Young, H., Mooney, H., Ceballos, G. (Eds.), Seasonally Dry Tropical Forest: Ecology and Conservation. Island Press, USA, pp. 279-299.
Melillo, J., Houghton, R.A., Kicklighter, D., McGuire, A., 1996. Tropical deforestation and the global carbon budget. Annu. Rev. Energy Environ 21, 293-310.
Mendoza, A., 2015. Vulnerability of biodiversity to land use change and climate change in Mexico. Physical Geography. University of Edinburgh, Edinburgh, UK.
Michaelsen, J., Schimel, D., Friedl, M., Davis., F., Dubayah, R., 1994. Regression Tree Analysis of satellite and terrain data to guide vegetation sampling and surveys. Journal of Vegetation Science 5, 673-686.
Miles, L., Newton, A., DeFries, R., Ravilious, C., May, I., Blyth, S., Kapos, V., Gordon, J., 2006. A global overview of the conservation status of tropical dry forests. Journal of Biogeography 33, 491-505.
Miller, G.T., 1992. Living in the environment. An introduction to environmental science. Wadsworth Publishing Co, California, USA.
Miranda, A., 1996. La Selva Tropical Estacional: Entre la vida y la muerte. Ocelotl, Revista Mexicana de Conservación. Méx. Pronatura AC, pp. 28-35.
Miranda, F., Hernández, E., 1963. Los tipos de Vegetación en México y su Clasificación. In: SARH (Ed.). Boletín de la Sociedad Botánica de México, Mexico, DF.
Mirmanto, E., Proctor, J., Green, J., Nagy, L., Suriantata, 1999. Effects of nitrogen and phosphorus fertilization in a lowland evergreen rainforest. Philosophical Transactions of the Royal Society B: Biological Sciences 354, 1825-1829.
Mitchard, E., Saatchi, S., Woodhouse, I., Nangendo, G., Ribeiro, N., Williams, M., Ryan, C., Lewis, S., Feldpausch, T., Meir, P., 2009. Using satellite radar backscatter to predict above-ground woody biomass: A consistent relationship across four different African landscapes. Geophysical Research Letters 36, L23401.
Mitchard, T.A., Saatchi, S., Baccini, A., Asner, G.P., Goetz, S.J., Harris, N.L., Brown, S., 2013. Uncertainty in the spatial distribution of tropical forest biomass: a comparison of pan-tropical maps. Carbon Balance and Management 8, 1-13.
Mitchard, T.A., Saatchi, S., Lewis, S.L., Feldpausch, T.R., Gerard, F.F., Woodhouse, I.H., Meir, P., 2011. Comment on 'A first map of tropical Africa's above-ground biomass derived from satellite imagery'. Environmental Research Letters 6, 049001.
Moisen, G.G., Frescino, T.S., 2002. Comparing five modelling techniques for predicting forest characteristics. Ecological Modelling 157, 209-225.
Moorcroft, O., Hurtt, G., Pacala, S., 2001. A method for scaling vegetation dynamics: The Ecosystem Demography Model (ED). Ecological Monographs 71, 557-586.
Murphy, P.G., Lugo, A.E., 1986a. Ecology of tropical dry forest. Annual review of Ecology and Systematics 17, 67-88.
Murphy, P.G., Lugo, A.E., 1986b. Structure and Biomass of a Subtropical Dry Forest in Puerto Rico. Biotropica 18, 89-96.
Mutanga, O., Adam, E., Cho, M.A., 2012. High density biomass estimation for wetland vegetation using WorldView-2 imagery and random forest regression algorithm. International Journal of Applied Earth Observation and Geoinformation 18, 399-406.
Nascimento, H.E.M., Laurance, W.F., 2002. Total aboveground biomass in central Amazonian rainforests: a landscape-scale study. Forest Ecology and Management 168, 311-321.
Návar, J., 2009. Allometric equations and expansion factors for Tropical Dry Forests trees of Eastern Sinaloa, Mexico. Tropical and Subtropical Agroecosystems 10, 45-52.
Návar, J., 2010. Biomass allometry for tree species of Northwestern Mexico. Tropical and Subtropical Agroecosystems 12, 507-519.

Návar, J., Estrada-Salvador, A., Estrada-Castrillón, E., 2010. The effect of land use change in the tropical dry forests of Morelos, Mexico on carbon stocks and fluxes. T. Journal of Tropical Forest Science 22, 295-307.
Ningthoujam, R., Mutum, D., 2010. Investigation of the tropical forest dynamics of the Northeast India. NeBIO 1, 28-33.
NOAA, 2015. NOAA Solar Calculator. Earth System Research Laboratory, Global Monitoring Division.
Noble, I., Dirzo, R., 1997. Forests as human dominated ecosystems. Science 277, 522-525.
O'Gorman, P., 2012. Sensitivity of tropical precipitation extremes to climate change. Nature Geoscience 5, 697-700.
Olsen, S.R., Cole, C.V., Watanabe, F.S., Dean, L.A., 1954. Estimation of available phosphorus in soil by extraction with sodium bicarbonate. Department of Agriculture. Circular, U.S. Washington, D.C.
Ometto, J.P., Aguiar, A.P., Assis, T., Soler, L., Valle, P., Tejada, G., Lapola, D.M., Meir, P., 2015. Amazon forest biomass density maps: tackling the uncertainty in carbon emission estimates. In: Ometto, J.P., Bun, R., Jonas, M., Nahorski, Z. (Eds.), Uncertainties in Greenhouse Gas Inventories. Springer International Publishing, pp. 95-110.
Ontl, T.A., Schulte, L.A., 2012. Soil Carbon Storage. Nature Education Knowledge 3, 35.
Palm, C.A., Houghton, R.A., Melillo, J.M., Skole, D.L., 1986. Atmospheric carbon dioxide from deforestation in southeast Asia. Biotropica 18, 177-188.
Pan, W.K.Y., Walsh, S.J., Bilsborrow, R.E., Frizzelle, B.G., Erlien, C.M., Baquero, F., 2004. Farm-level models of spatial patterns of land use and land cover dynamics in the Ecuadorian Amazon. Agriculture, Ecosystems & Environment 101, 117-134.
Pan, Y.D., Birdsey, R.A., Fang, J.Y., Houghton, R., Kauppi, P.E., Kurz, W.A., Phillips, O.L., Shvidenko, A., Lewis, S.L., Canadell, J.G., Ciais, P., Jackson, R.B., Pacala, S.W., McGuire, A.D., Piao, S.L., Rautiainen, A., Sitch, S., Hayes, D., 2011. A Large and Persistent Carbon Sink in the World's Forests. Science 333, 988-993.
Parmesan, C., Yohe, G., 2003. A globally coherent fingerprint of climate change impacts across natural systems. Nature 421, 37-42.
Peterson, F.S., 2012. Post-Harvest Establishment Influences ANPP, Soil C and DOC Export in Complex Mountainous Terrain. Forest Ecosystems and Society. Oregon State University, Oregon.
Petit-Aldana, J., Casanova-Lugo, F., Solorio-Sánchez, J., Ramírez-Avilés, L., 2011. Litterfall production and quality in pure and mixed fodder banks in Yucatan, Mexico. Revista Chapingo Serie Ciencias Forestales y del Ambiente 17, 165-178.
Piao, S., Luyssaert, S., Ciais, P., Janssens, I., Chen, A., Cap, C., Fang, J., Friedlingstein, P., Luo, Y., Wamg, S., 2010. Forest annual carbon cost: a global-scale analysis of autotrophic respiration. Ecology 9, 652-661.
Poillot, R., Delignette-Muller, M.L., Kelly, D.L., Denis, J.B., 2013. Tools for Two-Dimensional Monte-Carlo Simulations. The mc2d package.
Poisot, T., Bever, J.D., Nemri, A., Thrall, P.H., Hochberg, M.E., 2011. A conceptual framework for the evolution of ecological specialisation. Ecology Letters 14, 841-851.
Poorter, H., Niinemets, Ü., Poorter, L., Wright, I.J., Villar, R., 2009. Causes and consequences of variation in leaf mass per area (LMA): a meta-analysis. New Phytologist 182, 565-588.
Porter-Bolland, L., Ellis, E.A., Gholz, H.L., 2007. Land use dynamics and landscape history in La Montaña, Campeche, México. Landscape and Urban Planning 82, 198-207.
Portillo-Quintero, C.A., Sánchez-Azofeifa, G.A., 2010. Extent and conservation of tropical dry forests in the Americas. Biological Conservation 143, 144-155.
Powers, J.S., Becknell, J.M., Irving, J., Pèrez-Aviles, D., 2009. Diversity and structure of regenerating tropical dry forests in Costa Rica: Geographic patterns and environmental drivers. Forest Ecology and Management 258, 959-970.

Prentice, I.C., Farquhar, G.D., Fasham, M.J.R., Goulden, M.L., Heimann, M., Jaramillo, V.J., Kheshgi, H.S., Le Quéré, C., Scholes, R.J., Wallace, D.W.R., 2001. The carbon cycle and atmospheric carbon dioxide. In: Houghton, J.T., Ding, Y., Griggs, D.J., Noguer, M., van der Linden, P.J., Dai, X., Maskell, K., Johnson, C.A. (Eds.), Climate Change 2001. The Scientific Basis. Contribution of Working Group I to the Third Assessment Report of the Intergovernmental Panel on Climate Change Cambridge University Press, Cambridge, UK, pp. 183-237.

PSIG, 2015. Conjunto de Datos Vectoriales de la Carta de Uso de Suelo y Vegetación de: San Miguel del Puerto, San Pedro Pochutla, Santa María Colotepec, Santa María Huatulco y Santa María Tonameca. In: Procesos y Sistemas de Información en Geomática, S.A.d.C.V. (Ed.). PSIG, Naucalpan, Edo. de Mex.

Pyrcz, M.J., Deutsch, C.V., 2003. The whole story on the hole effect. Geostatistical Association of Australasia, Newsletter 18.

QGIS-2.6.0, 2014. Quantum GIS Development Team, Quantum GIS Geographic Information System. Open Source Geospatial Foundation Project.

R-Core-Team, 2014. R: A language and environment for statistical computing. Foundation for Statistical Computing, Vienna, Austria.

Rango, A., Tartowski, S.L., Laliberte, A., Wainwright, J., Parsons, A., 2006. Islands of hydrologically enhanced biotic productivity in natural and managed arid ecosystems. Journal of Arid Environments 65, 235-252.

Read, L., Lawrence, D., 2003. Recovery of Biomass following shifting cultivation in Dry Tropical Forests of the Yucatan. Ecological Applications 13, 85-97

Reich, P.B., Borchert, R., 1984. WATER STRESS AND TREE PHENOLOGY IN A TROPICAL DRY FOREST IN THE LOWLANDS OF COSTA RICA. Journal of Ecology 72, 61.

Réjou-Méchain, M., Tymen, B., Blanc, L., Fauset, S., Feldpausch, T.R., Monteagudo, A., Phillips, O.L., Richard, H., Chave, J., 2015. Using repeated small-footprint LiDAR acquisitions to infer spatial and temporal variations of a high-biomass Neotropical forest. Remote Sensing of Environment 169, 93-101.

Ribeiro, J., Diggle, P.J., 2001. geoR: A package for geostatistical analysis. R-NEWS 1.

Ribeiro, S.C., Fehrmann, L., Soares, C.P.B., Jacovine, L.A.G., Kleinn, C., de Oliveira Gaspar, R., 2011. Above- and belowground biomass in a Brazilian Cerrado. Forest Ecology and Management 262, 491-499.

Rincón, E., Álvarez, M., González, G., Huante, P., Hernández, A., 1999. Gaceta Ecológica, México-SEMARNAT-INE 53, 62-71.

Ripley, B., 2015. Package 'tree'.

Ripley, B., Venables, B., Bates, D.M., Hornik, K., Gebhardt, A., Firth, D., 2015. Package 'MASS'.

Ripley, B., Venables, W., 2015. Package 'nnet'.

Rodriguez-Veiga, P., 2016. Large-Scale Mapping of Forest Above-Ground Biomass Retrieval from Maximum Entropy using SAR and Optical Satellite Data. Physical Geography. University of Leicester, Leicester, UK.

Rodríguez-Veiga, P., Saatchi, S., Tansey, K., Balzter, H., 2016. Magnitude, spatial distribution and uncertainty of forest biomass stocks in Mexico. Remote Sensing of Environment 183, 265-281.

Rodriguez-Veiga, P., Saatchi, S., Wheeler, J.T., Ansey, K., Balzter, H., In Press. Methodology for Regional to Global Mapping of Above Ground Forest Biomass: Integrating Forest Allometry, Ground Plots, and Satellite Observations. In: Balzter, H. (Ed.), Earth Observation for Land and Emergency Monitoring - Innovative concepts for environmental monitoring from space. Wiley-Blackwell, Chichester.

Rodríguez, E., Ramos, R., Mata, J., Canizales, P., Jiménez, J., Uvalle, J., Valdecantos, A., Ruiz, M., 2010. Riqueza y diversidad de especies leñosas del bosque tropical caducifolio en San Luis Potosí, México. Ciencia UANL 13, 287-293.

Root, T.L., Price, J.T., Hall, K.R., Schneider, S.H., Rosenzweig, C., Pounds, A., 2003. Fingerprints of global warming on wild animals and plants. Nature 421, 57-60.
Rossi, J., Govaerts, A., De Vos, B., Verbist, B., Vervoort, A., Poesen, J., Muys, B., Deckers, J., 2009. Spatial structures of soil organic carbon in tropical forests - a case study of Southeastern Tanzania. Catena 77, 19-27.
Ruiz-Jaen, M.C., Potvin, C., 2011. Can we predict carbon stocks in tropical ecosystems from tree diversity? Comparing species and functional diversity in a plantation and a natural forest. New Phytologist 189, 978-987.
Ryan, C.M., Hill, T., Woollen, E., Ghee, C., Mitchard, E., Cassells, G., Grace, J., Woodhouse, I.H., Williams, M., 2012. Quantifying small-scale deforestation and forest degradation in African woodlands using radar imagery. Global Change Biology 18, 243-257.
Ryan, C.M., Williams, M., Grace, J., 2011. Above- and Belowground Carbon Stocks in a Miombo Woodland Landscape of Mozambique. Biotropica 43, 423-432.
Rzedowski, J., 1998. Diversidad y orígenes de la flora fanerogámica de México. In: T.P. Ramamoorthy, R.B., Fa, A.L.y.J. (Eds.), Diversidad biologica de Mexico: origenes y distribucion. Instituto de Biología-UNAM, Mexico, DF, pp. 129-145.
Rzedowski, J., 2006. La vegetación de México. In: (CONABIO), C.N.p.e.C.y.U.d.l.B. (Ed.). CONABIO, Mexico, DF.
Saatchi, S.S., Harris, N.L., Brown, S., Lefsky, M., Mitchard, E.T.A., Salas, W., Zutta, B.R., Buermann, W., Lewis, S.L., Hagen, S., 2011a. Benchmark map of forest carbon stocks in tropical regions across three continents. Proc Natl Acad Sci 108.
Saatchi, S.S., Harris, N.L., Brown, S., Lefsky, M., Mitchard, E.T.A., Salas, W., Zutta, B.R., Buermann, W., Lewis, S.L., Hagen, S., Petrova, S., White, L., Silman, M., Morel, A., 2011b. Benchmark map of forest carbon stocks in tropical regions across three continents. Proceedings of the National Academy of Sciences 108, 9899–9904.
Saatchi, S.S., Houghton, R.A., Dos Santos Alvalá, R.C., Soares, J.V., Yu, Y., 2007. Distribution of aboveground live biomass in the Amazon basin. Global Change Biology 13, 816-837.
Sabine, C.L., Heiman, M., Artaxo, P., Bakker, D.C.E., Chen, C.T.A., Field, C.B., Gruber, N., Le Quéré, C., Prinn, R.G., Richey, J.E., Romero-Lankao, P., Sathaye, J.A., Valentini, R., 2004. Current status and past trends of the carbon cycle. In: Field, C.B., Raupach, M.R. (Eds.), The Global Carbon Cycle: Integrating Humans, Climate, and the Natural World. Island Press, Washington, DC, USA, pp. 17-44.
Sagar, R., Singh, J., 2006. Tree density. basal area and species diversity in a disturbed dry tropical forest of northern India: implications for conservation. Environmental Conservation 33, 256-262.
Salas-Morales, S.H., Schibli, L., Nava-Zafra, A., Saynes-Vásquez, A., 2007. Flora de la costa de Oaxaca, México: lista florística comentada del parque nacional Huatulco. Boletín de la Sociedad Botánica de México 81.
Santilli, M., Moutinho, P., Schwartzman, S., Nepstad, D., Curran, L., Nobre, C., 2005. Deforestation and Kyoto Protocol: Tropical deforestation and the Kyoto Protocol: an editorial essay. Climatic Change 71, 267–276.
Schall, R., 1991. Estimation in generalized linear models with random effects. Biometrika 78, 719-727.
Seidel, D., Fu, Q., Randel, W.J., Reichler, T.J., 2008. Widening of the tropical belt in a changing climate. Nature Geoscience 1, 21-24.
SEMARNAP, 1998. Información Estadística de Incendios en Areas Forestales por Entidad Federativa, Informe Final Campaña. In: Secretaría de Medio Ambiente, R.N.y.P.S. (Ed.), Mexico, DF.
SEMARNAT-INE, 2009. México: Cuarta comunicación nacional ante la Convención Marco de las Naciones Unidas Sobre el Cambio Climático. In: (SEMARNAT), S.d.M.A.y.R.N. (Ed.). Instituto Nacional de Ecología (INE), Mexico DF, p. 274.

SEMARNAT, 2012. Inventario de Emisiones de Gases de Efecto Invernadero 1990-2006. In: (SEMARNAT), S.d.M.A.y.R.N. (Ed.).
Serrano-Medrano, M., Arias-Chalico, T., Ghilardi, A., Masera, O., 2014. Spatial and temporal projection of fuelwood and charcoal consumption in Mexico. Energy for Sustainable Development 19, 39-46.
Sherwood, S., Iingram, W., Tsushima, Y., Satoh, M., Roberts, M., Vidale, P., O'Gorman, P., 2010. Relative humidity changes in a warmer climate. Journal of Geophysical Research 115, DO9104.
Simmons, J.A., Fernandez, I.J., Briggs, R.D., Delaney, M.T., 1996. Forest floor carbon pools and fluxes along a regional climate gradient in Maine, USA. Forest Ecology and Management 84, 81-95.
Skutsch, M., McCall, K., Lovett, J., 2009. Carbon emissions: dry forests may be easier to manage. Nature 462.
Slik, J.W.F., Aiba, S.-I., Brearley, F.Q., Cannon, C.H., Forshed, O., Kitayama, K., Nagamasu, H., Nilus, R., Payne, J., Paoli, G., Poulsen, A.D., Raes, N., Sheil, D., Sidiyasa, K., Suzuki, E., van Valkenburg, J.L.C.H., 2010. Environmental correlates of tree biomass, basal area, wood specific gravity and stem density gradients in Borneo's tropical forests. Global Ecology and Biogeography 19, 50-60.
Slik, J.W.F., Paoli, G., McGuire, K., Amaral, I., Barroso, J., Bastian, M., Blanc, L., Bongers, F., Boundja, P., Clark, C., Collins, M., Dauby, G., Ding, Y., Doucet, J.-L., Eler, E., Ferreira, L., Forshed, O., Fredriksson, G., Gillet, J.-F., Harris, D., 2013. Large trees drive forest aboveground biomass variation in moist lowland forests across the tropics. Global Ecology & Biogeography 22, 1261-1271.
SMN, 2014. Servicio Metereologico Nacional. CONAGUA.
Snyder, K.A., Tartowski, S.L., 2006. Multi-scale temporal variation in water availability: Implications for vegetation dynamics in arid and semi-arid ecosystems. Journal of Arid Environments 65, 219-234.
Solé, R., 2007. Scaling laws in the drier. Nature 449, 151-153.
Sosa-Cedillo, V.E., 2008. Programa Estratégico Forestal del Estado de Oaxaca 2007-2030. In: SEMARNAT-CONAFOR (Ed.), Mexico, DF, p. 253.
Spadavecchia, L., Williams, M., Bell, R., Stoy, P.C., Huntley, B., van Wijk, M.T., 2008. Topographic controls on the leaf area index and plant functional type of a tundra ecosystem. Journal of Ecology 96, 1238-1251.
Sperry, J.S., Adler, F.R., Campbell, G.S., Comstock, J.P., 1998. Limitation of plant water use by rhizosphere and xylem conductance: results from a model. Plant Cell Environ 21, 347-359.
Sperry, J.S., Hacke, U.G., 2002. Desert shrub water relations with respect to soil characteristics and plant functional type. Funct. Ecol. 16, 367-378.
Strobl, C., Boulesteix, A.L., Zeileis, A., Hothorn, T., 2007. Bias in random forest variable importance measures: Illustrations, sources and a solution. BMC Bioinformatics 8, 25.
Sundquist, E.T., Visser, K., 2003. The geological history of the carbon cycle. In: Schlesinger, W.H. (Ed.), Treatise on Geochemistry. Elsevier Ltd, NY, USA, pp. 425-472.
Tanaka, K., Tomoaki, I., Daisuke, H., Joseph Jawa, K., Katsutoshi, S., Ikuo, N., 2010. Changes in above- and belowground biomass in early successional tropical secondary forests after shifting cultivation in Sarawak, Malaysia. Forest Ecology and Management 260, 875-882.
Thomas, S.C., Martin, A.R., 2012. Carbon Content of Tree Tissues: A Synthesis. Forests 3, 332-352.
Trejo-Vázquez, I., 1999. El clima de la selva baja caducifolia en México. Investigaciones Geográficas 39, 40-52.

Trejo, I., 1998. Distribución y diversidad de selvas bajas de México: relaciones con el clima y el suelo., Science Faculty. Universidad Nacional Autónoma de México (UNAM), Mexico, DF, p. 210.
Trejo, I., Dirzo, R., 2000. Deforestation of seasonally dry tropical forest: a national and local analysis in Mexico. Biological Conservation 94, 133-142.
Trejo, I., Dirzo, R., 2002. Floristic diversity of Mexican seasonally dry tropical forests. Biodiversity and Conservation 11, 2063- 2084.
Tucker, C.J., Townshend, J.R.G., 2000. Strategies for monitoring tropical deforestation using satellite data. International Journal of Remote Sensing 21, 1461-1471.
Turner, I.M., 2001. The ecology of trees in the tropical rain forest. Cambridge University Press, Cambridge , UK.
Turner, M.J., 2005. Landscape Ecology: What is the state of the science? Annual Review of Ecology, Evolution, and Systematics 36, 319-344.
Velázquez, A., Durand, E., Ramírez, I., Mas, J., Bocco, G., Ramírez, G., Palacio, J., 2003. Land use-cover change processes in highly biodiverse areas: the case of Oaxaca, México. Global Environmental Change 13, 175-184.
Vitousek, P.M., Mooney, H.A., Lubchenco, J., Melillo, J.M., 1997. Human domination of Earth´s ecosystems. Science 277, 494-499.
Walker, A.P., Zaehle, S., Medlyn, B.E., De Kauwe, M.G., Asao, S., Hickler, T., Parton, W., Ricciuto, D.M., Wang, Y.P., Wårlind, D., Norby, R.J., 2015. Predicting long-term carbon sequestration in response to CO2 enrichment: How and why do current ecosystem models differ? Global Biogeochemical Cycles 29, 476-495.
Walker, S.M., Desanker, P.V., 2004. The impact of land use on soil carbon in miombo woodlands of Malawi. Forest Ecology and Management 203, 345-360.
Walther, G.R., Post, E., Convey, P., Menzel, A., Parmesan, C., Beebee, T.J., Fromentin, J.M., Guldberg, O., Bairlein, F., 2002. Ecological responses to recent climate change. Nature 416, 3989-3395.
Watson, R.T., Zinyowera, M.C., Moss, R.H., Dokken, D.J., 1997. Regional impacts of climatic change: An assessment of vulnerability. Summary for Policymakers. A special report of the Intergovernmental Panel on Climate Change (IPCC) Working Group II. IPCC, Paris, France, p. 27.
Wick, B., Tiessen, H., Menezes, R.S.C., 2000. Land quality changes following the conversion of the natural vegetation into silvo-pastoral systems in semi-arid NE Brazil. Plant Soil 222, 59-70.
Wieder, W.R., Cleveland, C.C., Smith, W.K., Todd-Brown, K., 2015. Future productivity and carbon storage limited by terrestrial nutrient availability. Nature Geosci 8, 441-444.
Woollen, E., Ryan, C., Williams, M., 2012. Carbon Stocks in an African Woodland Landscape: Spatial Distributions and Scales of Variation. Ecosystems 15, 804-818.
Wright, J., van Schaik, C.P., 1994. Light and the phenology of tropical trees. The American Naturalist 143, 192-199.
Wright, J.S., Yavitt, J.B., Wurzburger, N., Turner, B.L., Tanner, E.V., Sayer, E., Santiago, L.S., Kaspari, M., Hedin, L.O., Harms, K.E., Garcia, M.N., Corre, M.D., 2011. Potassium, phosphorus, or nitrogen limit root allocation, tree growth, or litter production in a lowland tropical forest. Ecology 92, 1616-1625.
WWF, 2012. Selva seca mexicana. World Wild Foundation.
Yang, Y., Cheng, C., Yang, J., Li, S., Zhang, X., Zhu, D., 2012. Geographical Analysis of Maize Rough Dwarf Disease in the North China Plain: A Comparison of Four Spatial Regression Models. Sensor Letters 10, 349-361.
Yeaton, R.I., Travis, J., Gilinsky, E., 1977. Competition and spacing in plant communites. The Arizona Upland association. Journal of Ecology 65, 587.
Zimmerman, N., 1999. Toposcale AML. WSL, Birmensdorf, Switzerland.

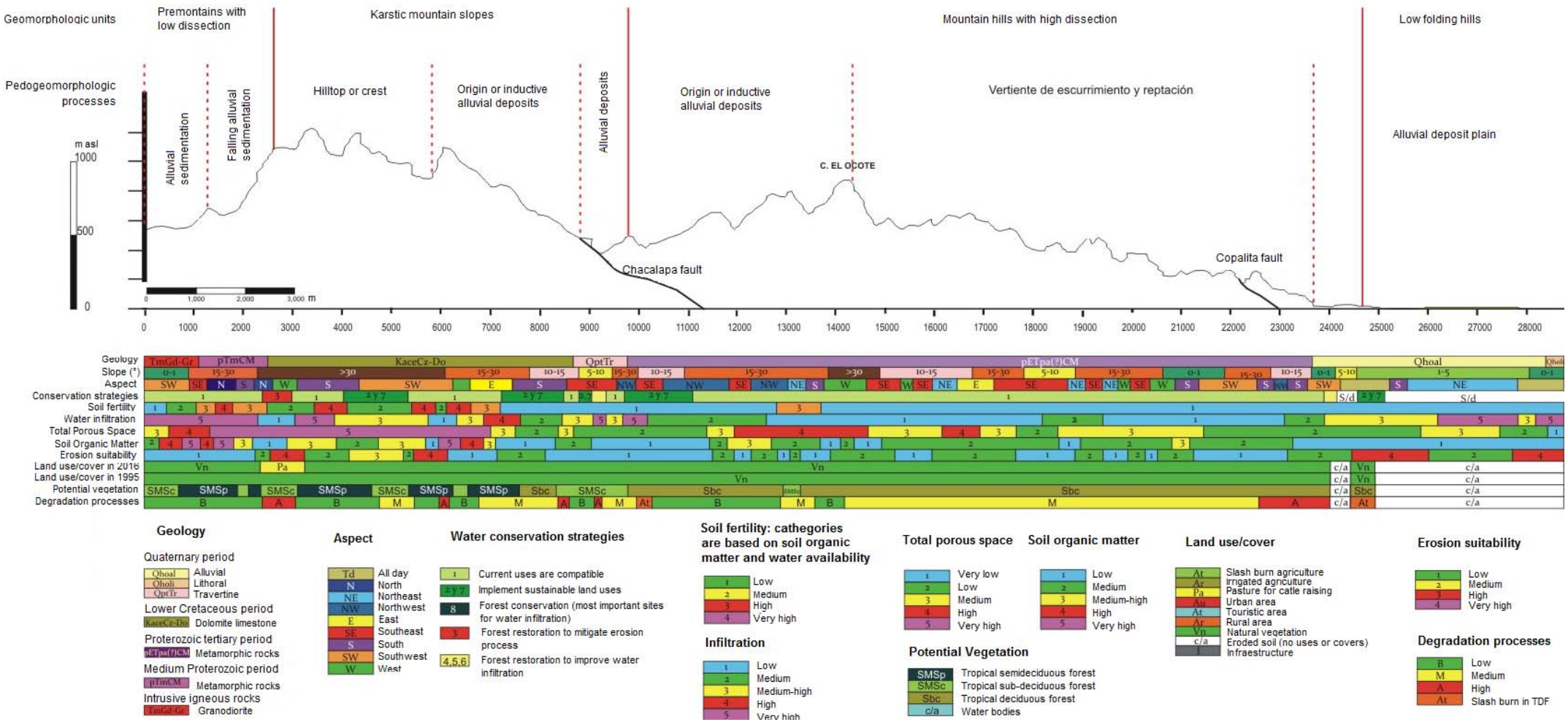

Annex 1. Pedogeomorphologic processes profile N-S. The figure was taken and traduced into English with the authorization of the author. Reference: Corona, N. **2009.** Programa de Manejo Forestal Sostenible y Aseguramiento de los Servicios Ambientales en Bahías de Huatulco, Oaxaca. FONATUR-PSIG. HUDU-8525-09-S-09.

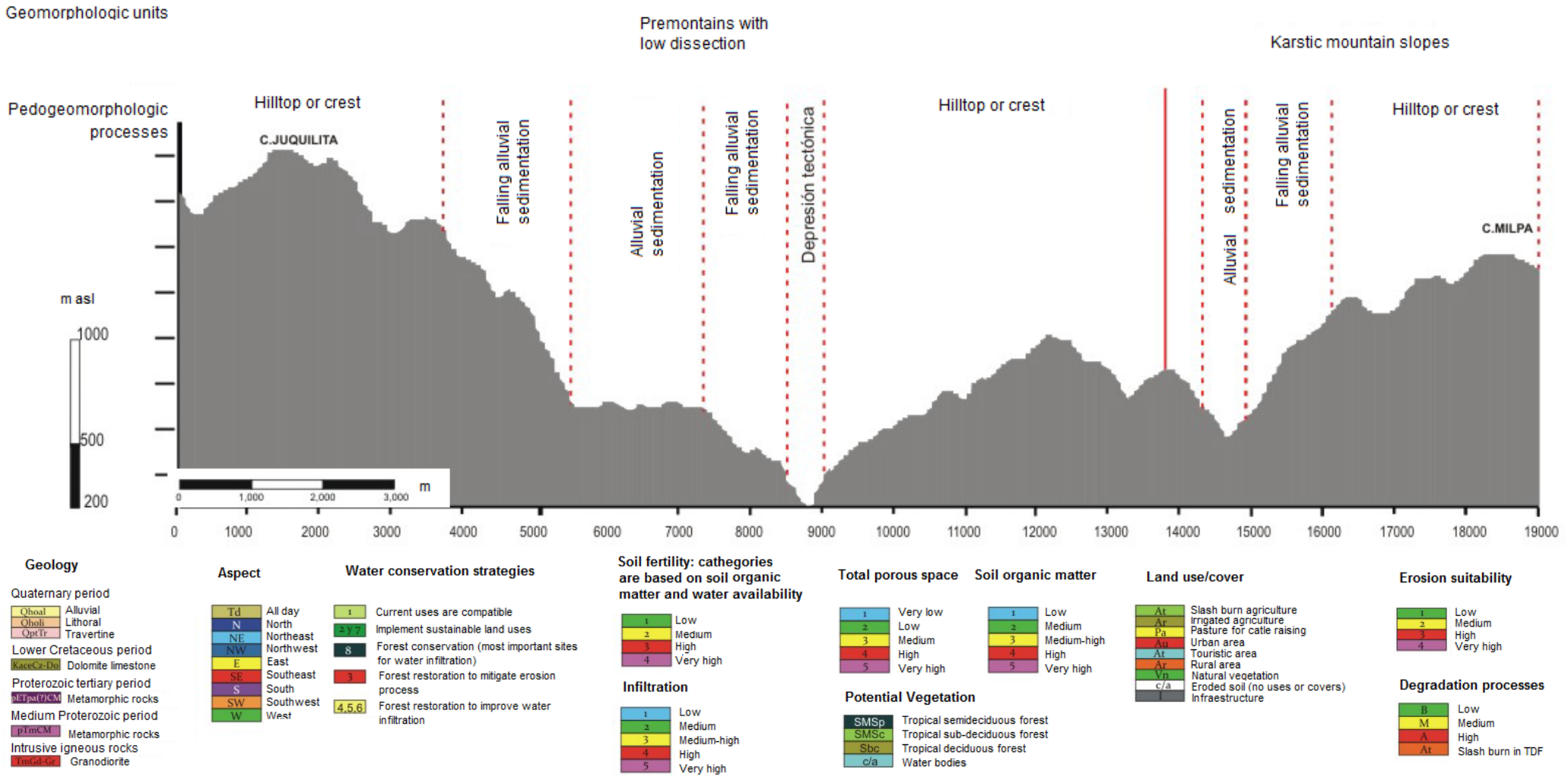

Annex 2. Pedogeomorphologic processes profile W-E. The figure was taken and traduced into English with the authorization of the author. Reference: Corona, N. **2009.** Programa de Manejo Forestal Sostenible y Aseguramiento de los Servicios Ambientales en Bahías de Huatulco, Oaxaca. FONATUR-PSIG. HUDU-8525-09-S-09.

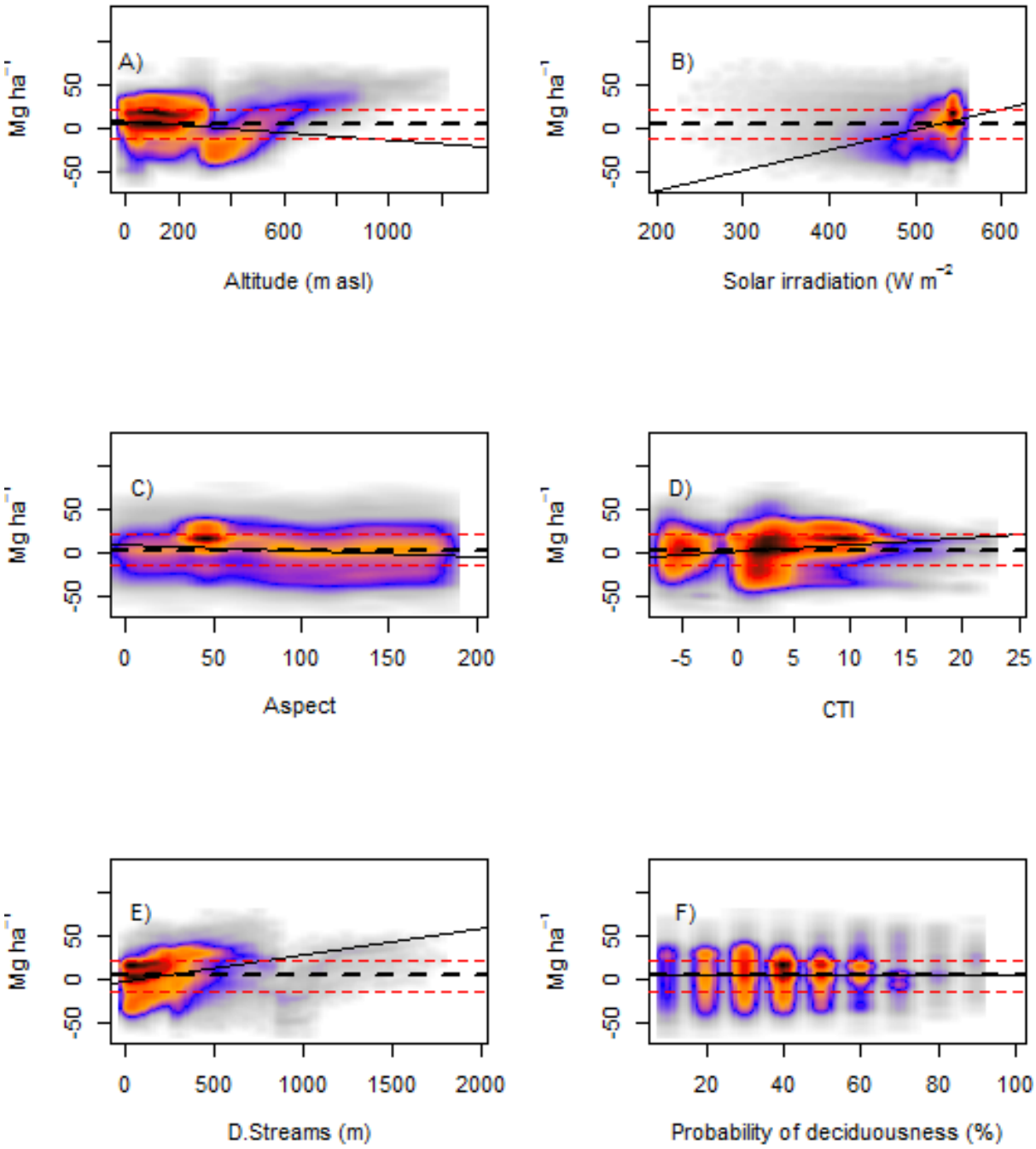

Annex 3. Lineal regressions of the differences in AGB estimated between Neural Networks and Regression Tree against different biophysical variables. Positive values in Y axis represent that NN predict higher AGB estimates for the same location than RT. The solid black line refers to the regression line of the scatterplot. Broken lines represent the mean difference between models (black) plus and minus one standard deviation (red).

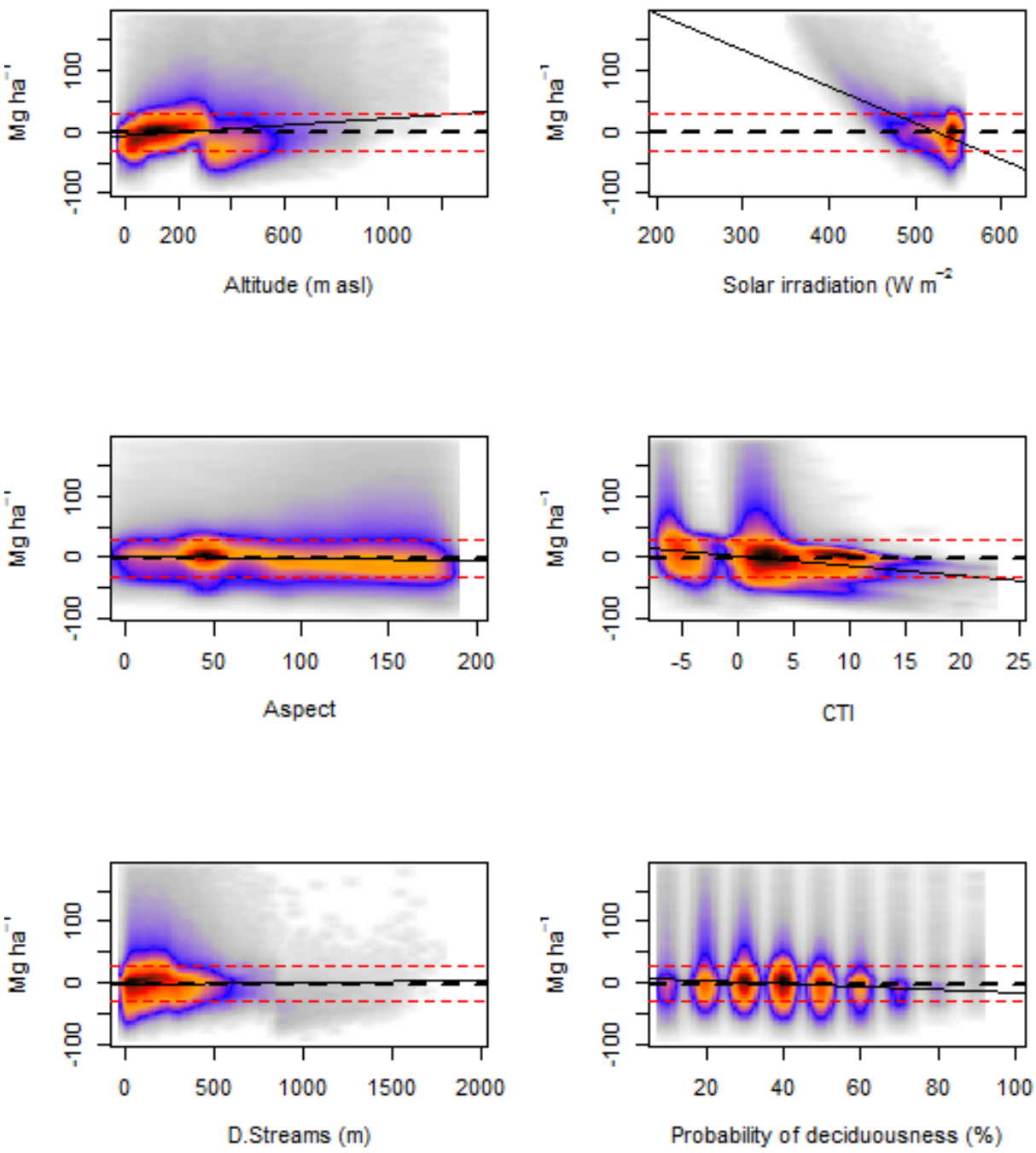

Annex 4. Lineal regressions of the differences in AGB estimated between GLM and Regression Tree against different biophysical variables. Positive values in Y axis represent that GLM predict higher AGB estimates for the same location than RT. The solid black line refers to the regression line of the scatterplot. Broken lines represent the mean difference between models (black) plus and minus one standard deviation (red).

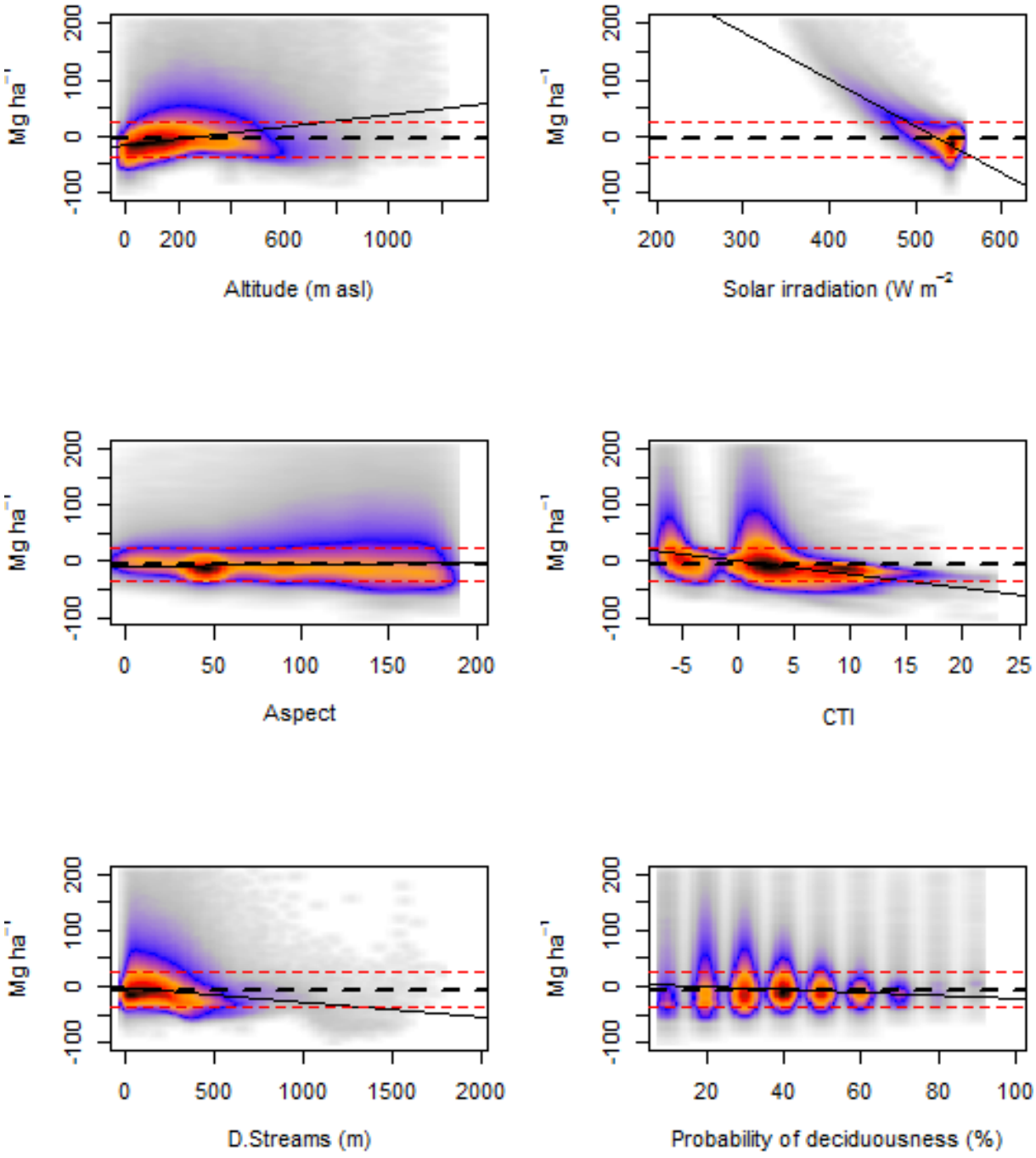

Annex 5. Lineal regressions of the differences in AGB estimated between GLM and Neural Networks against different biophysical variables. Positive values in Y axis represent that GLM predict higher AGB estimates for the same location than RT. The solid black line refers to the regression line of the scatterplot. Broken lines represent the mean difference between models (black) plus and minus one standard deviation (red).

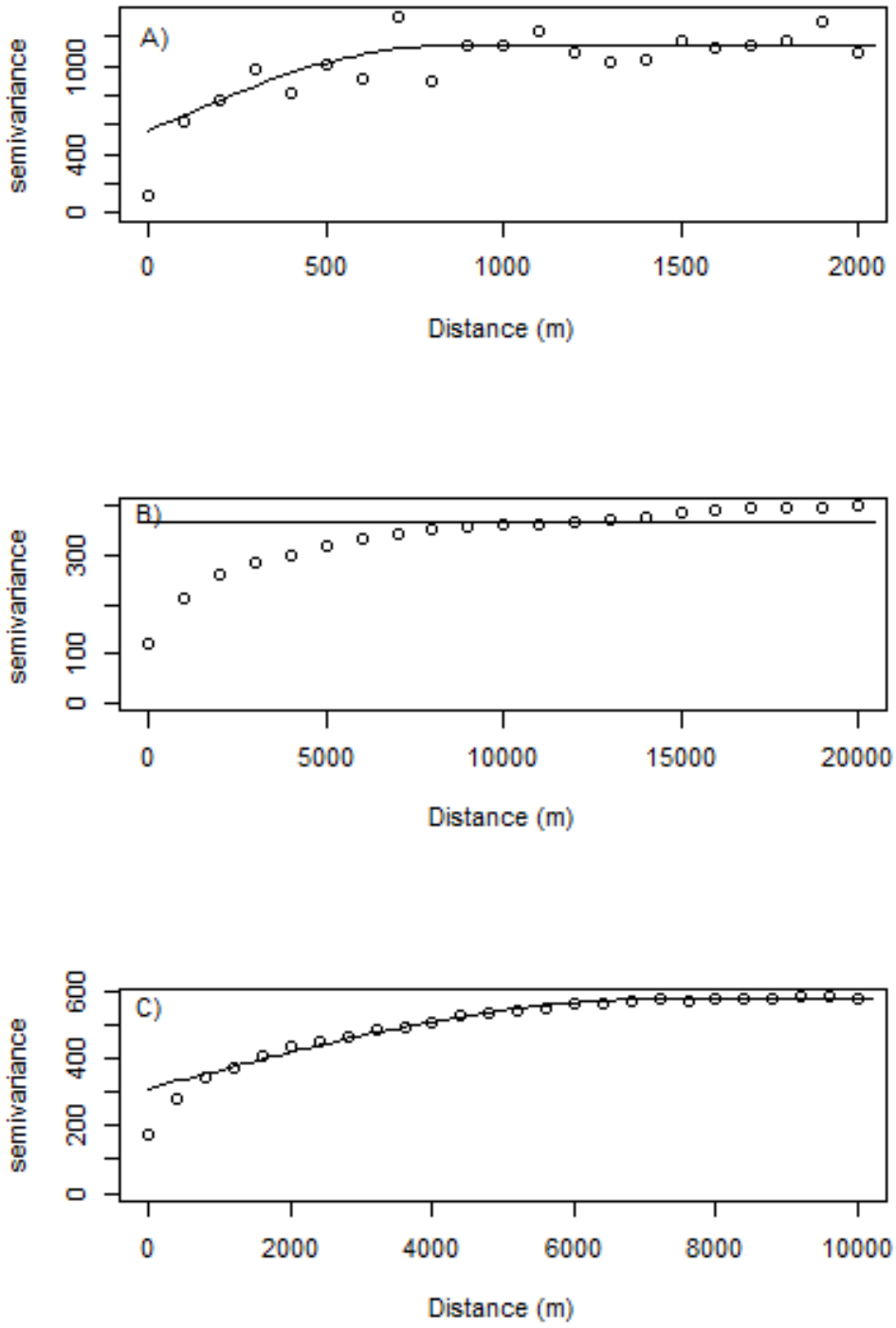

Annex 6. Spatial autocorrelation for the AGB predictions from the different models. Figure (A) refers to GLM, (B) to Neural Network and (C) to Regression Tree.